A Study of the Cytotoxic Mechanism of KP4 - Like Proteins

A Thesis

Presented in Partial Fulfillment of the Requirements for the

Degree of Master of Science

with a

Major in Biological Sciences in the

College of Graduate Studies University of Idaho

by

Marinda R. Stanton

Approved by:

Major Professor: Paul A. Rowley, Ph.D.

Committee Members: Allan Caplan, Ph.D., Doug Cole Ph.D., Patricia Okubara, Ph.D.

Department Administrator: Tanya Muira Ph.D.

December 2022

ABSTRACT

Crop loss and spoilage caused by fungi cost the global economy over $60 billion annually, with $21 billion in the United States alone. *Ustilago maydis* is known to produce an antifungal protein known as Killer Protein 4 (KP4). Using KP4 in transgenic plants resulted in increased resistance to multiple crop pathogens, including corn smut, head blight in wheat, stinking smut, and black rot. KP4 has been shown to inhibit fungal growth by blocking calcium channels. Homologs of KP4 (KP4-like; KP4L) have been identified, but the functions of the proteins remain unknown. These proteins could be a potential resource for creating new antifungals. A survey of KP4L proteins showed increased diversity and strongly conserved primary and secondary structures. Eight KP4L proteins were used to transform the model yeast *Saccharomyces cerevisiae* to study their expression and antifungal activities. However, the induction of KP4L genes caused growth arrest in *S. cerevisiae,* but with the resumption of growth when arrested cells were plated on non-inductive media. To identify if this toxicity was due to KP4L export outside of the cell, an N- terminal truncation mutant lacking an extracellular signal sequence was created. The N-terminal truncation mutant did not induce growth arrest. To confirm the extracellular export, a C-tag was fused to the KP4L C-terminus, and extracellular KP4L was detected by Western blotting. Importantly, the N-terminal truncation mutant that lacked a signal sequence did not get excreted outside of the cell. These results indicate that KP4L proteins are targeting the cell surface for toxicity like KP4 and could be utilized as novel antifungals in crops. Further experiments will be needed to confirm the KP4L mechanism.

ACKNOWLEDGEMENTS

I would like to acknowledge Dr. Paul A Rowley for advising me throughout this project. Jordan Hawley for starting the KP4L Project. Mark Lee for training me and being a critical person in the KP4L project. Additionally, I would like to acknowledge Dr. Shunji Li for teaching me the art of Western blots. Research reported in this publication was supported by the National Institute Of General Medical Sciences of the National Institutes of Health under Award Number P20GM104420. The content is solely the responsibility of the authors and does not necessarily represent the official views of the National Institutes of Health.

DEDICATION

Jo Kaya, thank you for your unending love and support throughout this degree. A big thank you to the entire Rowley lab specifically Dr. Shunji Li, Josie Boyer, Lance Fredricks, Mark Lee, and Mason Shipley for welcoming me into the Rowley Lab family so immediately and helping me get settled in the lab and in Moscow. Lastly, thank you to my mom, Carrie Holmes-Stanton. You never missed a single call of mine in the two years I was here. Thank you for reminding me what is important and that I can do anything one bite at a time.

TABLE OF CONTENTS

LIST OF TABLES

LIST OF FIGURES

CHAPTER 1: LITERATURE REVIEW

Importance of Novel Antifungals

Fungal infections in crops cost twenty-one billion dollars annually in the United States and sixty billion dollars worldwide (Rossman, 2009). Traditional fungicides for these infections, like azoles, are already becoming less effective. This is due to the plasticity of the fungal genome, allowing for quick adaptation to antifungals (Fisher et al., 2012). Novel treatments will be needed to keep crop loss to a minimum. Crop infection projections, like for *Fusarium graminearum*, a common grain disease, predict that disease severity and crop loss will increase significantly by 2050 due to the evolved resilience to common antifungals (Madgwick et al., 2011). Major crops like wheat, rice, potatoes, soybeans, and maize are all susceptible to various fungal pathogens that can dramatically reduce crop yield. Already, rice blast, a rice crop pathogen, can reduce crop yield by up to thirty percent, stem rust in wheat can cause crop losses of up to seventy percent, and maize loss due to corn smut can be up to twenty percent (Talbot, 2003; Allen et al., 2011). If extensive fungal outbreaks happened in these five major crops, it is estimated that only thirty-nine percent of the world's population would have sufficient food (Fisher et al., 2016). If this problem is left unaddressed, fungal infections could result in the commercially unviable crops. Fungi are already large contributors to biodiversity loss due to host extinction, including to a decline in many frog species decline (Fisher et al., 2012). Furthermore, as climate change progresses, the habitat area for pathogens will increase, and changes in weather and increases in severe weather will cause optimal conditions for disease. Pathogens can then infect plants earlier in the year and for a more extended period, resulting in greater crop loss (Fisher et al., 2012). It is important to note that fungal pathogens could also be negatively affected by climate change and cause reduction of some fungal species (Godfray et al., 2016).

The USDA projects a seventy percent increase in the human population by 2050 (Food Security USDA). The joint problem of an increase in world population and a decrease in crop yields due to fungal disease will make it difficult to feed everyone. A model of a rice crop epidemic predicts major rice price increases worldwide and an increase in hunger for some countries (Godfray et al., 2016). Even fungal disease in secondary crops (like fruits) can cause economic devastation for developing countries (Anderson et al., 2004). This shows a strong need to reduce crop yield losses and monetary losses. Developing novel antifungals is the first

step to minimizing fungal disease. Turning to plants and microorganisms for potential novel antifungals may be the key to doing this quickly. Plants and microorganisms have already developed many compounds as a way to inhibit or kill each other. Isolating these compounds from microorganisms and plants could lead to a new age of antifungal drug development.

Just as in the plant world, microorganisms face many obstacles to survival in the form of direct and indirect competition. Indirect competition primarily encompasses resource consumption, including finding the necessary nutrients for survival, nutrient uptake and extracellular digestion (Ghoul & Mitri, 2016). Direct competition generally consists of the elimination of other organisms and self-enhancing changes (Ghoul & Mitri, 2016). This can allow a species to take over more space or uptake more environmental nutrients. Direct competition between microbes can be thought of as a small-scale form of chemical warfare. Cells secrete various biocidal molecules or molecules to solidify attachment to a space rich in nutrients (Ghoul & Mitri, 2016). Two well-studied forms of direct competition are allelopathy (related to plants) and bacteriocins (related to bacteria).

Allelopathy

Allelopathy describes the process of one organism chemically affecting another and is often associated with plants' defense mechanisms (Cheng & Cheng, 2015). Plants can release defense molecules through their leaves and roots. The molecules, known as allelochemicals, are already positively utilized in agriculture for weed control or crop protection (Cheng & Cheng, 2015). One example is using plants on the sides of walkways in crop fields to prevent weed growth in walkways. For example, this has been used in field trials of tomato crops (Schulz et al., 2013). Fourteen different types of allelochemicals have been documented, and their functions range from influencing growth and development to respiration and metabolism (Chengxu et al., 2011). It has also been shown that secondary metabolites can function as allelochemicals. These can reduce neighboring plants' germination or water uptake, or damage photosynthesis machinery. Secondary metabolite allelochemicals are often found in invasive plant species (Chengxu et al., 2011). These tools help them invade new areas and establish dominance in already occupied areas. Targets of the allelochemicals are broad and include other plants, fungi, and bacteria. Utilizing these tools can be an environmentally friendly way to perform weed and pest management (Figure 1.1; Schulz et al., 2013; Cheng & Cheng, 2015).

Figure 1.1. Field trial using allelopathic cover for tomato crops (Schulz et al., 2013). *Left, is allelopathic rye mulch showing weed suppression. Right, is split into two treatments: left is untreated, and right is mechanical control. The image is taken from Schulz et al., 2013.*

Plants also produce natural antimicrobial peptides as a function of their immune system (Khan et al., 2019). Peptides known as defensins are a group within this immune system, and they can act against fungi and against both gram-negative and gram-positive bacteria (Khan et al., 2019). These are small, less than fifty-five residues, cationic peptides with three to five disulfide bonds (Khan et al., 2019). Defensins have a broad spectrum of activity that typically targets membranes in some way (Khan et al., 2019). Plant defensins MsDef1 and MtDef2 have been shown to inhibit root growth through calcium channel disruption in germinating *Arabidopsis thaliana* (Allen et al., 2008). Other defensins have been shown to create channels that allow for the influx of water or the outflow of ions (Khan et al., 2019). Plant defensin NaD1 punctures cell membranes and induces the production of reactive oxygen species, effectively killing any microorganism nearby. (Khan et al., 2018; Weerden et al., 2008). Upregulating plants' natural defense mechanisms has already been shown to reduce infections from fungal pathogens and has been used for crop protection (Lacerada et al., 2014).

Bacteriocins

Bacteria also must compete in the environment for nutrients and space. One example of direct competition between bacteria is through molecules known as bacteriocins. Bacteriocins are proteins produced by one bacteria strain and are used to inhibit strains of closely related bacteria (Benítez-Chao et al., 2021). The primary purpose is to remove the competition of other

microbes near the producer strain. Bacteriocins are small, positively charged peptides with many cysteine and disulfide bonds (Benítez-Chao et al., 2021). Both gram-negative and gram-positive bacteria produce bacteriocins, but gram-positive bacteria produce most of the known bacteriocins. Gram-positive bacteria produce two classes of bacteriocins: lantibiotics (peptides less than thirty-eight amino acids with post-translational modifications and unusually modified amino acids), and nonlantibiotics (small peptides less than sixty amino acids with no modifications besides disulfide bridges) (Hassan et al., 2012). Gram-negative bacteria also have four types of bacteriocins: colicins (size greater than ten kDa produced by *E. coli*), colicin-like (size greater than ten kDa not produced by *E. coli*), microcins (size lower than ten kDa), and phage tail-like (high similarities to phage tails) (Simons et al., 2020).

Bacteriocins can have bacteriostatic or bactericidal activity. Depending on the bacteriocin, it can also have a narrow or broad spectrum of activity. While there is an abundance of identified bacteriocins, only a portion has been studied to understand their structure and function. In general, they are known to interact with the cell membrane either through receptor-specific binding or through non-specific binding to the cell wall (Benítez-Chao et al., 2021; Simons et al., 2020). For example, Nisin bacteriocins bind to the cell walls and then form pores in bacterial cell membranes causing cell death Simons et al., 2020). Microbisporicin inhibit peptidoglycan synthesis and disrupt the bacterial cell membrane (Simons et al., 2020). Zoocin is known to disrupt the bacterial cell wall (Simons et al., 2020).

Bacteriocins have been used in a limited way with crops and in studies to attack crop pathogens (Mizeraa et al., 2021; Rooney et al., 2020; Grinter et al., 2012). There is a strong interest in using bacteriocins to combat multidrug resistant bacteria. Work has been done to understand the safety and toxicity of using bacteriocins in human health (Benítez-Chao et al., 2021). *In vitro* models have been shown to reduce drug-resistant pathogens (Benítez-Chao et al., 2021). *In vivo* testing in mouse models has also been shown to reduced pathogen infection (Benítez-Chao et al., 2021). Data has shown a lack of mammalian toxicity in the *in vivo* models (Benítez-Chao et al., 2021). Currently, bacteriocins are primarily used as food preservatives.

Killer Toxins produced by fungi

Similarly to plants and bacteria, growth-inhibiting molecules have been identified in fungi. While many fungal species have been identified to have antifungal molecules the best

studied are from *Saccharomyces cerevisiae.* Specifically *Saccharomyces cerevisiae* has nine different antifungal proteins that have been identified. These proteins have been named "killer toxins" after their purpose in killing fungi, which is a direct competition defense mechanism (Figure 1.2.). This has been proposed to help crops with fungal disease as a post-harvest treatment (Díaz et al., 2020).

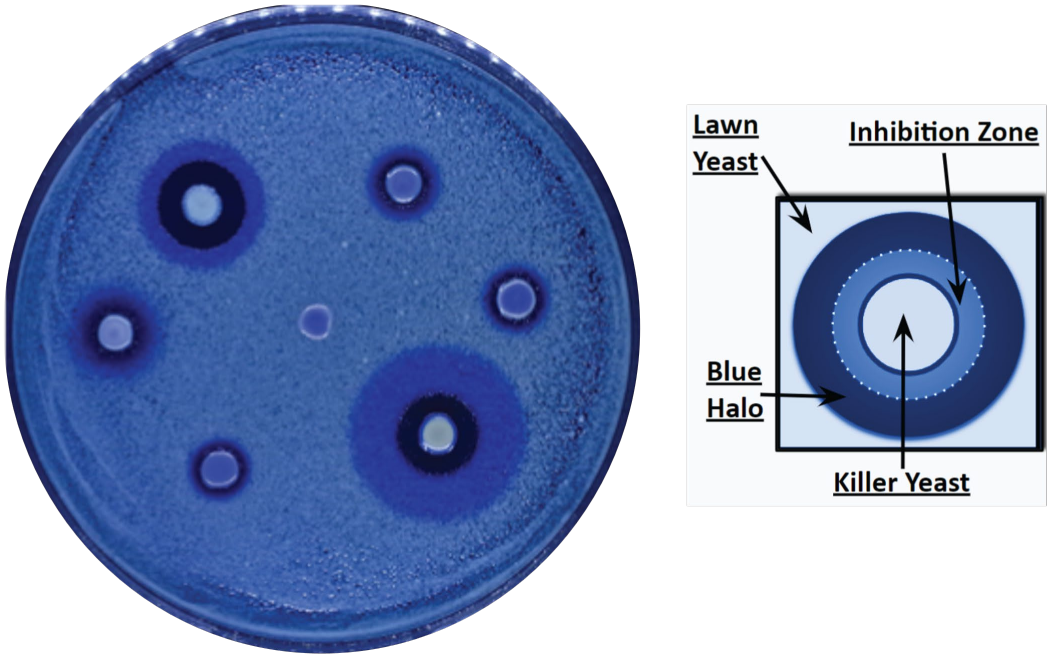

Figure 1.2. Left is a killer assay plate containing six killer toxins from Saccharomyces cerevisiae and the middle control is the lab strain of S. cerevisiae*. Right is a diagram describing the killer phenotype. The Inhibition zone and the blue halo are zones of cell death from the killer toxin producing cells. The dark blue colors come from a redox reaction with methylene blue when cells lyse.*

The three major killer toxins found in *Saccharomyces cerevisiae* are known as K1, K2, and K28. These toxins kill nearby sensitive strains and are thought of as a competitive advantage for producing killer strains. First detailed in the 1970s, the three canonical toxins are produced by dsRNA satellites and are associated with dsRNA totiviruses (Beavens et al., 1963, Schmitt & Breinig, 2006.). Both the dsRNA satellite and the dsRNA totivirus are needed for the killer phenotype (Schmitt & Breinig, 2006). The toxin itself is encoded on an dsRNA satellite residing in the cytoplasm. The killer toxin, or "M" virus, entirely depends on the totivirus or L-A virus replication machinery to persist in the cell. The L-A virus only has two open reading frames for a Gag capsid protein and a Gag-Pol fusion protein that encodes an RNA-dependent RNA polymerase (Schmitt & Breinig, 2006). The downstream processing is

done by the cell itself (Figure 1.3.). After processing, these toxins are secreted into the extracellular space. Then the killer toxin proteins interact with receptors on sensitive strains and ultimately kill them. The excreting cells survive the event through the presence of the "prepro-toxin." The prepro-toxin, or pptoxin, is the unprocessed version of the protein. The presence of the pptoxin conveys immunity only to the mature version of the toxin it creates and to no other killer toxins. That means a killer-producing cell can still be susceptible to other toxins with a different mechanism.

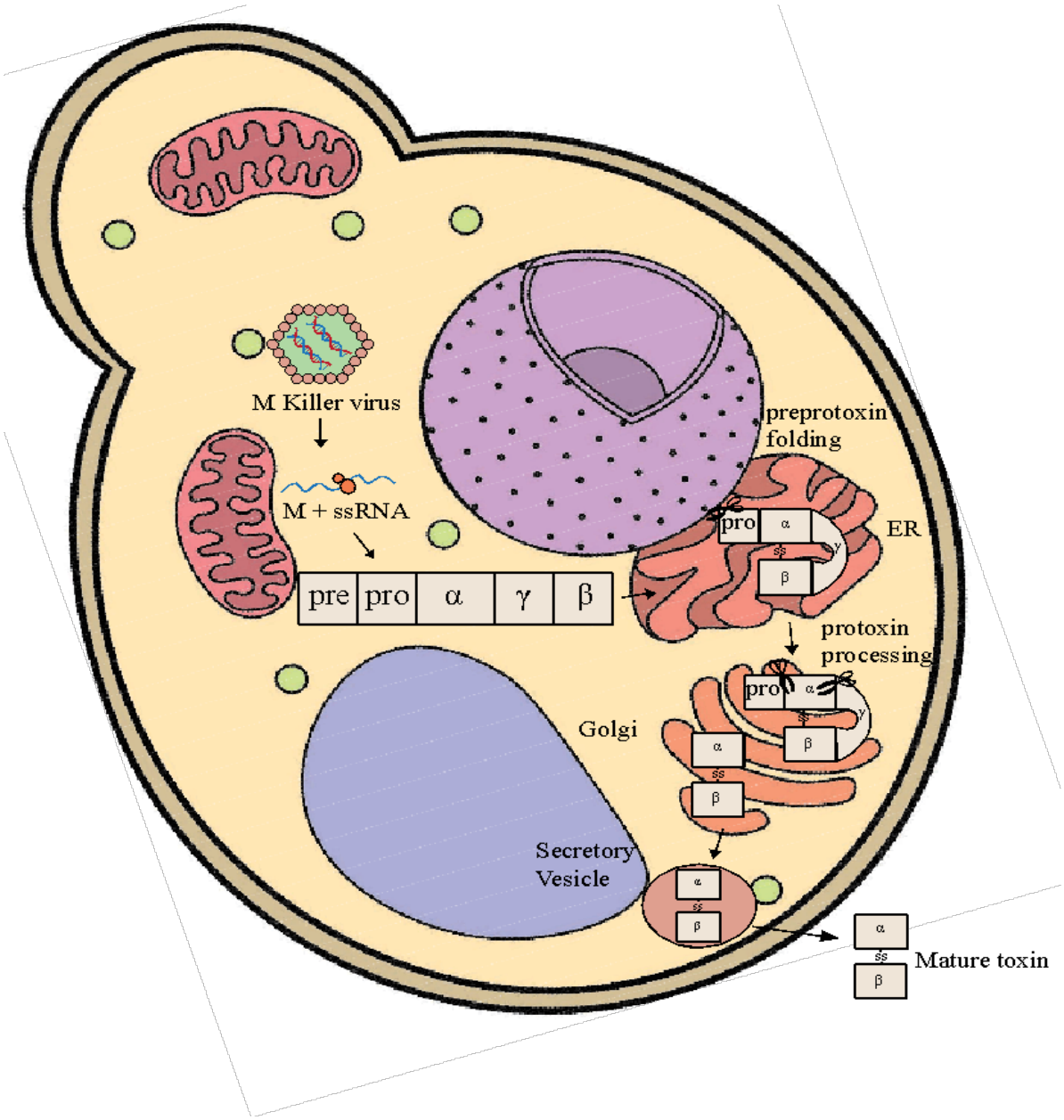

Figure 1.3. Example diagram of killer toxin production of K1. *The M Killer virus recruits the Gag-pol polymerase from the coinfecting totivirus for transcription. Translation is then performed by the cell itself. The preprotoxin is then folded in the endoplasmic reticulum and the pre portion of the toxin is removed. Further processing is performed in the Golgi. The Golgi apparatus then cleaves the pro region of the toxin and Kex2p removes the gamma domain of the protein. The mature toxin is then secreted out of the cell. Information about K1 processing from Schmitt and Breinig (2006).*

The mechanism of K1 is the best studied. K1 forms ion channels in the yeast membrane of sensitive cells. There are four subunits that make up the K1 toxin: delta, alpha, beta, and gamma. The removal of the signal sequence of the K1 toxin and the initial folding of the protein takes place in the endoplasmic reticulum of the killer yeast cell. The gamma subunit confers

immunity and eventually gets cleaved out by Kex2p in the Golgi of the killer yeast cell to form the mature toxin. After excretion, the beta domain binds to the cell surface of sensitive cells. Then the alpha domain attacks the membrane by "punching" holes, allowing ion leakage to occur. This breaks down the membrane gradient, ultimately leading to cell death. The first receptor for K1 is the beta-1,6-glucan in the cell wall which helps the toxin bind to the Kre1 receptor in the plasma membrane (Schmitt & Reiter, 2008).

Less is known about the killing mechanism of the killer toxin K2. K2 interacts with the plasma membrane and cell wall to cause cell death. Like K1, K2 also binds first to beta-1,6-glucan on the cell wall (Luksa et al., 2015). However, K2 does not have a gamma region and its optimal killing environment is pH four compared to pH 4.6 for K1 (Luksa et al., 2015). From this, it is assumed K2 operates with a different mechanism of action than K1.

The killer toxin K28 is different from both K1 and K2. K28 targets the nucleus of a sensitive cell for killing. This prevents cell division of target cells and ultimately causes growth arrest (Schmitt et al., 1989). K28 is folded by the endoplasmic reticulum and then processed by the Golgi to create an alpha-beta dimer mature toxin. Mature K28 toxins are endocytosed by the sensitive cell after binding to the cell surface via mannoprotein (Schmitt & Radler, 1987; Schmitt & Breinig 2006). After being taken up by the cell, the K28 toxin is then transported through the Golgi and the endoplasmic reticulum. The beta subunit is degraded, and the alpha subunit goes into the nucleus. The K28 toxin then targets host proteins in the nucleus involved in cell-cycle control to prevent DNA synthesis (Schmitt & Breinig 2006).

Killer Proteins from *Ustilago maydis*

Killer toxins have been identified in non-yeast fungi as well, specifically *Ustilago maydis* (Puhalla, 1968). *Ustilago maydis* is a member of the order Ustilaginales and phylum Basidiomycota (Martínez-Espinoza et al., 2001). *U. maydis* is included in a group known as smut fungi. Smut fungi are well-known, important plant pathogens that cause persistent agricultural losses (Martínez-Espinoza et al., 2001). *U. maydis*, commonly known as corn smut, causes grey galls to grow on the ears and kernels of the corn plants (Martínez-Espinoza et al., 2001). It is also known as "huitlacoche" and is considered a delicacy in the four corners area of the United States, as well as in Central America (Figure 1.4.; Ruiz-Herrera & Martínez-Espinoza, 1998). *U. maydis* has three killer proteins that were first identified in the 1970s. The

proteins are Killer Protein 1 (KP1), Killer Protein 4 (KP4), and Killer Protein 6 (KP6) (Koltin & Day, 1976). Similar to killer toxins in yeast, the killer proteins are encoded on a dsRNA satellite. Of wild *U. maydis* strains, it is estimated only about one percent contain killer protein-producing satellites (Day, 1973). Each virus type is insensitive to its own toxin due to a single recessive mutation in nuclear genes. The nuclear mutation for resistance is denoted as p1r, p4r, and p6r to correspond to the different toxin types (Koltin & Day, 1976). Resistance is specific to a single toxin so toxin producing strains are still sensitive to other toxin types.

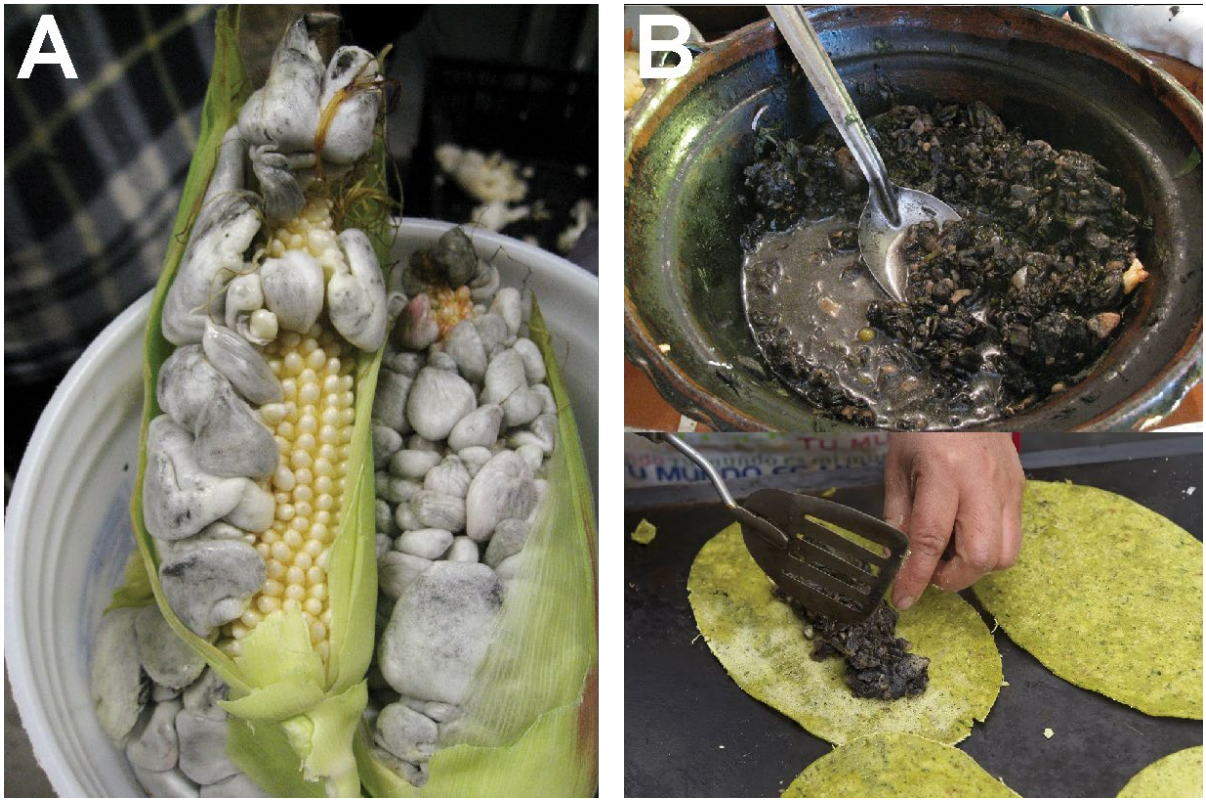

Figure 1.4. Ustilago maydis infected corn. *(A) An ear of corn infected with Ustilago maydis. (B) The preparation of Ustilago maydis infected kernels. Images from NPR 2015.*

KP1 is the least studied. The *U. maydis* cells encoding the KP1 killer toxin are known to have two M segments present, but it has been suggested that the M2 segment encodes the toxin. The KP1 toxin has a basic isoelectric point of 8.0, and it is 12.4 kDa with no glycosylation present (Park et al., 1996). It is known that the toxin does not require the cell wall to be present for its activity (Park et al., 1996).

KP6 is more studied. It is also a neutral protein with 219 acids (Allen et al., 2013). It is synthesized as one pre-protoxin but is later cleaved into two peptides known as the alpha and beta subunits, which are 79 and 81 amino acids respectively (Li et al., 1999). The alpha and beta subunits are covalently linked in downstream modifications (Allen et al., 2013). The subunits can fold properly independently, but they are not functional toxins until the linkage modification (Allen et al., 2012). The alpha subunit is proposed to create a pore (Li et al., 1999). The beta subunit is known to be responsible for toxicity (Allen et al., 2012). The alpha subunit binds to the cell wall and is thought to bring in the beta subunit to kill the sensitive cell (Allen et al., 2012). It has been proposed that the toxin could be disrupting potassium ion balance (Li et al., 1999; Tao et al., 1990). The subunits act independently and target the cell wall for activity. When sensitive spheroplast cells were treated with purified KP6, they were insensitive to the toxin—indicating that the cell wall is mandatory for proper functionality (Allen et al., 2013). Structure analysis identified KP6 as having a structure analogous to snake venom cytotoxins.

Killer Protein 4 from *Ustilago maydis*

For the purpose of this literature review, the KP4 toxin is the primary toxin of interest. KP4 is the most well-studied killer protein from *U. maydis* and was first discovered in 1968 (Puhalla, 1968). It was shown that grass smuts have reduced growth when in contact with KP4 and that it also inhibited root growth in *Arabidopsis thaliana* (Koltin & Day, 1976; Allen et al., 2007). KP4 is a small basic protein that has 127 amino acids (Gu et al., 1995). After signal sequence cleavage, the length is reduced to 105 amino acids (Gu et al., 1995). It is a non-glycosylated single polypeptide sequence (Gu et al., 1995). KP4 is a stable protein that resists the effects of temperature, organic solvents, and proteolytic enzymes (Gu et al., 1995). All the hydrophobic residues are concealed by hydrophilic residues, and the protein has five disulfide bonds, stabilizing the secondary structure (Gu et al., 1995). Unlike other killer toxins, it is extremely basic, with an isoelectric point above nine (Gu et al., 1995). The crystal structure of KP4 has been solved, allowing the protein to be categorized as an alpha-beta sandwich protein (Figure 1.5.; Gu et al., 1995). It has seven beta sheets, three alpha helices, and one split beta-sheet-alpha-helix-beta-sheet motif (Gu et al., 1995). There is weak similarity to scorpion toxins in the alpha-beta sandwich family (Gage et al., 1995). There is a highly basic protrusion from

the main beta-sheet in KP4, similar to the active site of scorpion toxins (Gu et al., 1995). Also, like scorpion toxins, there is a lysine residue in the basic protrusion (Gage et al., 2001). It is known for scorpion toxins that the lysine residue is part of the protein's active site. KP4 has one lysine present in the protein sequence (K42). When lysine 42 was mutated to glutamine, the antifungal activity was reduced by ninety percent (Gage et al., 2001). However, the similarity to the scorpion toxins mentioned is quite weak so caution should be used when comparing the two.

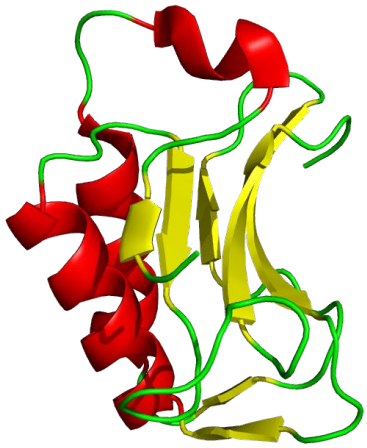

Figure 1.5. Crystal structure of KP4 (Gu et al., 1995; Schrodinger & DeLano, 2020). *Alpha helices colored red, beta sheets colored yellow, and the non-structured portions are colored green.*

The mechanism of KP4 was first discovered due to its structural similarity to scorpion toxins. Scorpion toxins are neurotoxins that inhibit cation channels. In comparison, KP4 has been indirectly shown to interact with calcium channels. In a plate assay, the antifungal activity was shown to be undone by excessive calcium ions present in growth medium (Figure 1.6.; Gu et al., 1995). Patch clamp data indicated that KP4 specifically blocked L-Gated Calcium Channels in mammalian cells (Gage et al., 2002). This channel is predicted to be analogous to its fungal calcium channel counterpart. *S. cerevisiae* has a potential homologous calcium channel, *CCH1*, and it is hypothesized that *Ustilago maydis* has a similar one that KP4 is acting upon (Gage et al., 2001;). It has been shown that the CCH1 calcium channel is activated by intracellular calcium depletion (Allen et al., 2013; Gage et al., 2001). Calcium is also known

to be important to the G1 and S transition in the cell cycle(Kahl & Means, 2003). KP4 is proposed to bind reversibly to the calcium channels on the cell surface and inhibit the growth of sensitive cells by blocking signaling pathways. Sensitive cells incubated with KP4 show constant viable cell count over 24 hours, indicating a fungistatic mechanism of action (Gage et al., 2001). Comparatively, untreated cells and cells treated with KP4 and calcium had normal growth (Gage et al., 2001). Additionally, when KP4-treated cells are washed with calcium, they resume standard growth patterns—furthering the proposed hypothesis about the inhibition of the cell cycle (Gage et al., 2001). The addition of cAMP molecules also causes cell growth recovery indicating that presence of excess signaling molecule is needed to negate fungistatic effect from KP4 (Gage et al., 2001). As a fungistatic protein, KP4 has been identified as a potential novel antifungal for use in agriculture.

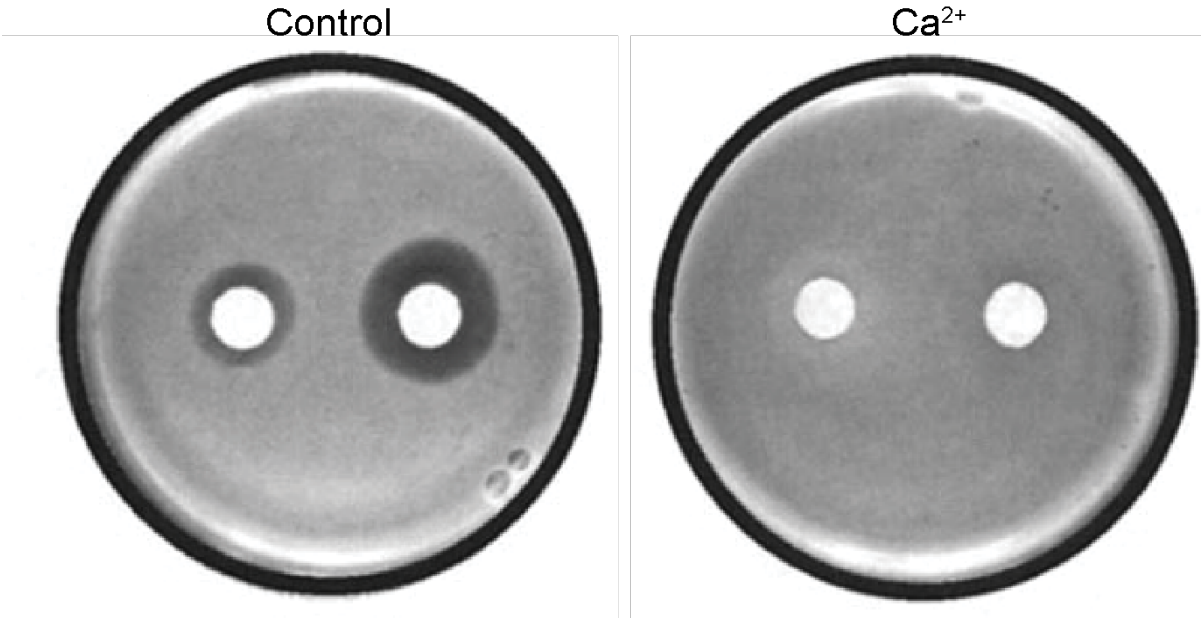

Figure 1.6. Inhibition of sensitive Ustilago maydis from purified KP4 protein. *Purified 0.8 um (left disc) and 8.0 um (right disc) KP4 plated on a sensitive lawn of Ustilago maydis (left), and KP4 plated on an excess of 0.1 M CaCl2 and a sensitive lawn of Ustilago maydis (right). Image taken from Gu et al., 1995.*

Due to KP4's success in inhibiting *U.* maydis, KP4 has been used to create transgenic corn, tobacco, and wheat plant strains (Clausen et al., 2000; Park et al., 1996; Deb et al., 2018; Schlaichet et al., 2006). Yield loss of corn from *U. maydis* alone varies from 2 percent to 20 percent (Allen et al., 2013). Greenhouse trials of transgenic maize strains showed that disease symptoms, post inoculation of *U. maydis,* were minimal to absent in strain lines expressing

high levels of KP4, compared to plant death in the wild-type lines (Allen et al., 2013). Transgenic corn kernels even show a zone of inhibition against sensitive strains of *U. maydis* surrounding the kernel (Clausen et al., 2000). After two weeks post-infection, the transgenic lines remained disease free and were shown to resist infection. The plants had normal development in a greenhouse environment over several months. There was also antifungal activity against *Fusarium graminearum* and other *Fusarium* species. One transgenic strain created did not have resistance, but it was shown to have low levels of KP4 mRNA compared to the transgenic lines with resistance (Clausen et al., 2000).

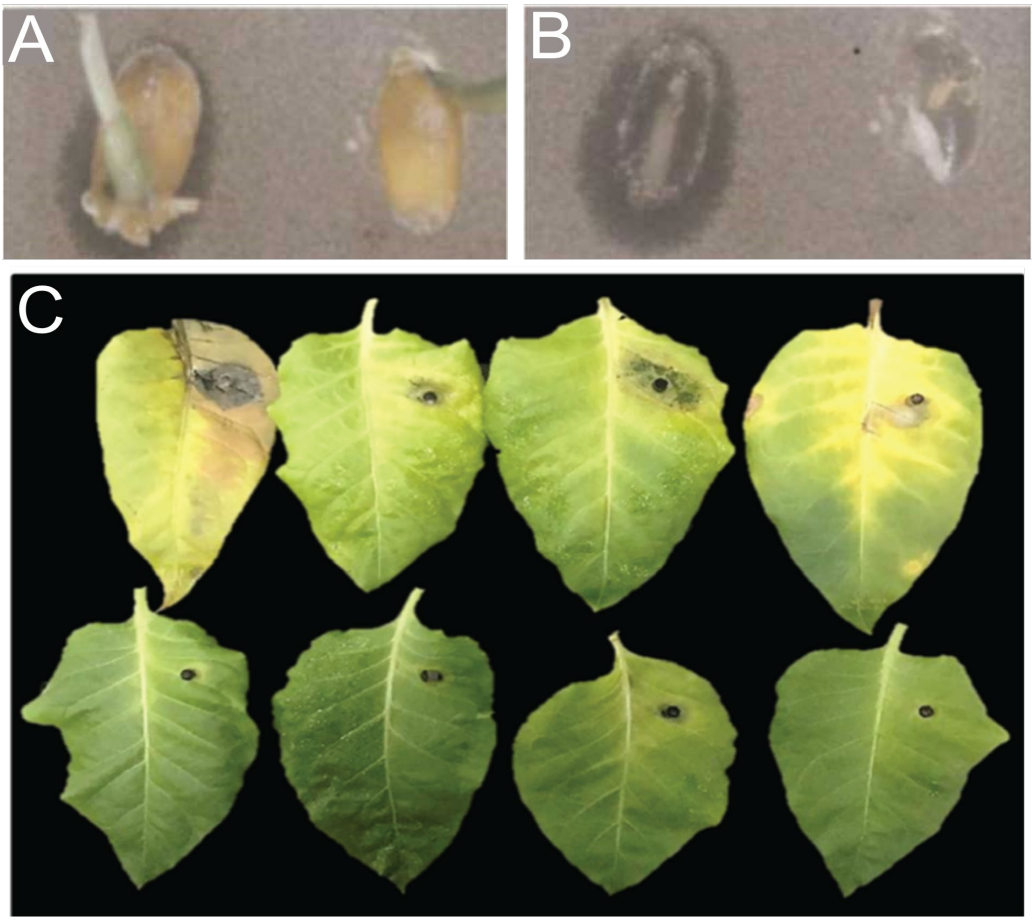

Figure 1.7. Transgenic plant strains resisting fungal infection. *(A) A transgenic corn strain (left) and wildtype corn strain (right) plated against a sensitive lawn of Ustilago maydis and (B) the same plate with the kernels removed (Claus et al, 2001). (C) Alternaria alternata infected wild-type tobacco plants (top) and KP4-containing transgenic strains (bottom) imaged two weeks post-infection (Deb et al., 2018).*

Other crops, like wheat and tobacco, also experience significant yield loss due to fungal disease and have had transgenic plant strains created with KP4. Field trials for transgenic wheat

expressing KP4 had a ten percent decrease in infections and crop symptoms from fungal pathogen *Tilletia carries,* compared to the wild-type wheat strain (Schlaichet et al., 2006). Transgenic tobacco also showed significant antifungal activity (Figure 1.7.). The tobacco was tested against Deuteromycetes phytopathogens *Alternata alternatia* and *Phoma exigua* var. *exigua* (Deb et al., 2018). There was no inhibition against another strain, *Verciullum dahliae*. These studies show that KP4 is a promising way to combat certain fungal diseases. In the transgenic tobacco trial, it was shown that there are many fungal pathogens that are not inhibited by the protein. However, there are many KP4 homologs that have been identified in other fungal species that could potentially be utilized to combat fungal pathogens.

Killer Protein 4-Like Proteins

There has been a vast diversity of KP4 homologs identified recently named "KP4-Like (KP4L)" proteins. KP4L was first identified and analyzed in twenty non-smut fungi in 2011 and then sixty additional proteins from fungi in 2019 (Brown, 2011; Lu & Faris, 2019). Since then, hundreds more have been identified (this study). KP4L proteins are found in plants, moss, amoeba, and fungi, mainly in Ascomycota and Basidiomycota lineages (Lu & Faris, 2019; Brown, 2011). Currently, there are only two publications about KP4L proteins. The lack of publications highlights a need for further understanding of the structure and function of these proteins (Brown, 2011; Lu & Faris, 2019).

Figure 1.8. KP4 and KP4L alignment showing the five segments of significantly conserved residues (Brown, 2011).

A significant difference between KP4 and KP4L is that KP4L proteins are genomically encoded. Phylogenetic analysis shows a common ancestor between KP4 and the KP4L genomic proteins (Brown, 2011). An analysis of seven KP4L proteins from *F. verticillioides* and KP4 show that the beginning and ends of the proteins have the most homology, with the

first eighteen residues having seventy-two percent identity, and the last twenty-eight residues having sixty-four percent identity (Brown, 2011). Additionally, for these eight sequences, there are five segments that have significantly conserved residues, including six cysteines (Figure 1.8.; Brown, 2011). Four of those cysteines are known to create cystine bonds in KP4 (Gu et al., 1995; Brown 2011). SignalP predicted similar signal sequence cleavage sites in the matching region to the KP4 signal sequence cleavage site (Brown, 2011). In an analysis of forty-one fungal KP4L proteins and two plant KP4L proteins, there is seventy-eight percent to one hundred percent identity within the five previously identified segments, and all six previously identified cysteines were conserved in all KP4L samples (Brown, 2011). There have also been single and double-domain KP4L proteins identified (Brown, 2011). Double-domain KP4L proteins indicate possible positive selection pressure on the genes due to the gene expansion. Although more data would be needed to identify if this was true.

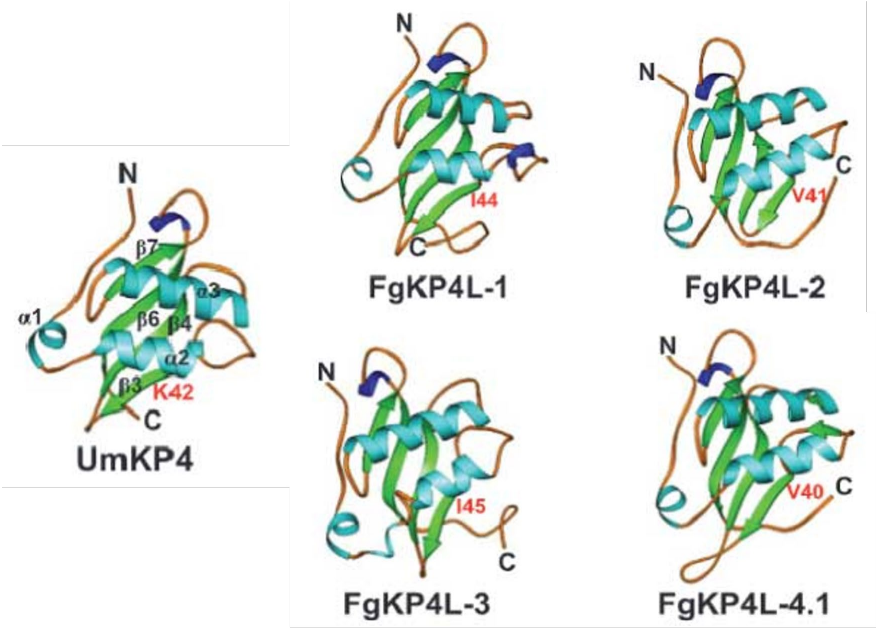

Figure 1.9. Structure prediction of four KP4L proteins compared to the crystal structure of KP4 (Lu & Faris, 2019). *Active site residue lysine 42 (K42) is highlighted and the aligned protein from the KP4L proteins.*

Similar to the conserved primary amino acid structure, the tertiary structure is also predicted to be highly conserved when compared to KP4 (Figure 1.9.; Lu & Faris, 2019). Structure predictions for four KP4L proteins from *F. graminearum* suggested that the KP4L proteins would form a three-dimensional structure like KP4 (Lu & Faris, 2019). The prediction included all three alpha helices and four of the larger beta sheets of the KP4 structure that

would form in the four KP4L proteins (Lu & Faris, 2019). Amino acid alignment also showed strong conservation of amino acids of the primary structure within the secondary structure from the KP4L proteins and KP4 (Lu & Faris, 2019). Conversely, it was predicted that the KP4L proteins would be acidic and have low isoelectric points of about four, which is different from the basic KP4 protein with an isoelectric point of nine (Lu & Faris, 2019; Gu et al., 1995).

Plant tests of KP4L from *F. graminearum* provided evidence that KP4L proteins are biologically active (Lu & Faris 2019). KP4L genes were expressed during fungal infection of wheat seedlings and were found to be biologically active when was tested on wheat seedlings (Lu & Faris, 2019). In a seedling assay, it was found that KP4L genes were upregulated during fourteen days of infection from *F. graminearum.* Eighty percent of infected seedlings did not emerge but when the KP4L genes were deleted, there was reduced virulence indicated by the increase in seedling emergence of wheat seedlings (Lu & Faris, 2019). The length of the average root treated with purified KP4L proteins was significantly shorter than the controls by about forty-eight percent (Figure 1.10.; Lu & Faris, 2019). These findings are comparable to those with KP4 and Arabidopsis (Allen, 2008). When wheat seedlings were treated with excess calcium, the root growth length resembled that of the controls (Lu & Faris 2019). Plant roots have numerous calcium channels, including voltage-gated calcium channels, because of calcium's importance as a plant nutrient and, among other aspects, the need for calcium in signaling and root growth (White, 1998). These results indicate that the KP4L genes could be functioning as a virulence factor for the pathogenesis of the fungal disease (Lu & Faris, 2019). KP4L proteins have been shown to have conserved primary and tertiary protein structure, signal sequence present, and have toxicity that is mitigated by excess calcium (Brown, 2011; Lu & Faris, 2019). KP4L proteins are different from KP4. The primary difference being that KP4L proteins are genomically encoded.

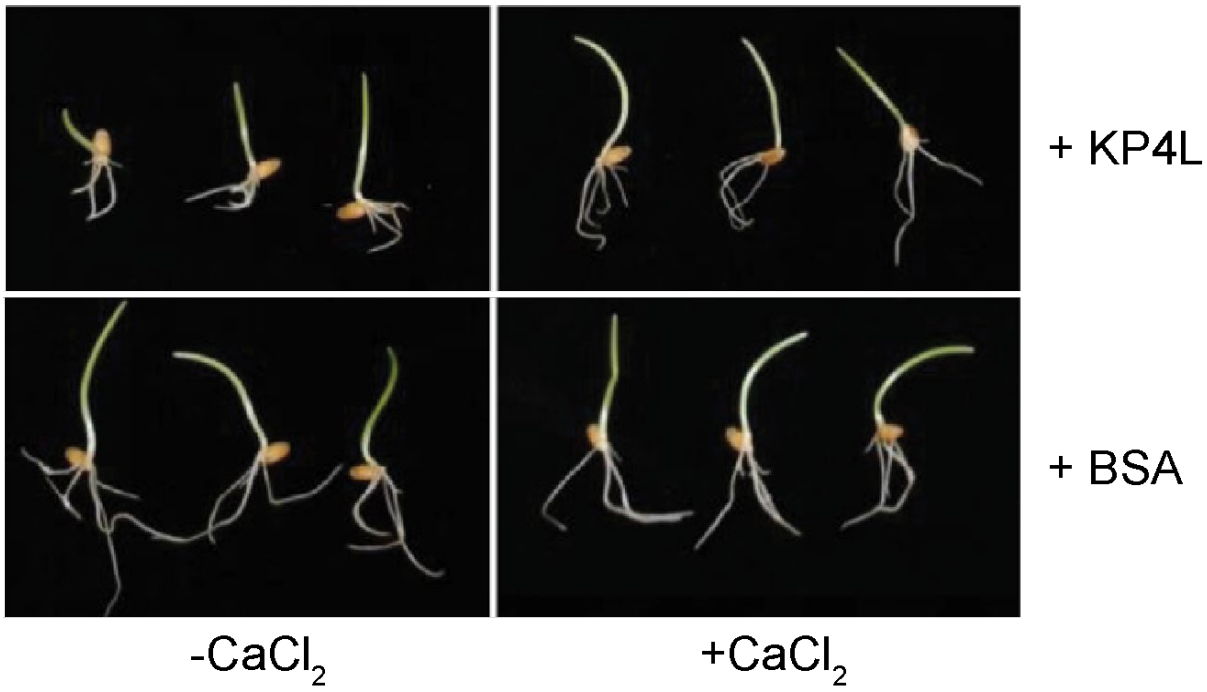

Figure 1.10. Purified KP4L proteins inhibiting wheat seedling root growth. *Purified KP4L protein was applied to the roots of germinating plants (top left), and the addition of excess CaCl2 to the KP4L proteins abrogates the root growth inhibition (top right). BSA control was added to germinating plants (bottom left) and BSA and CaCl2 were added to the germinating plants (Bottom right) (Lu & Faris, 2019).*

Previous work has shown that using antifungal proteins, such as KP4, is a successful approach to reducing crop loss. However, a variety of KP4L proteins will need to be explored because it currently it is not known how these proteins function. Fortunately, hundreds of KP4L genes have been identified. The large diversity of KP4L proteins could be an untapped resource for fighting fungal pathogens. Understanding their functions will be key to the future development of these proteins as novel antifungals.

Currently, there are multiple directions of research aimed at tackling resistant pathogens. Plant defensins, bacteriocins, and fungal killer toxins are all promising areas of research for potential novel antifungals. Furthering our understanding of these will help elucidate the best ways to decrease crop loss due to fungi. There is already promising research in each of these areas to reduce crop loss. This research is aimed at exploring the mechanism of KP4L proteins for the purpose of using them as a potential antifungal treatment.

CHAPTER 2: DETERMINING THE CONSERVED FEATURES OF THE KP4L PROTEINS.

Introduction

The KP4 protein from *Ustilago maydis* has no resemblance to other canonical killer toxins produced by yeasts, but many homologs have been identified and labeled as KP4-Like proteins (KP4L). Previous understanding of KP4L proteins is limited to two publications (Brown, 2011; Lu & Faris, 2019). The first was a review of thirty KP4L proteins, which identified five segments in the proteins and characterized the chromosomal location of the KP4L genes belonging to *Fusarium verticillioides* (Brown, 2011). In this first paper, single-domain KP4L proteins and double-domain KP4L proteins were identified, lending some evidence of gene expansion due to possible positive selection (Brown, 2011). The second publication created a phylogeny of a total of eight KP4L proteins, and further analyzed four KP4L proteins from *Fusarium graminearum* in their structure and their function in virulence (Lu & Faris, 2019).

This study aims to expand knowledge of the single domain KP4L proteins. In recent years, there has been an increase in sequence data available for KP4L proteins. There are now over 500 sequences that result from a search using the protein sequence of KP4 on the Basic Local Alignment Search Tool (Sayers et al., 2022). More information is needed to understand the structure and function KP4L proteins than is currently available. Protein sequence analysis, domain conservation analysis, and a phylogenetic tree were created from the new sequence data that are now available.

Materials and Methods

Identifying KP4L Proteins

A psi-blast search using the full viral KP4 protein sequence was performed to identify potential KP4-Like proteins (Sayers et al., 2022). The search yielded over 500 hits. The search was filtered to have records match with percent identity between 30% and 100%, e-value between 7e-87 (the maximum e-value) and 1e-08, and query coverage between 30% and 100%. The parameter change resulted in 233 sequences. Then the sequences were filtered for accession length with sequences of 200 amino acids or more removed. Longer sequences were removed to prevent double KP4 domain proteins, as identified in previous literature, from being included in the analysis (Brown, 2011). 167 sequences remained after filtering.

Determining the Presence of Signal Sequence

The 167 sequences were uploaded into SignalP 5.0 to identify the presence of signal sequences (Armenteros et al., 2019; https://services.healthtech.dtu.dk/service.php?SignalP-5.0). Sequences lacking signal sequences were removed or when signal sequence prediction probability was below 85%. This left 154 sequences. The sequences removed still had highly homologous sequences in the five segments including the sites that are 100% conserved.

Alignment of KP4L Proteins

A ClustalW alignment was used on the 154 protein sequences in MEGA-X version 11 (Thompson et al., 1994; Tamura et al., 2021). Then small adjustments to the alignment were made by eye for one area of the protein. The adjustment moved cysteines over by one site to match the KP4 protein.

ClustalW Options

Pairwise Alignment	10.00	Gap Opening Penalty
	0.10	Gap Extension Penalty
Multiple Alignment	10.00	Gap Opening Penalty
	0.20	Gap Extension Penalty
Weight	OFF	Negative Matrix
	30	Delay Divergent Cutoff (%)

Five Segment Analysis

The five segments identified in previous literature for KP4L proteins were used to identify segments in the sequence alignment of the 154 proteins. MEGA-X settings were chosen to indicate when an amino acid was 100% conserved across the alignment. The identity of each amino acid in all segments was calculated.

Phylogeny of KP4L Proteins

MEGA-X was used to calculate the best protein model for a Maximum Likelihood phylogenetic tree.

Settings

Tree	Neighbor-joining tree
Statistical Method	Maximum Likelihood
Substitution Type	Amino Acid
Gap Treatment	Use All Sites
Branch Swap Filter	None
Number of Threads	4

The model chosen was WAG + G because it was the model with the lowest Bayesian Informative Criterion score as instructed by the software. MEGA-X was then used to create a phylogeny using the following settings.

Settings

Statistical Method	Maximum Likelihood
Test of Phylogeny	Bootstrap Method
No. of Bootstrap Replicates	1000
Substitution Type	Amino Acid
Method	WAG + G
Rates among Sites	Uniform Rates
Gaps Treatment	Use all sites
ML Heuristic Method	Nearest-Neighbor-Interchange (NNI)
Initial Tree for ML	Make initial tree automatically
Branch Swap Filter	None
Number of Threads	4

Structure Predictions of Eight KP4L Proteins

Secondary structure prediction of the eight KP4L proteins was first done in JPred (Drozdetskiy et al., 2015). The 3D models were then created using AlphaFold2 (Skolnick et al., 2021). AlphaFold2 structure output was then colored according to the secondary structure and then imaged in PyMol (Schrodinger & DeLano, 2020).

Results

Determining the Presence of Signal Sequences in KP4L Proteins

From the original search of the KP4 protein sequence only 167 sequences matched the similarity and length requirements. For further examination the 167 sequences were inputted into SignalP to determine the presence of signal sequence. KP4 has a signal sequence present and is required for proper localization in the cell. Filtering for signal sequence allowed for removal of sequences that did not have proper localization and potentially are not extracellular toxins. From the original list of 167 sequences, only 154 sequences had a signal sequence present. Within the 154 sequences, only three did not have the matching sequence to KP4 of 'LGINC' or 'GIN' present immediately after signal sequence cleavage.

Alignment of KP4L Proteins

The length of KP4L proteins aligned in this study range from 111 residues to 177 residues. The total alignment of all proteins created a length of 262 sites (Figure 2.1.). Unlike previous alignments of KP4 and KP4L proteins, the lysine 42 was aligned with conserved cysteine residues (Identity 92.8%) among the KP4L proteins. Lysine 42 is known to be responsible for 95% of the killing activity from KP4. However, after alignment by eye to the KP4 cysteine (95% identity after alignment by eye), there was nothing aligned to this residue.

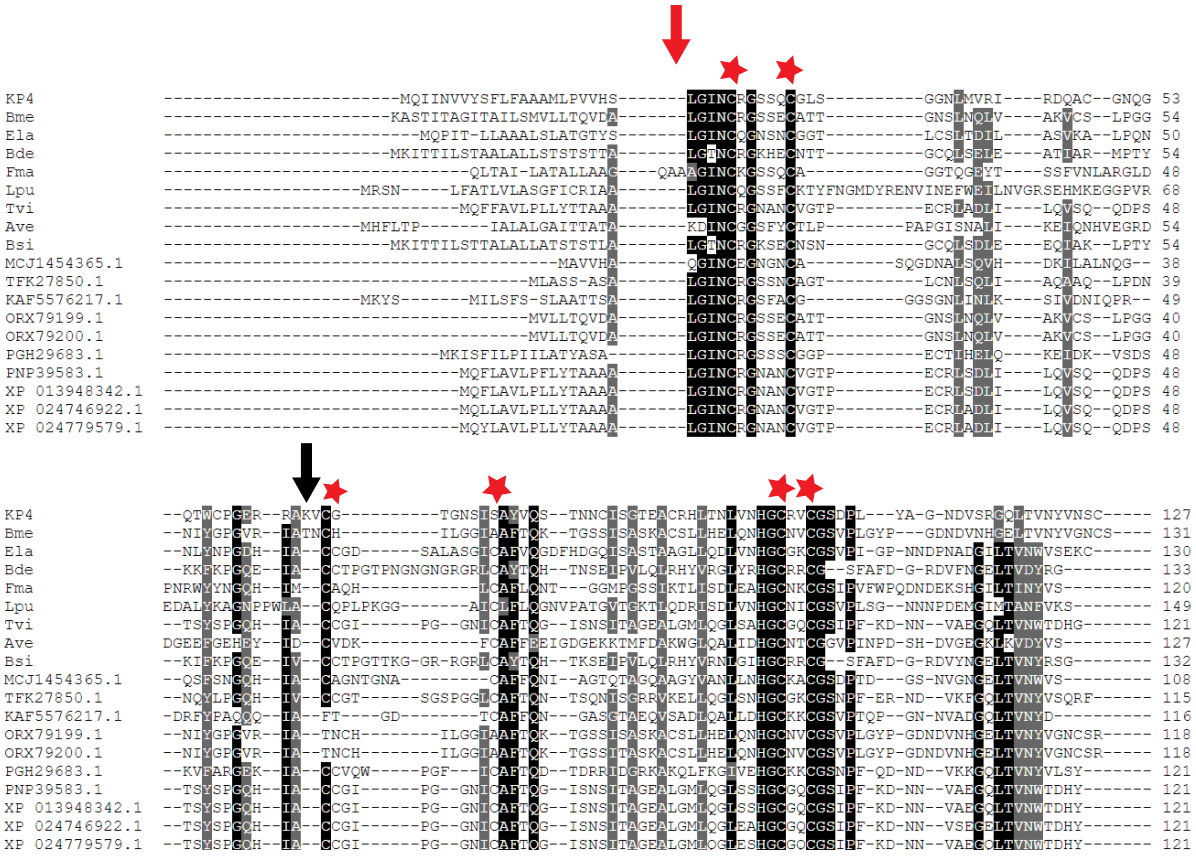

Figure 2.1. Alignment of KP4L protein sequence. *Red stars indicate conserved cysteines. Red arrow indicates signal sequence cleavage site. Black indicates complete conservation and gray indicates greater than 75% conservation. Black arrow indicates the lysine residue responsible for 95% of KP4 activity (K42).*

Five-Segment Analysis

The analysis of the previously defined five segments revealed strong conservation across (Brown, 2011). All amino acids of each segment were present in a minimum of 80% of sequences (Figure 2.2.). Nine amino acids were completely conserved across all sequences (N57, C58, G60, C64, H159, C161, C164, G165, G181). Four of the completely conserved amino acids were cysteines (Figure 2.2.).

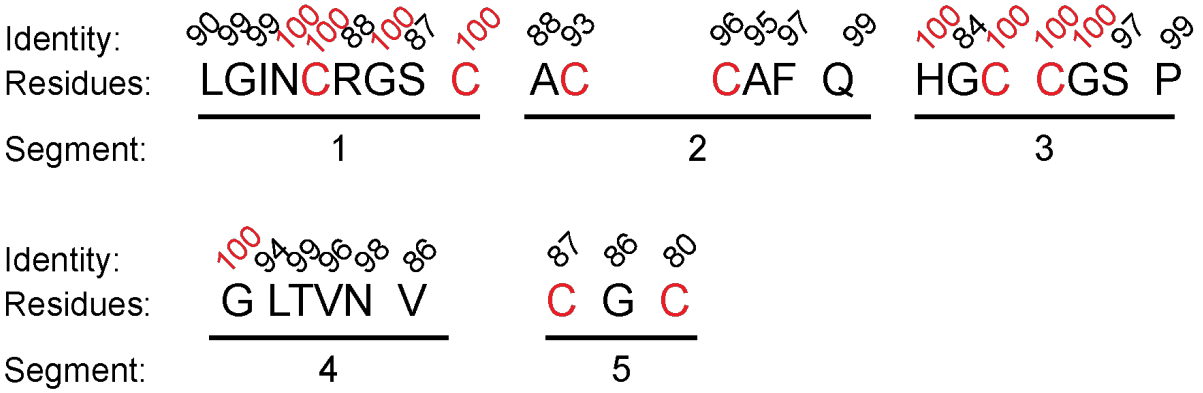

Figure 2.2. KP4L Segment identity in the 154-protein alignment. *Percent identity is above each residue. Residues with 100% identity are labeled in red. Conserved cysteines are also labeled in red. Segments correspond to the segments previously identified in Brown (2011).*

In segment 1, identified previously as GINCxGSxxC, four of the identical residues were present (N57, C58, G60, C64). Analysis of aligned sequences revealed strongly conserved residues surrounding this segment. This segment was expanded to LGINCRGSxxC because of the strong retention of leucine and arginine. All residues were maintained at a minimum of 87% across the 154 KP4L proteins which is well above the 78% threshold established in Brown (2011) (Figure 2.2.). Segment 2, CxxxxxxCAFxQ, was present in all sequences and the lowest identity score is 93% for C115. This segment was expanded to ACxxxxxxxxCAFxxQ because A114 is conserved in 88% of sequences. Of the nineteen changes, only four were not conservative replacements. Segment 3 HGCxxCGSxP was also strongly conserved with four completely conserved amino acids present in this segment (H159, C161, C164, G165). Segment 4, GxLTxxNxV, with V188 having the lowest conservation at 86% sequence identity, was amended to GxLTVxNxV because V185 was present in 96% of the proteins. G181 was completely conserved across all sequences and is the ninth and final residue to be completely conserved. The final segment, segment 5 CxxGxxC was present in only 99 of the 154 KP4L sequences. In 55 sequences when the protein ended before the final segment. C215 was present in 87% of the 99 sequences, C217 was retained in 86% of the sequences, and C219 was retained in 80% of the 99 sequences. It should be noted that segment 5 is only present in KP4L proteins and not in the KP4 protein. Additionally, segment 2 is only found in KP4L proteins. Only the two cysteines are found in the viral KP4 protein. These five

segments can be used to specifically describe KP4L proteins due to KP4 lacking some of the highly retained portions of the sequence.

Phylogeny of KP4L Proteins

The alignment shown in Figure 2.1. was used for the input of for the phylogenetic analysis (Figure 2.3.). The phylogeny indicates evidence for possible horizontal gene transfer. The groupings of *Fusarium* spp. and *Cordyceps* spp. especially support the possibility of horizontal gene transfer. A wide variety of fungal species from the Ascomycota lineage and the Basidiomycota lineage were identified, as well as a moss species from the plantae kingdom (*Ceratodon purpureus*).

The phylogeny groups together all the KP4L proteins that are used for further examination and the viral KP4 protein from *Ustilago maydis* (Figure 2.3). The KP4L *Basidiobolus meristosporus* protein is grouped as the sister taxa to the viral KP4 protein. Clade One has *Fusarium* sps, *Basidiobolus meristosporus*, *Hypoxylon* sps, *Coprinopsis marcescibillus,* and *Trichoderma* sps groups. Notably, the groups of *Basidiobolus meristosporus* and *Coprinopsis marcescibillus* are made up of multiple KP4L proteins from one species. The phylogeny does not group by species which indicates horizontal gene transfer.

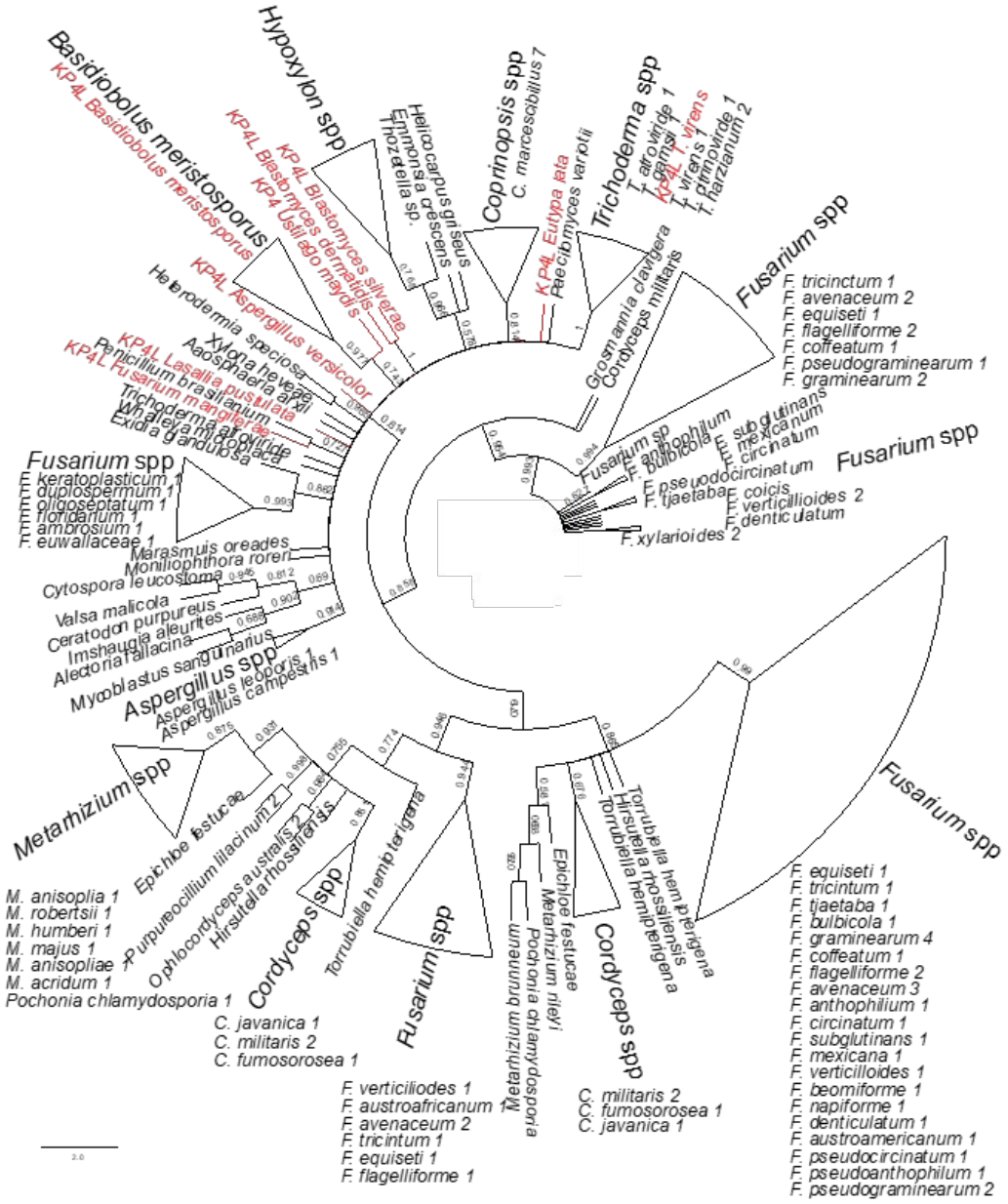

Figure 2.3. Phylogeny of KP4L proteins. *The evolutionary history was inferred by using the Maximum Likelihood method and Whelan And Goldman model. The bootstrap consensus unrooted tree inferred from 1000 replicates is taken to represent the evolutionary history of the taxa analyzed. Branches corresponding to partitions reproduced in less than 50% bootstrap replicates are collapsed. The percentage of replicate trees in which the associated taxa clustered together in the bootstrap test (1000 replicates) are shown next to the branches. Initial tree(s) for the heuristic search were obtained automatically by applying Neighbor-Join and BioNJ algorithms to a matrix of pairwise distances estimated using the JTT model, and then selecting the topology with superior log likelihood value. This analysis involved 154 amino acid sequences. There were a total of 262 positions in the final dataset. Evolutionary analyses were conducted in MEGA X and formatting was performed in FigTree. The numbers next to species names indicate the number of times that species was found in that location. The red highlight indicated the KP4 protein from U. maydis and the eight KP4L proteins used for further study.*

Structure Predictions of Eight KP4L Proteins

Eight different KP4L proteins with the most amino acid similarity to KP4 were chosen for further study (Table 2.1.). These eight proteins come from *Basidiobolus meristosporus, Eutypa lata, Trichoderma virens, Fusarium mangiferae, Blastomyces silverae, Lasallia pustulata, Blastomyces dermatitides,* and *Aspergillus versicolor.* These fungal species represent a diversity of organisms that are involved in crop spoilage and human disease.

Table 2.1. Amino Acid Similarity to KP4 Protein. The similarity was determined by Sequence Manipulation Suite Identity and Similarity (Stothard, 2000).

Organism	**Percent Similarity to KP4**	**Percent Identity to KP4**
Basidiobolus meristosporus	49.24	39.39
Eutypa lata	45.04	32.33
Trichoderma virens	43.09	32.56
Fusarium mangiferae	41.48	24.29
Blastomyces silverae	38.52	30.60
Lasallia pustulata	36.08	22.15
Blastomyces dermatitidis	35.77	27.94
Aspergillus versicolor	31.85	21.74

The protein sequences were aligned via ClustalW using the default parameters (Thompson et al., 1994). The results show the retention of cysteines in all sequences and of conservation of sequences within the five segments identified previously (Figure 2.4.; Brown, 2011).

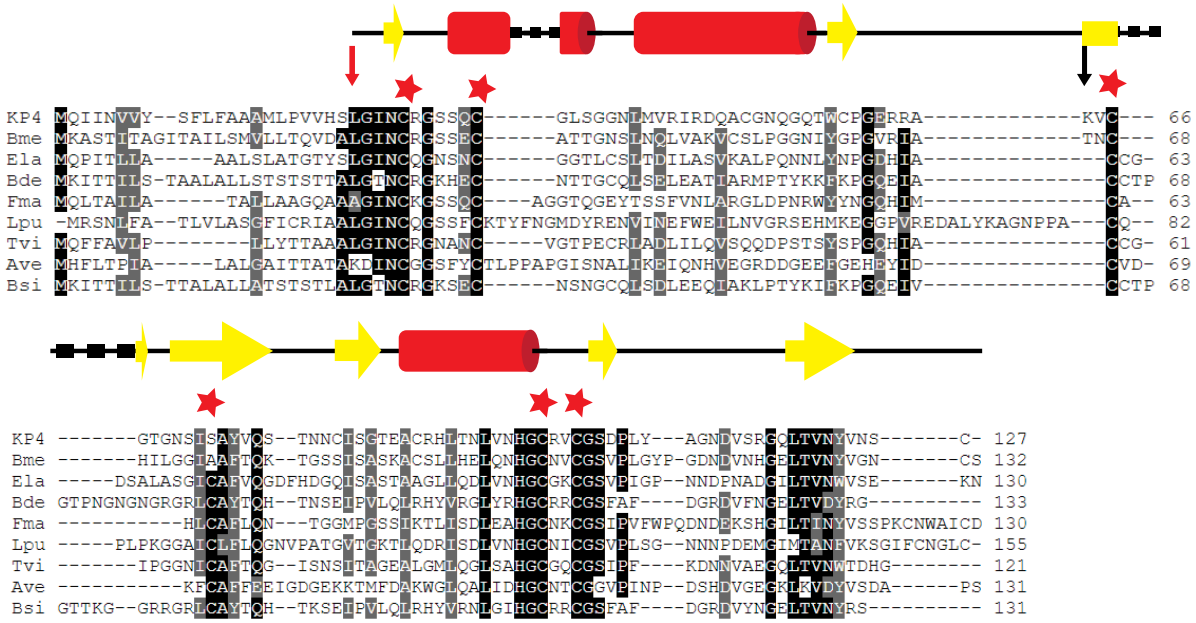

Figure 2.4. Sequence alignment of the eight studied KP4L proteins and KP4 from U. maydis. *Alignment created using MEGA-X ClustalW. Image generated using The Sequence Manipulation Suite using eighty-percent similarity settings. The red arrow indicated the signal sequence cleavage site for all proteins. Black arrow indicates the lysine 42 residue from KP4 that is responsible for 95% of killing activity. Red stars indicate conserved cysteines. Yellow arrows indicate beta sheets and red rectangles indicate alpha helices. Dotted lines reflect spacing from the alignment. Secondary structure reflects protein structure from KP4. Three letter abbreviation used for all KP4L proteins: Bme = Basdiobolus meristosporus, Ela = Eutypa lata, Tvi = Trichoderma virens, Fma = Fusarium magniferae, Bsi = Blastomyces silverae, Lpu = Lasallia pustulata, Bde = Blastomyces dermatitidis, Ave = Aspergillus versicolor.*

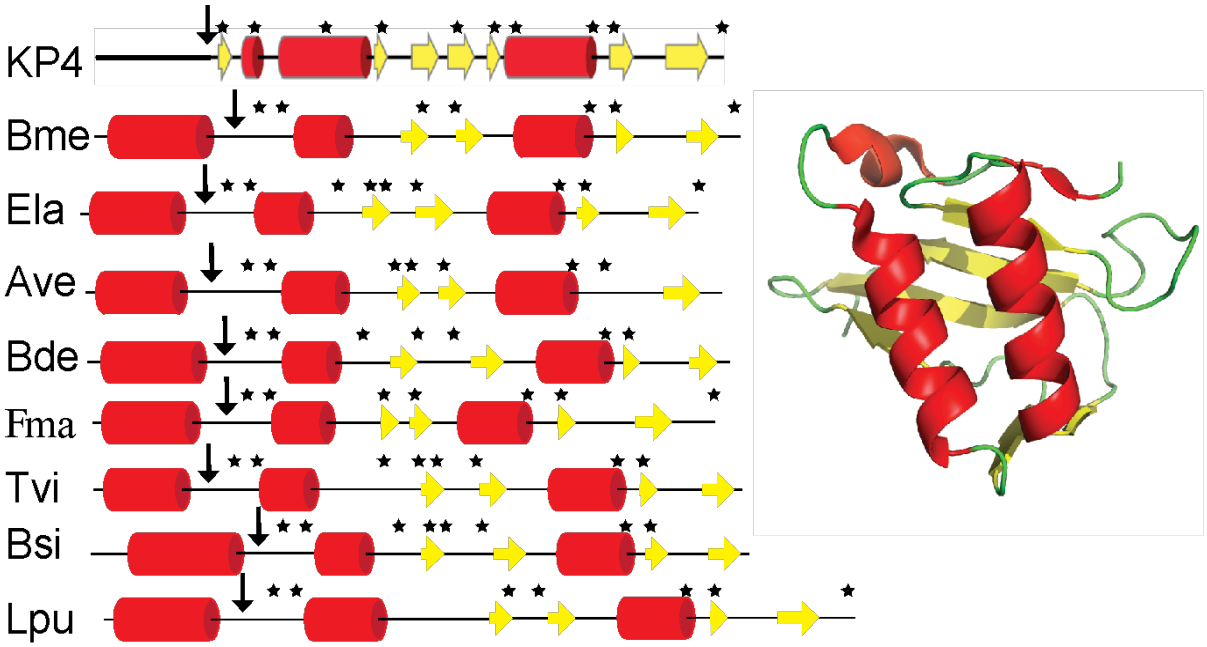

Figure 2.5 Predicted secondary structures for the eight KP4L proteins. *The eight KP4L proteins are compared to KP4 from U. maydis. The structure predictions were made using Phyre2. The yellow arrows indicate beta sheets, and the red cylinders are alpha helices. The black arrows indicate signal sequence cleavage points. The black stars are cysteines present in the sequence. Three letter abbreviation used for all KP4L proteins: Bme = Basdiobolus meristosporus, Ela = Eutypa lata, Tvi = Trichoderma virens, Fma = Fusarium magniferae, Bsi = Blastomyces silverae, Lpu = Lasallia pustulata, Bde = Blastomyces dermatitidis, Ave = Aspergillus versicolor.*

Secondary structure prediction of the eight KP4L proteins also showed two alpha helices within the protein-coding sequence and one within the signal sequence portion (Figure 2.5; Drozdetskiy et al., 2015). Four of the seven beta sheets were also predicted for the eight KP4L proteins. AlphaFold2 predictions also showed strong conservation of three-dimensional structure among the KP4L proteins and the KP4 protein. The AlphaFold2 prediction showed three alpha helices for all KP4L proteins matching the three alpha helices in the viral KP4 protein (Figure 2.6). *Fusarium magniferae* was predicted to have four alpha helices. All AlphaFold2 predications had a confidence greater than 90%.

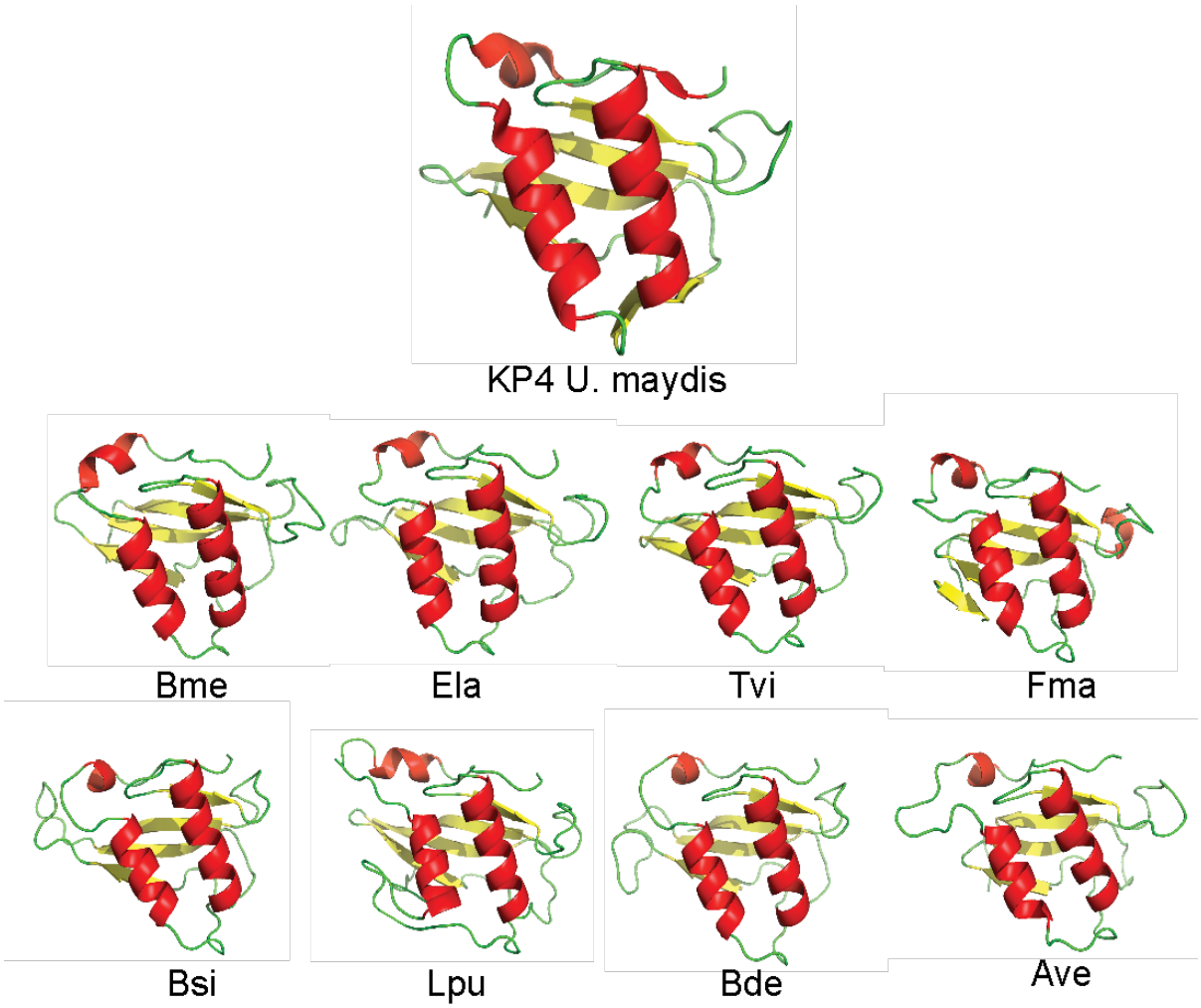

Figure 2.6. AlphaFold2 3D structure predictions of the eight KP4L proteins. *The structure predictions show strong retention of the three alpha helices of KP4 and four of the beta sheets. All predictions had greater than 90% confidence. The yellow arrows are beta sheets, the alpha helices are colored red, and the green is nonstructured portion of the protein. The three-letter abbreviation used for all KP4L proteins are: Bme = Basdiobolus meristosporus, Ela = Eutypa lata, Tvi = Trichoderma virens, Fma = Fusarium. magniferae, Bsi = Blastomyces silverae, Lpu = Lasallia pustulata, Bde = Blastomyces dermatitidis, Ave = Aspergillus versicolor.*

Discussion

The alignment of the KP4 and KP4L proteins had strong conservation of eight cysteines ranging from 80% to 100% (Figure 2.1.). Lysine 42 is a critical residue for KP4 and is responsible for 95% of fungistatic activity. In the alignment of KP4L proteins, nothing was aligned to this residue. Lysine only appears once in the KP4 protein but is plentiful in the KP4L proteins. *B. meristosporus*, the most closely related protein to KP4, has three lysines present in its protein sequence. *Trichoderma gamsii* has ten lysines in its protein sequence. It is possible that another lysine or completely different residue is present in the active site. Another possibility is that the active site is changed in the KP4L proteins.

A review of the five segments posed by Brown in 2011 was conducted on the 154 data set of KP4L proteins (Figure 2.2.). From this analysis, the first, second, and fourth segments could be expanded to LGINCRGSxxC, ACxxxxCAFxxQ, and GxLTVNxxV, respectively. The second segment would expand to include the first alanine because it is found in 88% of the sequences. The fourth segment would include the first valine (96% identity). The fifth segment (CxxGxxC) is not found in all sequences, including the viral KP4 protein. Only about 64% of the sequences were long enough to have the fifth segment. Primarily, but not exclusively, *Fusarium* sps and *Cordyceps* sps have the fifth segment. This segment may have been an expansion exclusive to the KP4L proteins. Overall, the KP4L proteins have low levels of identity to the KP4 protein but the strong retention of the primary structure in the five segments indicates that functionality could also be conserved in the KP4L proteins.

The phylogeny included ascomycota, basidiomycota, and moss sequences (Figure 2.3.). *Fusarium* spp had five subclades found throughout the tree. *Cordyceps* spp., *Trichoderma* spp., *Torrubiella* spp is also found throughout the phylogenetic tree. Species within the same genus found throughout the phylogenetic tree indicates horizontal gene transfer occurring several times. If vertical transmission was the main form of transmission the spreading of KP4L genes, then species found in the same genus would group together strongly. Horizontal transmission could explain the wide variety of the fungal species that have the KP4L protein present as well.

To further investigate the similarity between KP4 and the KP4L homologs a subset of the most similar proteins to KP4 was created. The eight KP4L proteins chosen for further study were grouped within the clade that held the KP4 protein. Structure prediction had strong

secondary structure conserved in all eight KP4L proteins compared to KP4. The AlphaFold2 also had strong predicted conservation in the three-dimensional structure of the KP4L proteins. The three-dimensional folding of the KP4L proteins also strongly resembles the KP4 structure. The strong conservation of structure is sign of conservation of function.

In this study, the KP4L protein phylogeny was expanded using 154 protein sequences. Primary structure conservation was expanded from previous literature (Brown, 2011). Secondary and tertiary structure was identified to be conserved across eight of the KP4L proteins most similar to KP4. The strongly conserved structure of the KP4L proteins to the KP4 protein is a strong indicator of the conserved toxin functionality. If function is conserved, then KP4L proteins could be used for possible novel antifungals. Further research will be required to elucidate the function of the KP4L proteins.

CHAPTER 3: CHARACTERIZE THE CYTOTOXIC MECHANISM OF KP4L PROTEINS IN *SACCHAROMYCES CEREVISIAE*.

Introduction

The protein KP4 from *Ustilago maydis* has been shown as a potential antifungal agent. Patch clamp data shows that the small basic protein blocks calcium channels (Gage et al., 2001; Gage et al., 2002; Gu et al., 1995, Allen et al., 2013). Specifically, it has been shown to block L-Gated Calcium channels in mammalian cells (Gage et al., 2002). Transgenic plant strains have shown a significant increase in resistance to various fungal pathogens in seedling, greenhouse, and field trials (Clausen et al., 2001; Allen et al., 2011; Deb et al., 2018). However, KP4 is not active against all fungal pathogens (Deb et al., 2018). A multitude of homologs of KP4 (KP4L) have been identified in other fungi, plants, and moss. The previous chapter of this thesis explored the structure of the KP4L proteins compared to KP4. This chapter aims to further the understanding of the functionality of the KP4L proteins for the potential use of novel antifungals.

Eight proteins most structurally similar to KP4 were chosen for further study. The KP4L proteins include proteins from *Basidiobolus meristosporus, Eutypa lata, Trichoderma virens, Fusarium mangiferae, Blastomyces silverae, Lasallia pustulata, Blastomyces dermatitides,* and *Aspergillus versicolor.* These proteins will be studied within in the model organism of *Saccharomyces cerevisiae.* These proteins were selected because they were shown in the previous chapter to have primary, secondary, and tertiary conservation to KP4. The structural similarity to KP4 implies that they also are ion channel inhibitors. However, very little is known mechanistically about KP4L proteins. It is unconfirmed how these proteins benefit the species they are found in. Some research data has shown that they may function in virulence, they are secreted, and they target neighboring cells for toxicity (Lu & Faris, 2019). The mechanistic hypothesis is that the KP4L proteins are secreted from the cells and target the cell surface for cytotoxicity.

Materials and Methods

Growth Analysis of KP4L Proteins

Generating KP4L Plasmids

The KP4L genes were inserted into a high copy number galactose inducible yeast expression vector (pAG426-GAL-ccdB) using Gateway cloning from oligonucleotides ordered from Twist Biosciences (Figure 3.1.; Reece-Hoyes & Walhout, 2018). Gateway cloning was done per the manufacturer's instructions in a quarter reaction size. Restriction digest with gel electrophoresis and sequencing were used to confirm correct sequence and orientation of the KP4L gene insert into the destination vector.

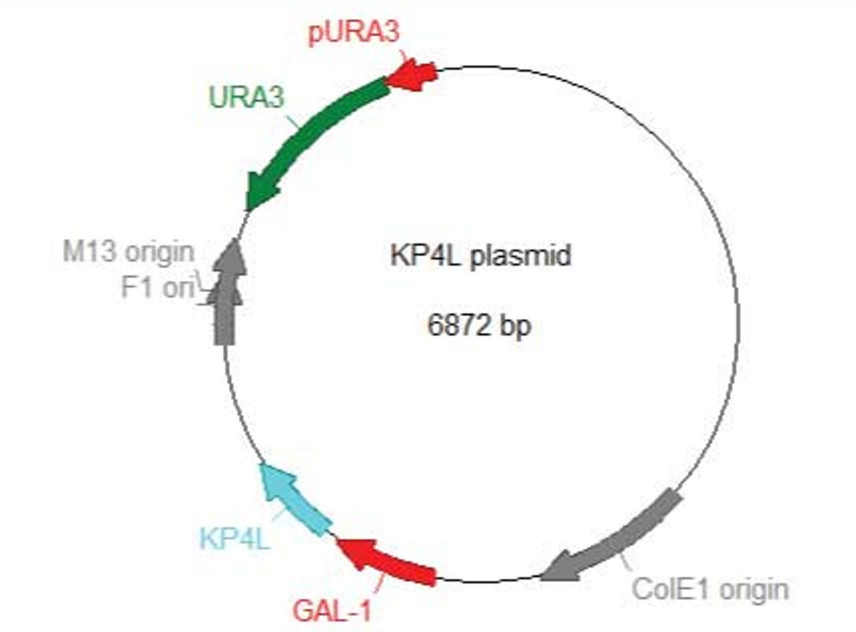

Figure 3.1. Diagram of the two-micron-like pAG426-GAL-ccdB plasmid system used for KP4L proteins. *The selectable marker was for the ura3 gene, which encodes for uracil production. The promoter system was a galactose inducible promoter for the KP4L promoter. pURA3 is the promoter for the uracil selective marker and URA3 is the uracil selective marker gene. ColE1 is replication origins for the plasmid. GAL1 is the inducible promoter. KP4L is the KP4L genes used in the study. Image created in Ape.*

Yeast Transformation

The eight plasmids encoding the KP4L gene from eight different fungi (*Basidiobolus meristosporus, Eutypa lata, Trichoderma virens, Fusarium mangiferae, Blastomyces silverae, Lasallia pustulata, Blastomyces dermatitides,* and *Aspergillus versicolor*) were transformed into the lab strain of *S. cerevisiae* BY4741. A 2 mL YPD overnight culture of BY4741 was created the night before. The next morning OD_{600} was recorded to confirm the yeast were in stationary phase. Then a 1:50 dilution in YPD of the overnight culture was created. The 50 mL culture was grown at 30°C for six hours until it had an OD_{600} between 1.0 and 0.5 for the yeast to be in exponential growth. There are enough cells in the 50 mL culture for three transformation reactions. The cells were then spun for 30 seconds at 1,900 x *g* and the supernatant was discarded. The pellet was suspended in a one-to-one ratio of sterile water and incubated at room temperature for ten minutes. The culture was then spun again for the same duration and the supernatant was removed. The pellet was then suspended in 5 mL of 100 mM lithium acetate solution per reaction (15 mL total). The suspension was then incubated for ten minutes at 30°C. After incubation, the suspension was spun for 1,900 x *g* for 30 seconds and the supernatant was removed. The cells were then suspended in the residual lithium acetate, and equal amounts were transferred to sterile 1.5 mL microcentrifuge tube tubes. The suspensions were then spun for thirty seconds for 4,000 x *g*. Then the pellets were overlaid with the following:

240 µL PEG_{4000} (50% w/v)

36 µL Lithium acetate [1M]

50 µL Carrier DNA (ssDNA, 2 mg/mL)

50 µL of plasmid (500 ng to 1000 ng)

The overlay had to be done in order and gently. Then the cells were suspended in the transformation overlay by stirring the pipette tip gently. Controls for the experiment were water (negative control) and GFP plasmid pPAR100 (positive control). The suspension was then incubated for thirty minutes at 30°C and then twenty minutes at 42°C. It is important to note that strains containing gene deletions were incubated at 36°C for twenty minutes instead. Samples were then spun for 30 seconds at 4,000 x *g*, and then the supernatant was removed via pipetting. Cells were then gently suspended in 100 µL of sterile ddH_20, plated on selective

plates (complete media with dextrose lacking uracil), and grown for 48 hours (room temperature for deletion collection strains).

Serial Dilution Assay

The eight strains of transformed BY4741 with the KP4L plasmids were used for serial dilution assays. Two mL dextrose selective media overnight cultures were created of the BY4741 KP4L strains. The strains were then washed in water twice to the original culture volume the next morning. The cultures were then standardized to an OD_{600} of 1.5 in a 1500 µL volume of sterile ddiwater in sterile 1.5 mL microcentrifuge tube tubes. Sterile water was added via a multichannel pipette in a sterile deep well plate. The last five columns were filled to a volume of 1350 µL. The next step was to pipette 1500 µL of the 1.5 mL microcentrifuge tube tubes of 1.5 OD_{600} to the first column of the deep well plate. Then the plate was serially diluted via multichannel pipetting of 150 µL to the following five columns. This diluted out the original culture to 10^{-6} of the original culture. The cultures were then pinned from the well plate to dextrose and galactose solid plates medium, using a long-armed pinner. In between each plate media type, the pinner was flamed using ethanol.

Doubling Time Assay

20 mL cultures were inoculated with a colony of the corresponding KP4L plasmid strain of BY4741 and standardized to 0.01 OD_{600}. Cultures grown overnight in Complete Media lacking uracil with raffinose media ("CM-u raffinose") and time points of OD_{600} were recorded starting the following morning. Cultures were induced with either 2% galactose (to induce KP4L expression) or 2% dextrose (as a control). Four time points were recorded before and after the induction of the media. Doubling time was calculated using an exponential growth curve in excel.

Cell Count and Budding Index

20 mL raffinose cultures were inoculated with the strains BY4741 transformed with KP4L *B. meristosporus* and a GFP plasmid and incubated overnight. At an OD_{600} of 1.5, 5 mL of each culture were spun down and suspended into 500 µL of sterile ddH_20. A 1:4 dilution of the 500 µL was used for a cell count.

A hemocytometer slide was used to calculate the total cell amount. 10 µL of the 1:4 dilution of each culture was used with the hemocytometer. Three counts of five boxes on the hemocytometer were averaged for the total cell count for the culture. A counter was used to

count the cells. A budding index was also done for each round of counting. Identification was completed regarding how many cells per box of the count are large/medium bud, small bud, or no bud to distinguish. The bud count was averaged per round to find the differences in budding between the cultures. After the cell count, the cultures were induced with 2% galactose for two hours. After two hours, another cell count and budding analysis were performed to compare pre- and post-induction. After eight hours, a 1:1,000,000 dilution was plated on complete media lacking uracil with dextrose ("CM-ura dextrose") plates.

Identifying Genes Important for Cytotoxicity

Yeast Genome Deletion Collection of 4000+ Single Gene Knock-Out Transformation

The Yeast Genome Deletion Collection *S. cerevisiae* strains were transformed with a plasmid encoding the KP4L gene from *B. meristosporus* and plated on dextrose and galactose (Figure 3.2.; Giaever et al., 2002). Jordan Hawley and Mark Lee developed the transformation protocol.

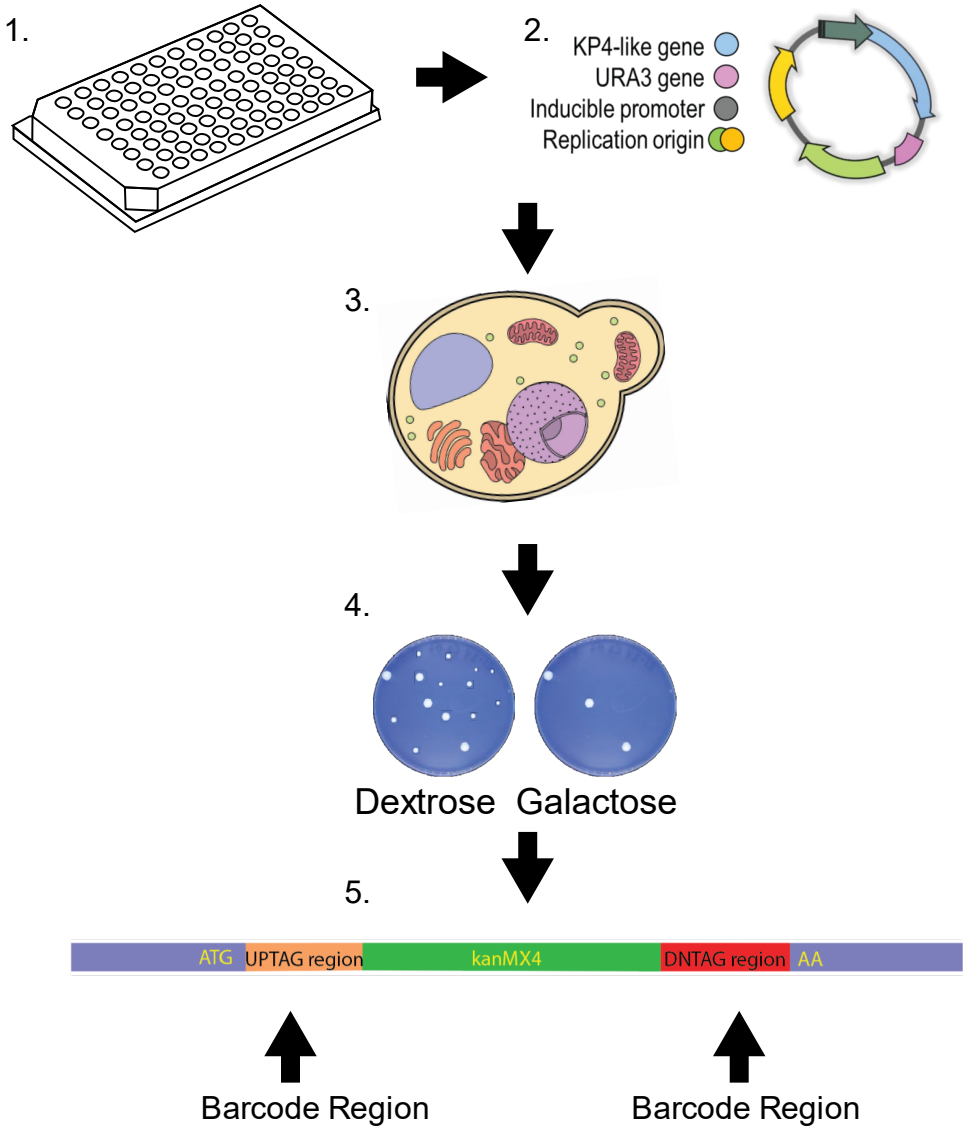

Figure 3.2. Methods diagram of the transformation of the Yeast Genome Deletion Collection with KP4L B. meristosporus. *The diagram shows the transformation of KP4L B. meristosporus into the deletion collection and then identification of deletion strains that have a growth revival on galactose through sequencing the deletion collection barcodes.*

The deletion collection was plated onto G418 YPD plates. Before the transformation, the deletion collection plates were imaged in the Phenobooth to determine how equally represented each strain would be. The plates were then scraped using 2 to 3 mL of YPD and gently homogenized with a cell spreader. Once plates were scraped clean, the liquid was placed into a 50 mL conical tube and brought to a volume of 25 mL. The suspension was diluted to an OD_{600} of 1.0. The media was then partitioned into three 1.5 mL tubes with an OD_{600} of 1.0,

0.5, and 2.0 respectively. The tubes were then spun for five minutes at 8,000 x *g* and the supernatant was removed. Each tube was then suspended in one mL of sterile water to wash and then spun again at 8,000 x *g* for five minutes. The pellet was then suspended in one mL of 100 mM of lithium acetate and mixed gently by inversion. The cell suspension was then incubated at 30°C for ten minutes in a water bath. Then it was spun for 1 minute at 8,000 *x g*. The supernatant was removed, and then the cell pellet was overlaid with the following:

240 µL	PEG_{4000} (50% w/v)
36 µL	1 M Lithium Acetate
50 µL	Carrier DNA (2.0 mg/mL)
25 µL	Plasmid
25 µL	ddH_20

The cells were then suspended in the transformation mixture using the pipette tip to stir gently. The mixture was then incubated at 30°C for 30 minutes. Then at 36°C for 20 minutes. The mixtures were then spun for 1 minute at 8000 *x g*. The supernatant was then removed, and the cells were resuspended in 100 µL of sterile water.

To plate the transformation mixture, a 1:10 dilution series was created out to 10^{-4}. Then the dilution series was plated onto CM -ura dextrose plates as a control. The remaining amount of the transformation mixture was plated onto complete media lacking uracil with galactose ("CM-ura galactose") plates.

Yeast Genome Deletion Collection Identification

Jordan Hawley and Mark Lee developed the transformation protocol. Galactose survivors were picked, and the identifying tag was DNA was isolated from galactose survivors via the Isolation of Yeast Chromosomal DNA protocol. For each survivor colony, a 2 mL overnight culture was grown in selective media. The following day, the overnight was spun for 5 minutes at 1200 x *g*. The supernatant was then removed, and the cells were suspended in 0.5 mL of sterile ddH_2O. The suspended cells were then transferred to a microcentrifuge tube and spun ay 1,200 x *g* for 5 seconds at room temperature. The supernatant was then removed. The cell pellet was then disrupted by vortexing briefly. The cells were then suspended in a breaking buffer. Then 0.3g of glass beads were added, and 200 µL of phenol/chloroform/isoamyl alcohol was added and vortexed for three minutes. Then 200 µL of TE buffer was added and vortexed briefly. The tubes were then spun for 5 mins at 10,000 *x g* at room temperature. The aqueous

layer was then transferred to a new tube. 1 mL of 100% ethanol was then added and mixed by inversion. The tubes were then spun for 3 minutes at 20,000 *x g*. The supernatant was removed and the pellet was resuspended in 400 µL TE buffer. Then 3 µL of 10 mg/mL of DNase-free RNase A was added to the tube. Then the suspension was mixed and incubated for 5 minutes at 37°C. After, 10 µL of 4 M ammonium acetate and 1 mL of 100% ethanol were added to the tube. This mixture was mixed by inversion. The tube was then spun for 3 minutes at high speed. The supernatant was then discarded, and the pellet was dried. The DNA was then suspended in 100 µL TE buffer. A 1:10 dilution in sterile H_2O was used for PCR.

Breaking Buffer

2% (w/v) Triton X-100

1% (w/v) SDS

100mM NaCl

10 mM Tris-HCl, pH 8.0

1 mM EDTA, pH 8.0

TE Buffer

0.5 mL 1 M Tris-HCl, pH 8.0

100 µL 0.5 M EDTA, pH 8.0

Diluted to 45 mL with H2O and pH to 8.0

Topped off to 50 mL and filter sterilized.

The extracted DNA was then used to identify the barcodes for the deletion collection. Barcodes were used to determine the specific strain of the deletion collection that conferred resistance.

Table 3.1. Primers used to identify the barcodes of the deletion collection.

Primer	**Target**	**Sequence**
pRUI158	Up-tag Region	GATGTCCACGAGGTCTCT
KANB	Up-tag Region	CTGCAGCGAGGAGCCGTAAT
pRUI160	Down-tag Region	CGGTGTCGGTCTCGTAG
KANC	Down-tag Region	TGATTTTGATGACGAGCGTAAT

The PCR product was then confirmed via gel electrophoresis and then sent for sanger sequencing. The PCR settings were as follows:

Table 3.2. of PCR settings for the amplification of the deletion collection barcode.

Barcode of Deletion Collection PCR Settings	
Denature	30 seconds at 94°C Extend
Anneal	30 seconds at 65°C
Extend	1 minute at 72°C
Repeat Cycle	30 cycles
	72°C 10 minutes
	4°C infinite hold

Confirmation of Deletion Strains with Growth Revival

Of the survivor strains identified from the deletion collection screen a subset was chosen for further analysis. The survivor strains are strains that can grow in the presence of KP4L Bme and were used for identifying the location of the KP4L protein. The subset of the survivor strains was chosen based on categories from the GO analysis and reconfirmed for survival on galactose. In total fourteen strains were chosen (YLR267W, YLR326W, YLR309C, YBR188C, YLR307W, YBR078W, YER027C, YMR175W-A, YGR014W, YPL277C, YGL140C, YER120W, YEL022W, YGL163C), one from each category, and then all strains relating to the cell wall or membrane. Deletion strains were streaked out from stock plates onto G418 selective media.

Table 3.3. Deletion Collection Strains Picked for Reconfirmation.

ORF name	Strain	GENE	Function
YLR267W	BY4741	*BOP2*	Unknown
YLR326W	BY4741		Cell Periphery Protein
YLR309C	BY4741	*IMH1*	Vesicular Transport
YBR188C	BY4741	*NTC20*	Splicing
YLR307W	BY4741	*CDA1*	Cell Wall
YBR078W	BY4741	*ECM33*	Cell Wall and Plasma Membrane
YER027C	BY4741	*GAL83*	Galactose Metabolism
YMR175W-A	BY4741		Phospholipid Binding
YGR014W	BY4741	*MSB2*	Signaling
YPL277C	BY4741		Plasma Membrane
YGL140C	BY4741		Plasma Membrane
YER120W	BY4741	*SCS2*	Plasma Membrane
YEL022W	BY4741	*GEA2*	Vesicular Transport
YGL163C	BY4741	*RAD54*	Stress

Then strains were confirmed via PCR and gel electrophoresis. This was done to compare the length of the knock-out gene kanMX to the wild-type gene of interest. The kanMX gene is approximately 1700 bp. For all chosen genes (except *ECM33*/YBR078W) there was a difference of at least 1kb in size between the wildtype gene and kanMX knock-out. Strains were identified by band presence at the size of 1700 bp. The strain YBR078W was determined via restriction digest.

Table 3.4. Primers used for confirmation of deletion collection strains.

Primer	Target	Sequence
MS001	YBR078 (ECM33) 5’	TTTCAACAAGTCCCTTTGAGC
MS002	YBR078 (ECM33) 3’	AAAATTCAGTGATGAACCAACC
MS003	YLR309C (IMH1) 5’	CAGAAACGTCAAATAGTAAGCAACAGG
MS004	YLR309C (IMH1) 3’	ATCAATCAACAGTTTCTCATTGTGTCG

Continuation of Table 3.4.		
MS005	YBR188C (NTC20) 5’	GGCTAGCCGTTCCTTCAAAGC
MS006	YBR188C (NTC20) 3’	TTGCTAAGTTCATCGCTTTTCTTTCC
MS007	YER027C (GAL83) 5’	AAAACGTGGCAAAGAAAACAATACC
MS008	YER027C (GAL83) 3’	CATGGAGAGCTATAATGGAAAAATCG
MS009	YGR014W (MSB2) 5’	ATTCTGTTCATCTCTAGCTGGCTTCC
MS010	YGR014W (MSB2) 3’	CGCACTTTCTTCTCGTGTCAGG
MS011	YLR207W (CDA1) 5’	AGCAGCTTCAACATTTCTCTTTTCC
MS012	YLR207W (CDA1) 3’	TGACGCTTTTCCTTATACATTCAAGC
MS016	YEL022W (GEA2) 5’	GGCGTTTAAATAATAAACACACCAACC
MS017	YEL022W (GEA2) 3’	TTTGATGGTCAAAACTTATCCTTCACC
MS018	YER120W (SCS2) 5’	GCAAAGTGCATTGTTTATTGTGTGG
MS019	YER120W (SCS2) 3’	GGTTTCCCTAGTGTAGTAGGCGCTA
MS020	YGL140C 5’	TTCAAGCGAGAAAATCTTCCTTATCC
MS021	YGL140C 3’	GTTCGCCACCATTCTAGTTATGACC
MS022	YGL163C (RAD54) 5’	ACGCTCAGAACTTAGCTCTATTTCAAGG
MS023	YGL163C (RAD54) 3’	CTGACAGCGTGAGATTTTCTTGC
MS024	YLR267W (BOP2) 5’	TTGTGCAATATATAGGCTGTGATTTCG
MS025	YLR267W (BOP2) 3’	CCTCAACGCTTTTTGTTTTCATTTT
MS026	YLR326W 5’	GCTAGAGAGCATTGGAAGAATTTGC
MS027	YLR326W 3’	TGCCCATATTTGTTGATAAGAATGTAGC
MS028	YMR175W 5’	AAAGATGAACGCTGGCAGAGG
MS029	YMR175W 3’	CGCCCTTGAGCTTAAAACAACC
MS030	YPL277C 5’	TTAGCTCTCGAAGAATCCATTGACC
MS031	YPL277C 3’	CTCTCACAACGGTAATTTAGTTCAATCC

Table 3.5. PCR settings for deletion collection strain confirmation.

Deletion Collection Confirmation PCR Settings	
Denature	30 seconds at 94°C Extend
Anneal	30 seconds at 65°C
Extend	1 minute at 72°C
Repeat Cycle	30 cycles
	72°C 10 minutes
	4°C infinite hold

Serial Dilution Assay of Deletion Collection

The confirmed deletion collection strains were transformed with the KP4L gene *B. meristosporus* with the C-tag. A spot assay was performed as previously described to identify resistance to the cytotoxicity of the KP4L *B. meristosporus* protein expression.

Determining the Cellular Location of the KP4L Proteins

Tagging KP4L genes

A C-tag epitope tag (EPEA) was added to the C terminus of the KP4L *B. meristosporus* protein and the N-truncation mutant of KP4L *B. meristosporus.* After primer addition using the primers PRUI260 (C-tag) and PRUI1925, TOPO TA was used to clone the PCR product into the pCR8 backbone. TA ends were added after the PCR product was purified using a Monarch PCR & DNA purification kit with the following reaction:

19 µL of PCR product

1 µL of dNTPS

5 µL 10X Taq Buffer

1 µL of Taq polymerase

24 µL Hyclone H_20

This reaction was then incubated for twenty minutes at 72°C. The TA product was then cloned into the pCR8 backbone using the following reaction:

1 µL of PCR-TA end product

0.25 µL of Salt Solution

0.25 µL of pCR8 vector backbone

The reaction was then incubated at room temperature for two hours.

E. coli transformation

The pCR8 with the tagged KP4L product was then immediately transformed into *E. coli* using NEB chemically competent one-shot cells. The cells were allowed to thaw on ice for ten minutes. Then 25 µL of the *E. coli* cells were added to the TA cloning 1.5 mL microcentrifuge tube. The tube was then incubated on ice for thirty minutes. Then the reaction was heat shocked at 42°C for thirty seconds. The reaction was then placed on ice for two minutes. 250 µL of prewarmed SOC media was added to the tube and then was incubated at 37°C shaking at 250 rpm for one hour. Then cells were spread on LB-spectinomycin plates and incubated on the plates overnight. The following day eight *E. coli* colonies were streaked out and incubated overnight. Single colonies of each streak out were picked, and overnight cultures were created. The plasmid was extracted from the culture using the miniprep kit from hi-speed mini plasmid kits from IBI.

Restriction Digest of C-tagged KP4L gene in PCR8 Vector

Restriction digest was used to confirm the successful addition of the mutated KP4L gene from the eight single colonies using the following reaction:

1 µL NcoI

1 µL Xbal

1 µL Cutsmart buffer

2 µL nuclease-free water

The reaction was incubated in a water bath overnight at 37°C.

Sequencing of C-tagged KP4L gene in pCR8 Vector

Successfully forward-orientated inserts were sent for Sanger sequencing to confirm the presence of the C-tag and no gene-altering mutations.

1 µL M13 primer

500 ng of plasmid

Fill to 15 µL of nuclease-free water

LR Gateway of Entry clone to Destination Vector

For sequencing confirmed plasmid, Gateway cloning was used to insert the KP4L gene and C-tag into the pAG426GAL yeast expression vector:

0.5 µL of KP4L *B. meristosporus* NTD C-tag in pCR8

0.5 µL of destination clone pAG426GAL

1 µL of nuclease-free water

0.5 µL of LR Clonase

The Gateway reaction was incubated at room temperature for three hours. Then 0.25 µL of Proteinase K was added to the reaction and incubated at 37°C for ten minutes. The gateway reaction was then transformed into *E. coli* using the previously described protocol. *E. coli* colonies were then picked, grown overnight, and underwent DNA extraction using the hi-speed mini plasmid kits from IBI mini prep kit, and stored at -20°C. Yeast expression plasmids were then transformed into the lab strain BY4741 of *S. cerevisiae* using the protocol previously described in this chapter.

Transformation of Subset of Yeast Genome Deletion Collection

Deletion collection strains mutant (YER120W, YGL140C, YGL163C, YBR188C, YLR326W, YBR078W) confirmed to have a revival of growth with KP4L protein induction were also transformed with the KP4L *B. meristosporus* C-tag protein to be used for Western blotting. The deletion collection protocol was used for the yeast transformation with a reduced heat shock temperature of 36°C, instead of 42°C.

Sample Preparation for Western Blotting

The identified deletion collection strains (YER120W, YGL140C, YGL163C, YBR188C), BY4741 with the wild-type KP4L *B. meristosporus* protein, and a separate

BY4741 strain with the signal sequence truncation mutant of the *B. meristosporus* KP4L protein were the strains used for Western blotting.

Strains were grown in dextrose media overnight to achieve the preferred optical density (about 3.0 OD_{600}), and then they were washed with sterile water. The spun-down cells were then transferred into 50 mL selective raffinose media with an OD of 1.5 for overnight growth. The next day cultures were confirmed to have at least an OD of 3.0, and then protein induction was done with 20% liquid galactose and grown for three hours. Total galactose content in the culture was 10%.

Protein Precipitation

A time-point trial was done to determine the best time point to collect samples and precipitate protein. Identifying a time-point was important due to the lethality of expression of the KP4L protein in BY4741. At about three hours the culture was given optimal time to produce and excrete the C-tagged proteins. It was found that three hours was the sweet spot between protein production and provided the best performance. Earlier time points did not have a strong precipitant from spent media.

All samples were standardized to an OD_{600} of 3.0, through dilution of sterile water, if needed. Cells were spun and the spent media was filtered with a 0.22 micrometer filter into a new 50 mL conical tube. Then 0.5% of NP40 and twenty percent trichloroacetic acid ("TCA") of the total sample were added to the spent media. Ammonium sulfate precipitation was tried, but it was unable to precipitate the low amount of protein found in the spent media. Spent samples were incubated on ice for 15 minutes and then spun at 15000 x g for fifteen minutes at 4°C. The sample, when placed on ice, had two clear phases present: a clear supernatant, and a cloudy portion on the bottom of the tube. The clear supernatant of the samples was then removed. However, it was important to leave a small bit of clear supernatant for protein precipitation. Then 750 μL of 100% acetone was added. At this point, an oily layer was observed. The oil layer was then gently flicked to dissolve into the acetone, and then the sample was incubated on ice for five minutes. Then it was spun again for fifteen minutes at 4°C. The supernatant was removed, and then any remaining acetone was allowed to evaporate. Then the white precipitate was dissolved into a 6X SDS PAGE buffer. The sides of the tubes were well scraped during this portion to ensure protein stuck to the side of the tube was recovered. A

small amount of SDS PAGE buffer (less than one hundred µL) was needed to ensure a concentrated sample. Otherwise, the required exposure time for the membrane was quite large.

Protein Precipitant Sample Preparation

Twenty microliters of solubilized protein precipitation were combined with SDS-Page Sample Buffer with beta-mercaptoethanol added and heated to 95°C. If the protein sample turned green, more Tris pH 8.0 was added until the dye returned to purple.

Cell Fractionation for Cell Lysate Sample

The cell pellet was moved to a 1.5 mL microcentrifuge tube tube and washed in 500 µL of sterile ddH_20. lysis buffer with protease inhibitor (in a ratio of 100 µL: 1 mL) and glass beads were added in a 1:1:1 ratio to the physical volume of cells in the 1.5 mL microcentrifuge tube tube. At 1.5 OD_{600}, the twenty-four-mL culture was checked to make sure fifty µL of cells were concentrated. All ingredients, including 1.5 mL microcentrifuge tube tubes used, were chilled before use. The cell suspensions were vortexed for two minutes and then chilled on ice for two minutes. This was repeated three additional times. Then the tubes were spun for eight minutes at 1000 *x g* at 4°C. The supernatant was transferred to new chilled 1.5 mL microcentrifuge tube tubes, without disturbing the cell and bead pellet at the bottom. The new tubes contained the cell lysate.

Cell Lysate Sample Preparation

20 µL of cell lysate were combined with four microliters of SDS-page sample buffer with beta-mercaptoethanol added.

SDS-PAGE Gel Creation

Due to the low molecular weight of the protein, about 15 kDa, a 15% gel was used for running the samples. The recipes for the gels are as follows:

15% Resolving Gel (5mL/ 1 gel)

1.1 mL	H_20
2.5 mL	30% Acrylamide Mix
1.3 mL	1.5 M Tris (pH 8.8)
0.05 mL	10% SDS
0.05 mL	10% Ammonium persulfate
0.002 mL	TEMED

15% Separating Gel (2 mL/ 1 gel)

1.4 mL	H_20
0.33 mL	Acrylamide Mix
0.25 mL	1.0 M Tris (pH 6.8)
0.02 mL	10% SDS
0.02 mL	10% Ammonium persulfate
0.002mL	TEMED

Running the Protein Gel

The gel was loaded with 20 µL of buffered sample and then run for one-and-a-half to two hours at 40 amps. Two gels were used. One gel was loaded with cell lysis samples, and one gel was loaded with the spent media precipitant sample.

Gel Transfer to Membrane

After running the gel, it was transferred to a nitrocellulose membrane, using the mixed-weight protocol on the Bio-Rad Trans-Blot Turbo Transfer System. After running the gel, the gel and membrane were soaked in the transfer buffer for 15 minutes prior to transfer. Within the cassette of the Trans-Blot instrument, a sandwich of filter paper, gel, and the membrane was created. Three pieces of filter paper, soaked in transfer buffer, were the base of the sandwich. Then the membrane was placed directly on top of the filter paper. The gel was then carefully aligned on the membrane. One piece of soaked filter paper was then placed on top of the gel. A blot roller was then used to remove air bubbles between the gel and the membrane. Then two pieces of filter paper, soaked in transfer buffer, were placed on top to complete the sandwich. A final round of rolling with the blot roller was done to create consistent contact between layers.

1X Transfer Buffer Recipe (500 mLs)

40 mL	10X Stock
360 mL	dH_20
100 mL	100% Methanol

Membrane Incubation

The membrane was then incubated in blocking buffer for forty minutes.

Blocking Buffer

6 g	Milk Powder
200 mL	1% TBST

1X 1% TBST (1000mL)

50 mL	20X TBS Stock
949 mL	dH_20
1 mL	Tween20

After blocking, the membrane was rinsed three times for five minutes with 1% TBST solution, and the tray was changed. After the rinse, the membrane was cut with a razor blade at the 26 kDa band across the gel. The top portion of the membrane was incubated for one hour with a 1:1000 dilution of the GAPDH antibody. The lower portion of the membrane was incubated with a 1:1000 dilution of the C-tag antibody. The portion probed for the C-tag needed a second incubation with a 1:2000 dilution of the streptavidin secondary antibody for an additional hour to visualize the protein. After each antibody incubation, the membrane was rinsed three times in 1% TBST for five minutes, and the tray was changed.

Membrane Imaging

After the final rinse, the membrane was imaged via chemiluminescence, using the Cytiva Amersham ImageQuant 800. Auto exposure was selected for all imaging. If needed, the time was increased up to five minutes. If an exposure increase was needed, the corresponding GAPDH control exposure time was also increased. It occasionally was necessary to increase the exposure time to visualize the protein precipitated bands but reducing the amount of buffer the protein was solubilized in also helped reduce the time needed.

Results

Growth Analysis of KP4L Proteins

To assay the function of the KP4L proteins, eight of the identified KP4L genes were cloned from eight fungal species into *S. cerevisiae* expression plasmid named pAG426-Gal-ccdB through Gateway cloning. *S. cerevisiae* was then transformed with the eight KP4L plasmids. The transformants were assayed on CM-ura dextrose and CM-ura galactose plates. The KP4L proteins were expressed to assay their function when exported from the cell. When the eight KP4L proteins were expressed, an unpredicted phenotype was discovered in some of the strains. Induction on solid plate media resulted in a lethality phenotype and reduced growth phenotype from *B. meristosporus* (Bme)*, E. lata* (Ela), and *T. virens* (Tvi) KP4L proteins (Figure 3.3.). The other KP4L proteins did not noticeably disrupt growth of *S. cerevisiae* on solid growth media.

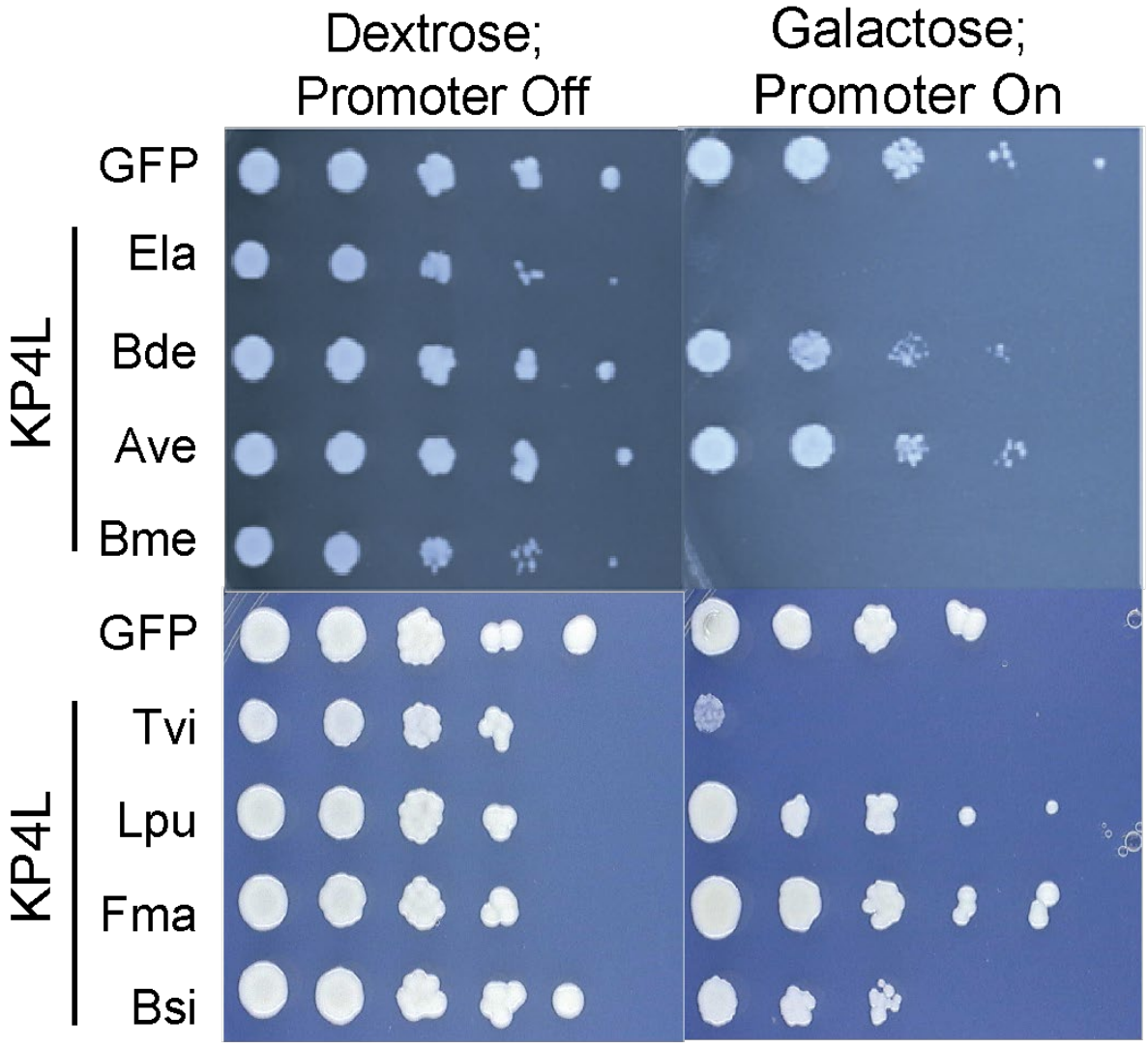

Figure 3.3. Ectopic expression of eight KP4L proteins in Saccharomyces cerevisiae. *The control is a plasmid on the pAG426GAL backbone encoding GFP. Ela = Eutypa lata, Bde = Blastomyces dermatitidis, Ave = Aspergillus versicolor, Bme = Basidiobolus meritosporus, Tvi = Trichoderma virens, Lpu = Lasallia pustulata, Fma = Fusarium mangiferae, and Bsi = Blastomyces silverae. Cultures were standardized at OD600 1.5 and then a 1:100 dilution out to 10-6. Plated on a dextrose control and galactose for protein induction, B. meristosporus and E. lata had the strongest lethality phenotype of the eight KP4L proteins.*

To further assess the effect of KP4L expression on the growth of *S. cerevisiae*, strains that were assayed in Figure 3.1. were grown in liquid CM-ura raffinose media and induced with galactose (Figure 3.4.). An increased doubling time was observed for KP4L proteins from *B. meristosporus* and *E. lata* compared to dextrose controls. After induction of KP4L expression, the OD_{600} of the liquid culture immediately plateaued with galactose induction for

KP4L protein from *B. meristosporus*. The KP4L protein from *E. lata* also plateaued, but not as quickly as the KP4L *B. meristosporus.* The KP4L *B. meristosporus* strain had a doubling time of 41 hours and KP4L *E. lata* had a doubling time of 18 hours when grown under conditions that induced KP4L expression. In comparison, cultures with dextrose had doubling times that were approximately three hours for all strains tested, including the strain with KP4L *B. meristosporus*. Similar results were found for the other six KP4L proteins with similar doubling times from galactose and dextrose induction. ANOVA test showed that there was a significant difference in doubling time between GFP control strains and the KP4L *B. meristosporus* and KP4L *E. lata* ($p<0.05$). Paired t-test also showed significant differences between KP4L *B. meristosporus* and KP4L *E. lata* dextrose and galactose induction doubling times ($p<0.05$).

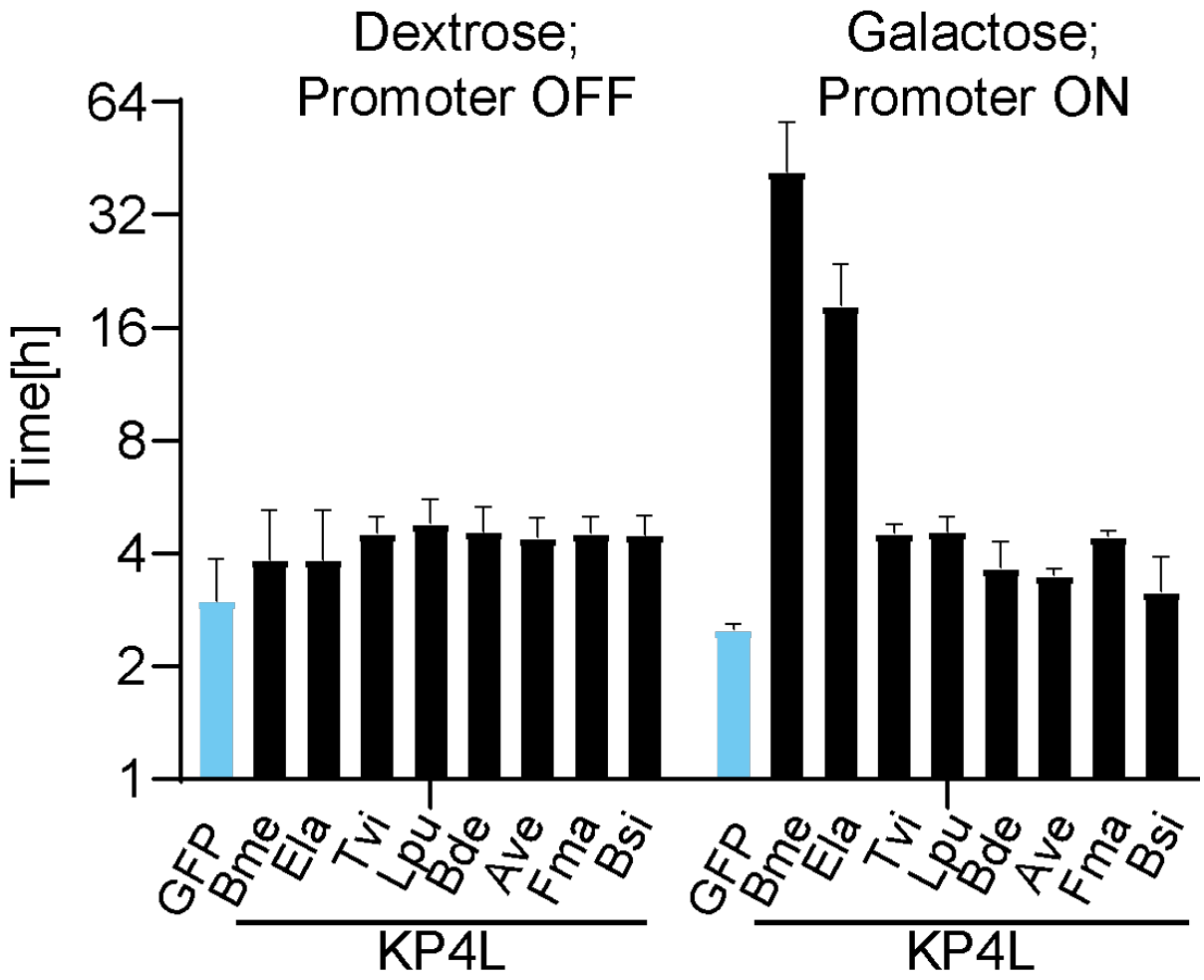

Figure 3.4. Doubling time calculations for the eight KP4L proteins. *Growth assays were performed, starting the eight strains in 20 mL CM -uracil raffinose media. After four time points were collected, indicating that cultures were in exponential growth phase, protein production was induced to be 10% galactose or 10% dextrose in the culture. After induction, an additional four-time points were taken. Doubling time was calculated from the exponential growth equation and performed in excel. Ela = Eutypa lata, Bde = Blastomyces dermatitidis, Ave = Aspergillus versicolor, Bme = Basidiobolus meritosporus, Tvi = Trichoderma virens, Lpu = Lasallia pustulata, Fma = Fusarium mangiferae, and Bsi = Blastomyces silverae.*

The expression of a non-native protein raised questions about the inherent toxicity of expression in *S. cerevisiae.* Signal sequences are known for endoplasmic reticulum localization and plays a role in exportation. A signal sequence truncation mutant was created to investigate whether the exportation of the protein was causing toxicity. Induction of the N-terminal truncation mutant of the KP4L protein from *B. meristosporus* caused a restoration of growth similar to the GFP control (Figure 3.6.). A natural variant of the KP4L *B. meristosporus* gene

was identified with two mutations in the signal sequence, when compared to the wildtype KP4L *B. meristosporus* gene (KP4L Bme α; Figure 3.5.).

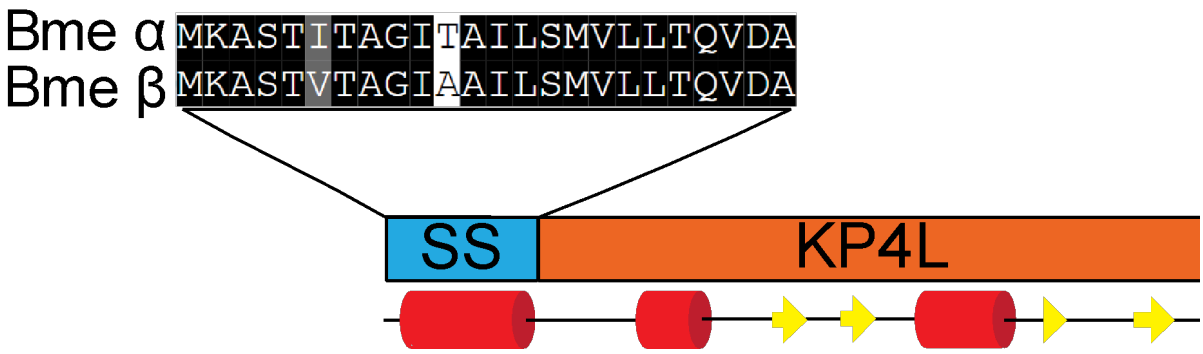

Figure 3.5. Diagram of amino acids differences between B. meristosporus α and β. *Bme β = natural variant of B. meristosporus KP4L protein. Bme α = wildtype KP4L B. meristosporus protein. The blue box indicates signal sequence. The orange is the KP4L domain. The boxes size reflects length within the protein. Secondary structure diagram is provided below for B. meristosporus. Alpha helices are red rectangles, and the beta sheets are yellow arrows. Signal sequence is colored for conservation. Black is 100% conserved, gray is conservative mutation, and white indicates a non-conservative mutation. The diagram is to highlight the two amino acid changes between B. meristosporus α and β.*

The remainder of the protein had no other amino acid substitutions. The two mutations in the signal sequence caused a revival of growth upon induction (Figure 3.6.). Doubling time calculations for the variant also reflected growth revival phenotype (Figure 3.7.). To compare, a signal sequence truncation mutant was also created for the natural variant of *B. meristosporus* (Bme β). The NTD mutant had a slightly increased growth revival upon induction (Figure 3.6.).

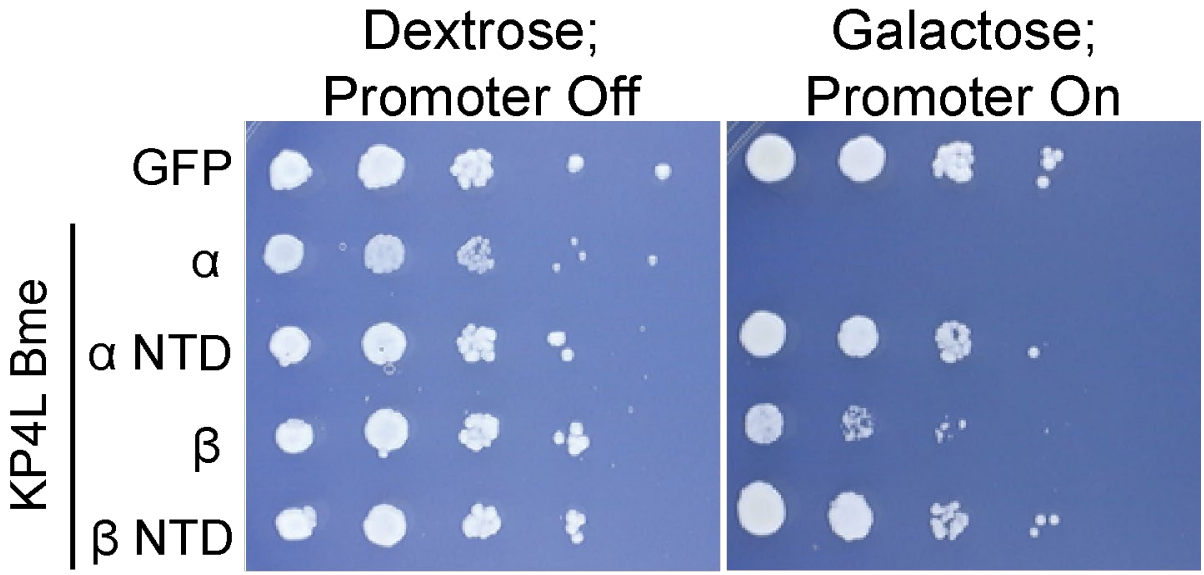

Figure 3.6. Ectopic expression of the KP4L B. meristosporus and the variants in S. cerevisiae. *KP4L B. meristosporus α and β and their N terminal truncation mutants lacking the signal sequence plated on dextrose and galactose. Bme α = WT KP4L protein from B. meristosporus, NTD Bme α = N terminal truncation of signal sequence mutant of Bme α, Bme β = Natural variant of B. meristosporus, NTD Bme β = N terminal truncation of the natural variant of B. meristosporus. Cultures were standardized at OD600 1.5 and then had a 1:100 dilution out to 10-6. Plated on a dextrose control and galactose for protein induction. B. meristosporus and E. lata had the strongest lethality phenotype of the eight KP4L proteins.*

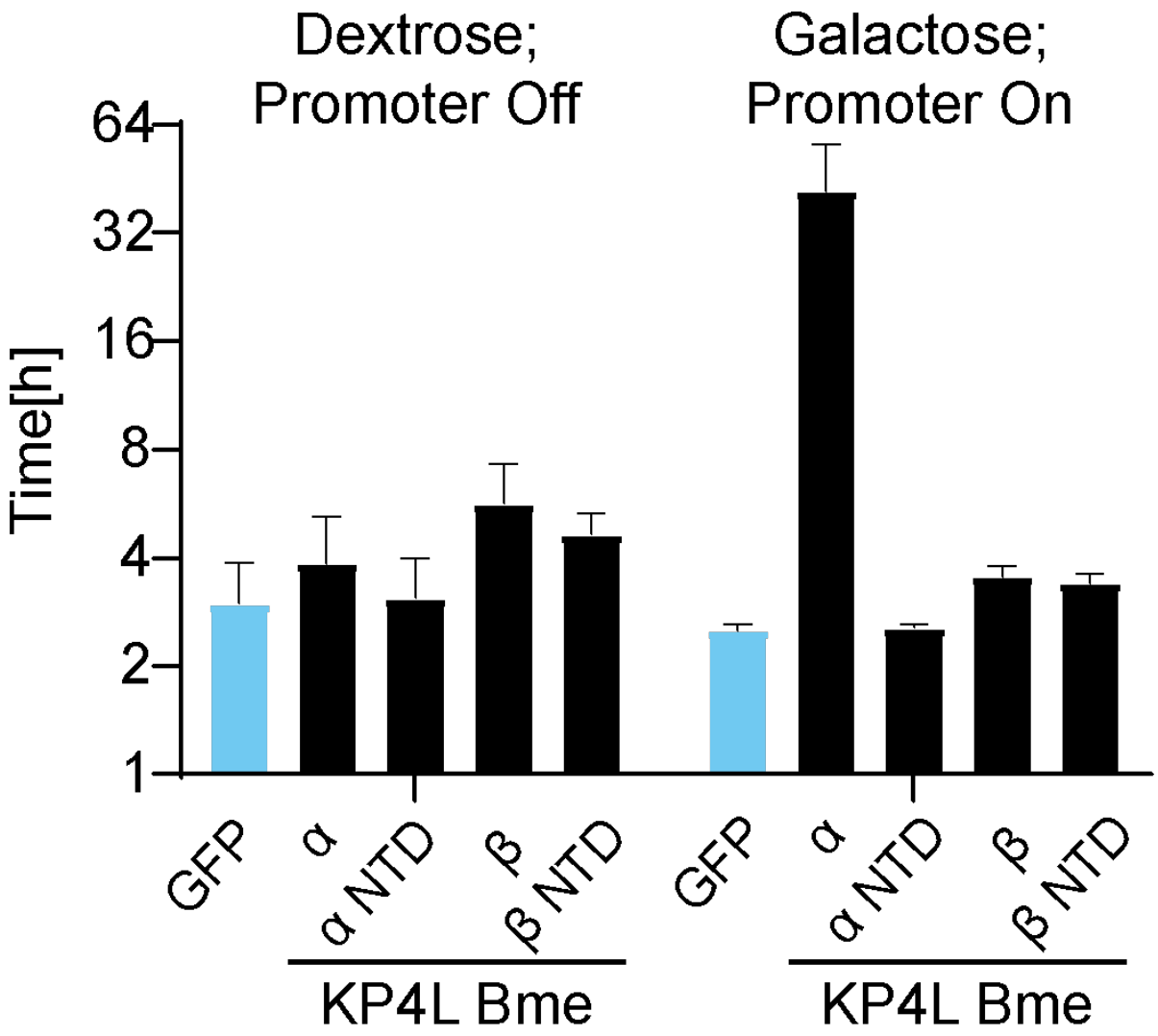

Figure 3.7. Doubling time calculations for the KP4L B. meristosporus α and β and their N terminal truncation in S. cerevisiae. *Growth assays were performed by starting the eight strains in 20 mL CM -uracil raffinose media. After four time points were collected that indicated cultures were in exponential growth phase, protein production was induced with 10% galactose or 10% dextrose in the culture. After induction, an additional four-time points were taken. Doubling time was calculated from the exponential growth equation and performed in excel. Bme α = WT KP4L protein from B. meristosporus, NTD Bme α = N terminal truncation of signal sequence mutant of Bme α, Bme β = Natural variant of B. meristosporus, NTD Bme β = N terminal truncation of the natural variant of B. meristosporus.*

Cell Count and Budding Index

Since KP4 is predicted to inhibit growth by preventing cell division the KP4L *B. meristosporus* containing strain was assayed for further understanding the halt of cell growth in protein induction. Cell counts included over 1000 cells for the GFP control and of the KP4L *B. meristosporus* strain of BY4741. The budding analysis revealed a decrease of 20.3% in large buds and a decrease of 9.5% in small buds for the KP4L *B. meristosporus* strain (Figure 3.8.; Figure 3.9.). There was an increase of 29.8% in cells with no buds for the same strain. Conversely, for the GFP control strain, there was only about a 13.2%, 7.4%, and 5.8% change in no buds, small buds, and large buds when grown in galactose-containing media, respectively. The change in budding index for GFP brought the budding index to equally represented by the three bud types.

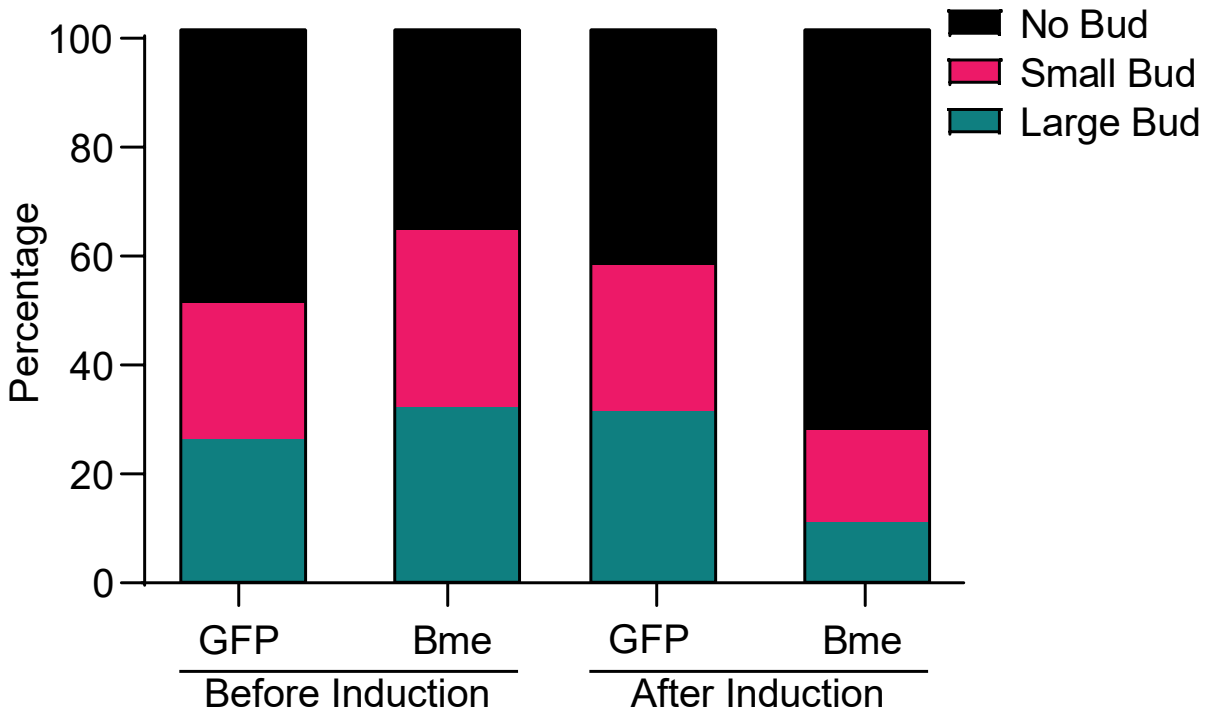

Figure 3.8. Budding index percentages of the strains containing GFP and KP4L B. meristosporus. *Cell count and budding analysis was done once cultures reached OD600 of 1.5. After the first count the cultures were induced with 2% galactose. After two hours of growth a cell count and budding analysis was repeated. N of GFP strain cells prior to induction = 1527. N of GFP strain cells after induction = 1932. N of KP4L B. meristosporus strain cells prior to induction = 1361. N of KP4L B. meristosporus strain cells after induction = 1527.*

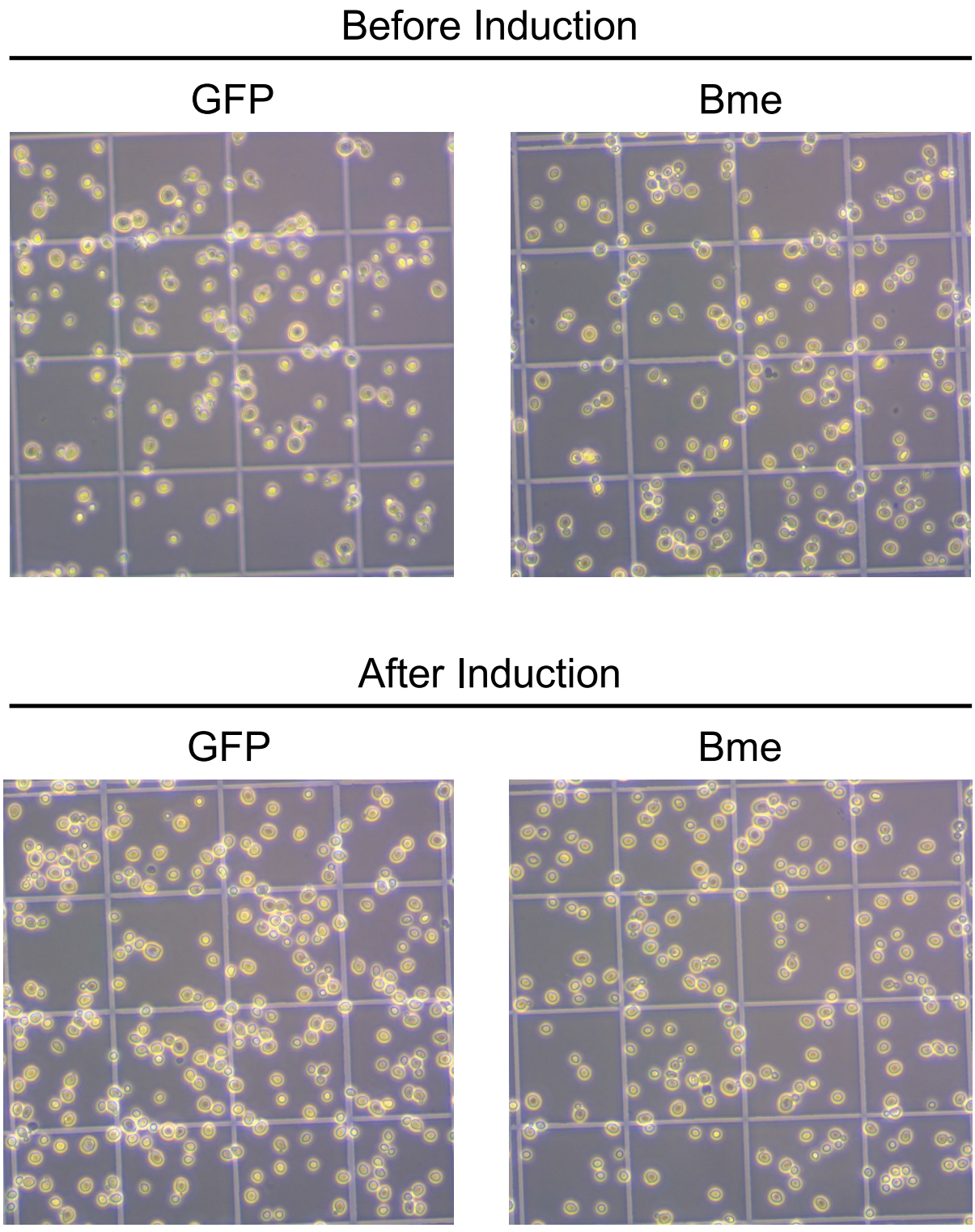

Figure 3.9. Cell images of GFP and KP4L B. meristosporus containing strains of S. cerevisiae before and after protein induction. *Images were taken prior to induction and then two hours after galactose induction.*

Excess Ions and Cytotoxicity

Previous literature showed the presence of excess calcium abrogated the cytotoxic effect of KP4 (Gu et al., 1995; Gage et al., 2001; Gage et al., 2002). To see if a similar effect would happen with KP4L proteins excess ion assays were performed. Serial dilution assays and growth assays were conducted in excess ion concentrations, varying from 40 mM to 0.2 M of $CaCl_2$, NaCl, KCl, and $MgCl_2$. KP4L *B. meristosporus,* KP4L NTD *B. meristosporus,* KP4L *E. lata,* and the GFP control were used for the serial dilution assays. Growth assays only included KP4L *B. meristosporus* and GFP control. There was no growth revival on any concentration of $CaCl_2$, NaCl, KCl, and $MgCl_2$ on the serial dilution assays (Figure 3.10.). The doubling time of KP4L *B. meristosporus* was reduced to 16 hours, but non-induction doubling time (Dextrose induction) was not achieved by providing excess ions (Figure 3.11.). GFP had an increased doubling time of about 45 minutes.

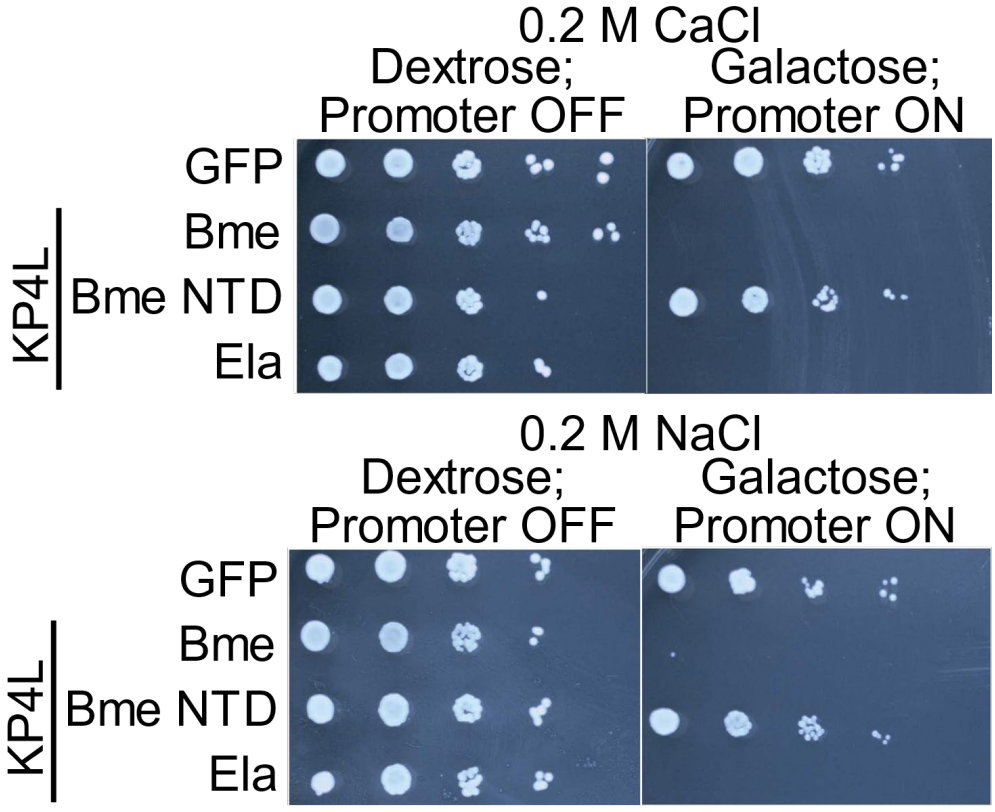

Figure 3.10. Ectopic expression of KP4L B. meristosporus and the N terminal truncation, KP4L E. lata, and GFP control. *Bme = KP4L B. meristosporus, Bme NTD = KP4L B. meristosporus N terminal truncation, Ela = KP4L Eutypa lata. Cultures were standardized at OD600 1.5 and then had a 1:100 dilution out to 10-6. Plated on a dextrose control and galactose for protein induction.*

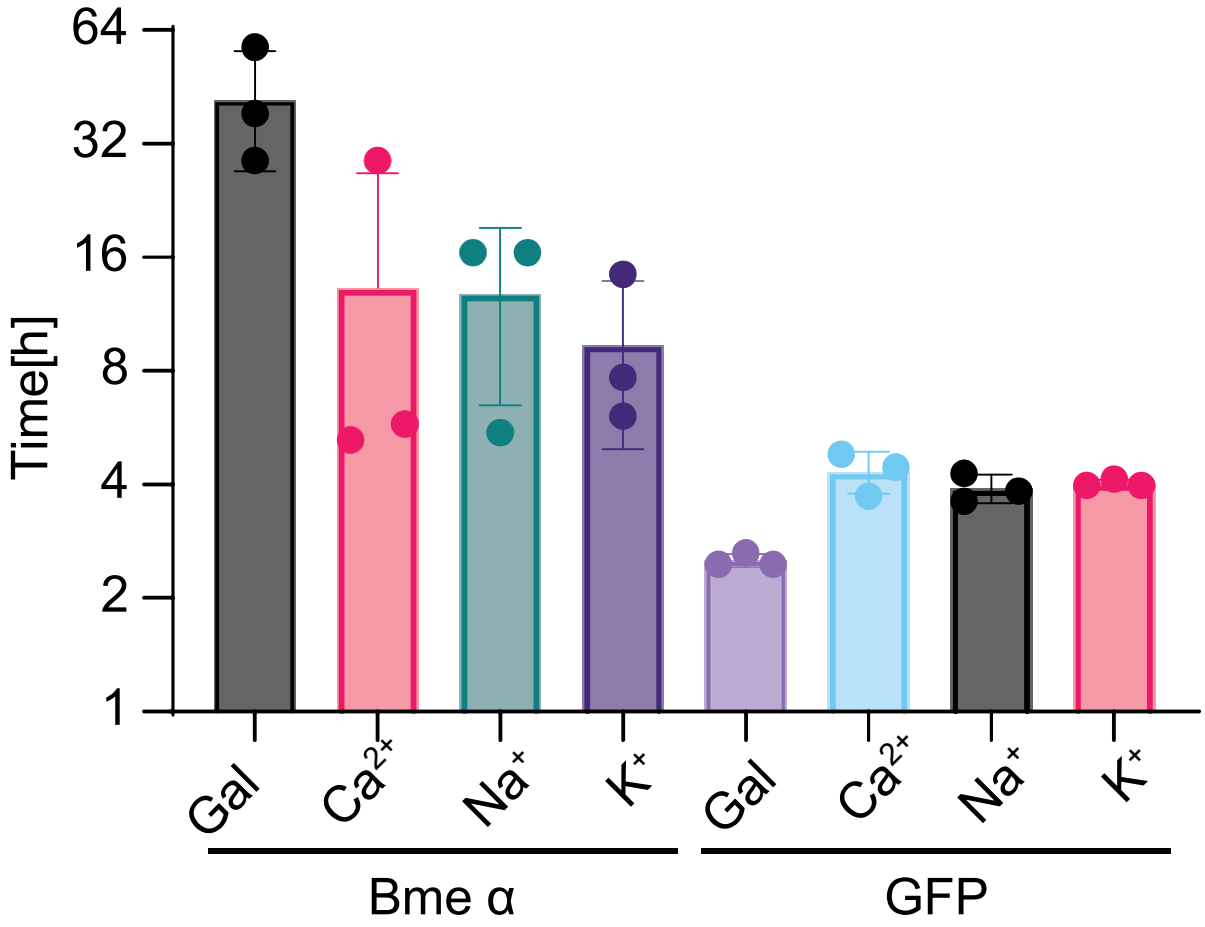

Figure 3.11. Doubling time of GFP and KP4L B. meristosporus with excess ions. *Bme = KP4L B. meristosporus. Growth assays were performed, starting the eight strains in 20 mL CM -uracil raffinose media. After four time points were collected that indicated cultures were in exponential growth phase, protein production was induced with 10% galactose in the culture. After induction, an additional four time points were taken. Doubling time was calculated from the exponential growth equation and performed in excel.*

Identifying Genes Important for Cytotoxicity

To determine the host genes that are important for the lethality of KP4L proteins, a screen of the haploid yeast deletion collection (containing gene deletions of more than four thousand nonessential genes) was transformed with the plasmid expressing the KP4L gene from *B. meristosporus* (experiment performed by Mark Lee and Jordan Hawley; Gaiver et al., 2002). Deletion strains that had a revival of the growth phenotype of KP4L and grown on galactose were identified by their unique molecular barcode through PCR and sequencing. 44 gene knockouts were found to suppress KP4L cytotoxicity (Table 3.6). Gene categories were then used for GO analysis (Figure 3.12.)

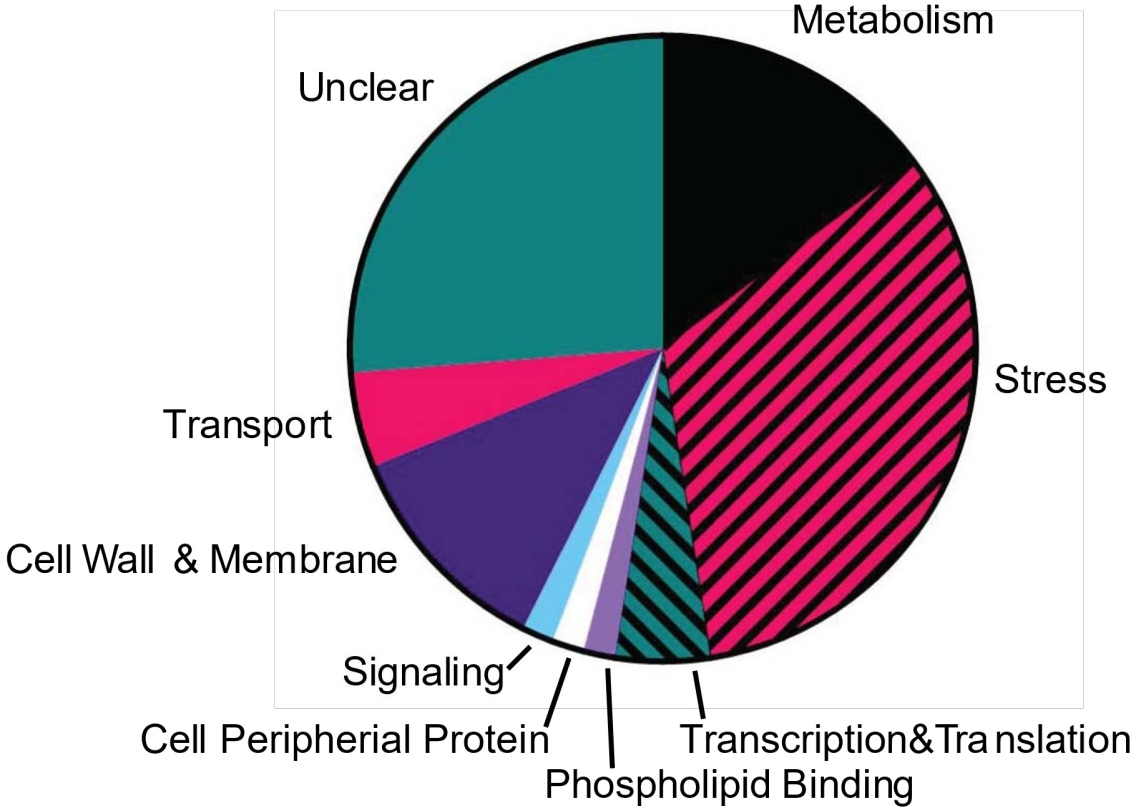

Figure 3.12. GO analysis of the 44 genes identified in the Yeast Genome Deletion Collection Screen. *The most prominent categories were stress, unclear or unknown, metabolism, and cell wall and membrane.*

Table 3.6. Identified growth revival strains from the deletion collection transformation with KP4L *B. meristosporus.*

Gene tag	Number of Repeats	Gene	Gene tag	Number of Repeats	Gene
YBR188C	5	*NTC20*	YGL230C	1	
YBR078W	4	*ECM33*	YLR267W	1	*BOP2*
YEL006W	3	*YEA6*	YLR279W	1	
YPL258C	3	*THI21*	YLR416C	1	
YLR309C	2	*IMH1*	YOR342C	1	
YER131W	2	*RPS26B*	YPL067C	1	*HTC1*
YJL218W	2		YBR223C	1	*TDP1*
YMR254C	2		YER162C	1	*RAD4*
YLR364W	2	*GRX8*	YFL010W-A	1	*AUA1*
YBR148W	1	*YSW1*	YGL163C	1	*RAD54*
YEL022W	1	*GEA2*	YGR004W	1	*PEX31*
YER120W	1	*SCS2*	YHR177W	1	*ROF1*
YGL140C	1		YJL197W	1	*UBP12*
YPL277C	1		YKR091W	1	*SRL3*
YGR289C	1	*MAL11*	YLR278C	1	
YAR030C	1		YML060W	1	*OGG1*
YAR044W	1		YMR030W	1	*RSF1*
YBL083C	1		YMR052W	1	*FAR3*
YDR417C	1		YMR226C	1	
YER158C	1		YNL200C	1	*NNR1*
YGR014W	1	*MSB2*	YOR346W	1	*REV1*
YLR307W	1	*CDA1*	YOR354C	1	*MSC6*
YLR326W	1		YPL072W	1	*UBP16*
YLR374C	1		YPL074W	1	*YTA6*
YMR175W	1	*SIP18*	YPL138C	1	*SPP1*
YOR053W	1		YPL165C	1	*SET6*

Continuation of Table 3.6.					
YPL079W	1	*RPL21B*	YPL206C	1	*PGC1*
YDR491C	1		YBR218C	1	*PYC2*
YGL023C	1	*PIB2*	YDR216W	1	*ADR1*
YGL177W	1		YDR345C	1	*HXT3*
YJR090C	1	*GRR1*	YER027C	1	*GAL83*
YPL244C	1	*HUT1*	YHR094C	1	*HXT1*

GO analysis from identified genes from the screen, included many genes related to the categories of galactose metabolism, stress, and membrane transport (Figure 3.13). Of the subset chosen, only six strains showed a strong revival of growth phenotype after protein induction (YER120W, YGL140C, YGL163C, YBR188C, YBR078W, YLR326W). A strong revival of growth was categorized as growth that occurred within one week of plating (Figure 3.13). Doubling time analysis was also used to confirm strong growth revival (Figure 3.15.).

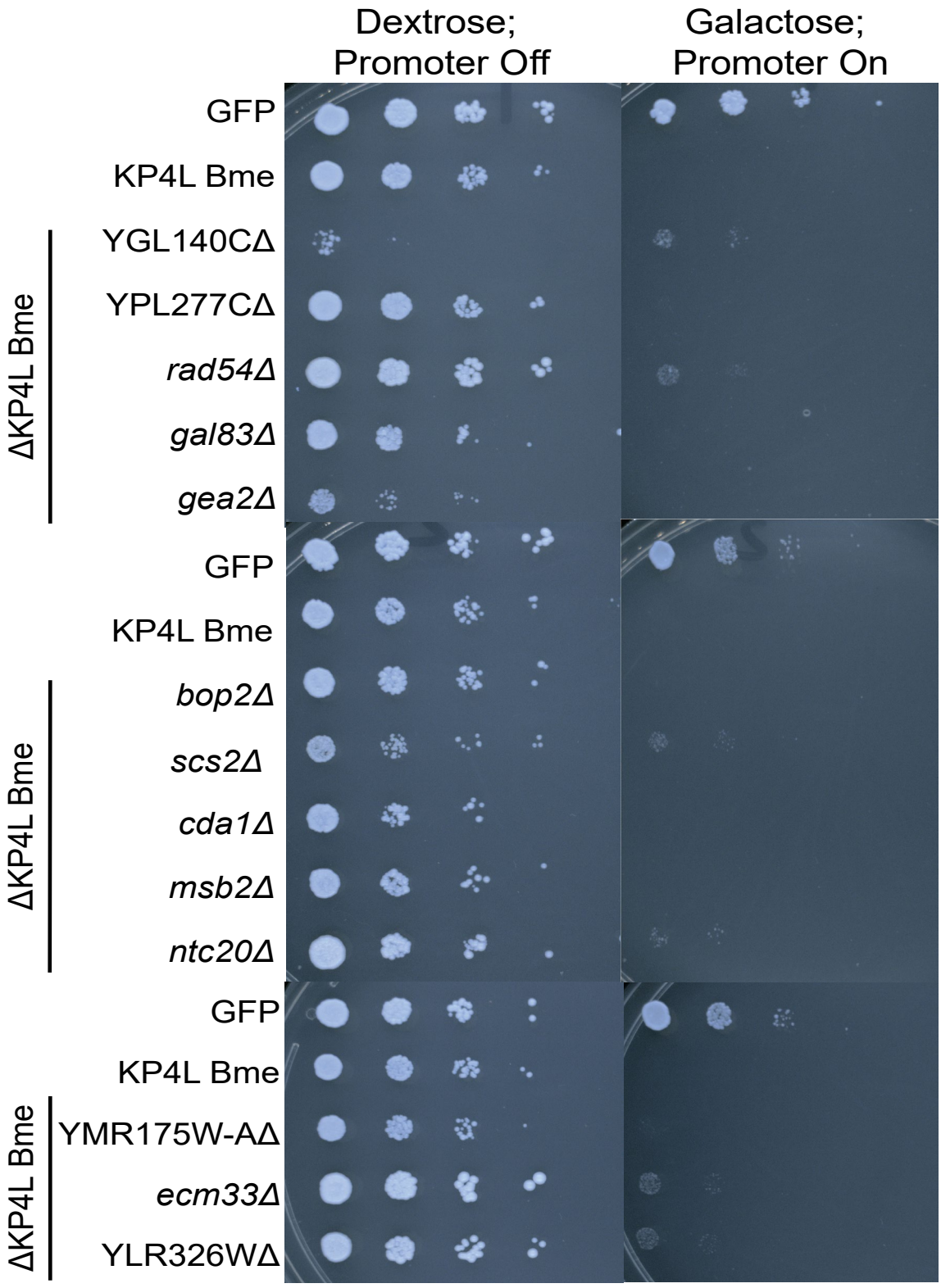

Figure 3.13. Ectopic expression of Yeast Genome Deletion Collection strains transformed with KP4L B. meristosporus. *Bme = KP4L B. meristosporus. Cultures were standardized at OD600 1.5 and then had a 1:100 dilution out to 10-6. Plated on a dextrose control and galactose for protein induction.*

If incubated for an extended period, all strains showed small levels of growth, compared to KP4L *B. meristosporus,* which never showed any growth. Almost all strains had growth revival after a month of incubation (Figure 3.14.). This is supported by the deletion collection screen data because strains were allowed several weeks of growth to identify slow growing resistance strains. The Yeast Genome Collection strains with a strong growth revival phenotype were chosen as strains to be used for Western blotting.

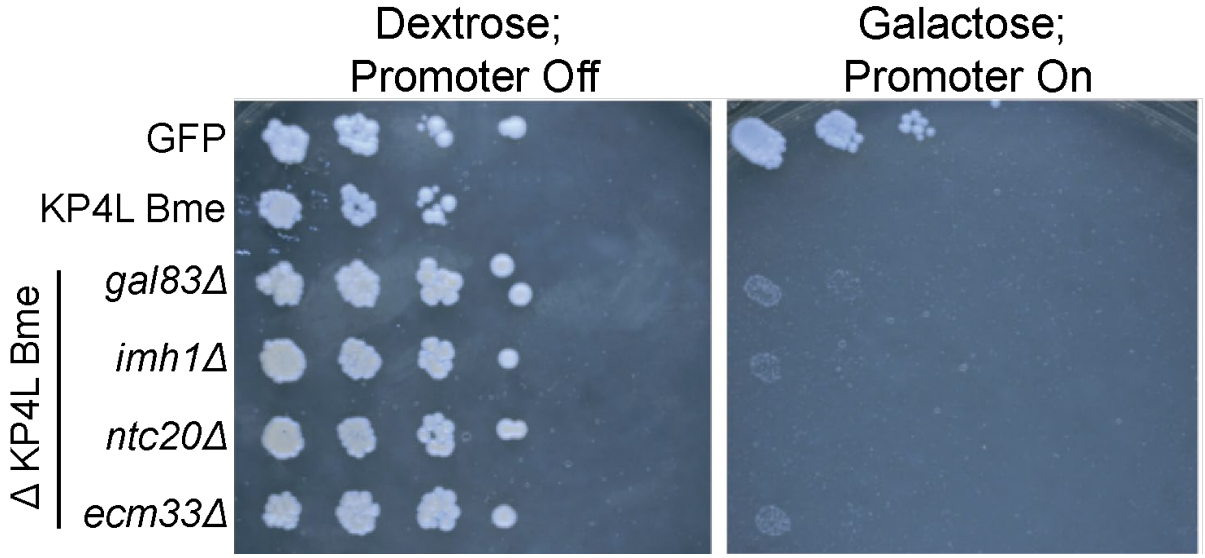

Figure 3.14. Long-term incubation of Yeast Genome Deletion Collection strains that confer resistance compared. *Serial dilution assay with KP4L B. meristosporus and GFP as controls. All deletion strains show growth revival with a long enough incubation compared to BY4741 with KP4L B. meristosporus α which had no growth even after a month of incubation. Bme = KP4L B. meristosporus α. Cultures were standardized at* OD_{600} *1.5 and then had a 1:100 dilution out to* 10^{-6}*. Plated on a dextrose control and galactose for protein induction.*

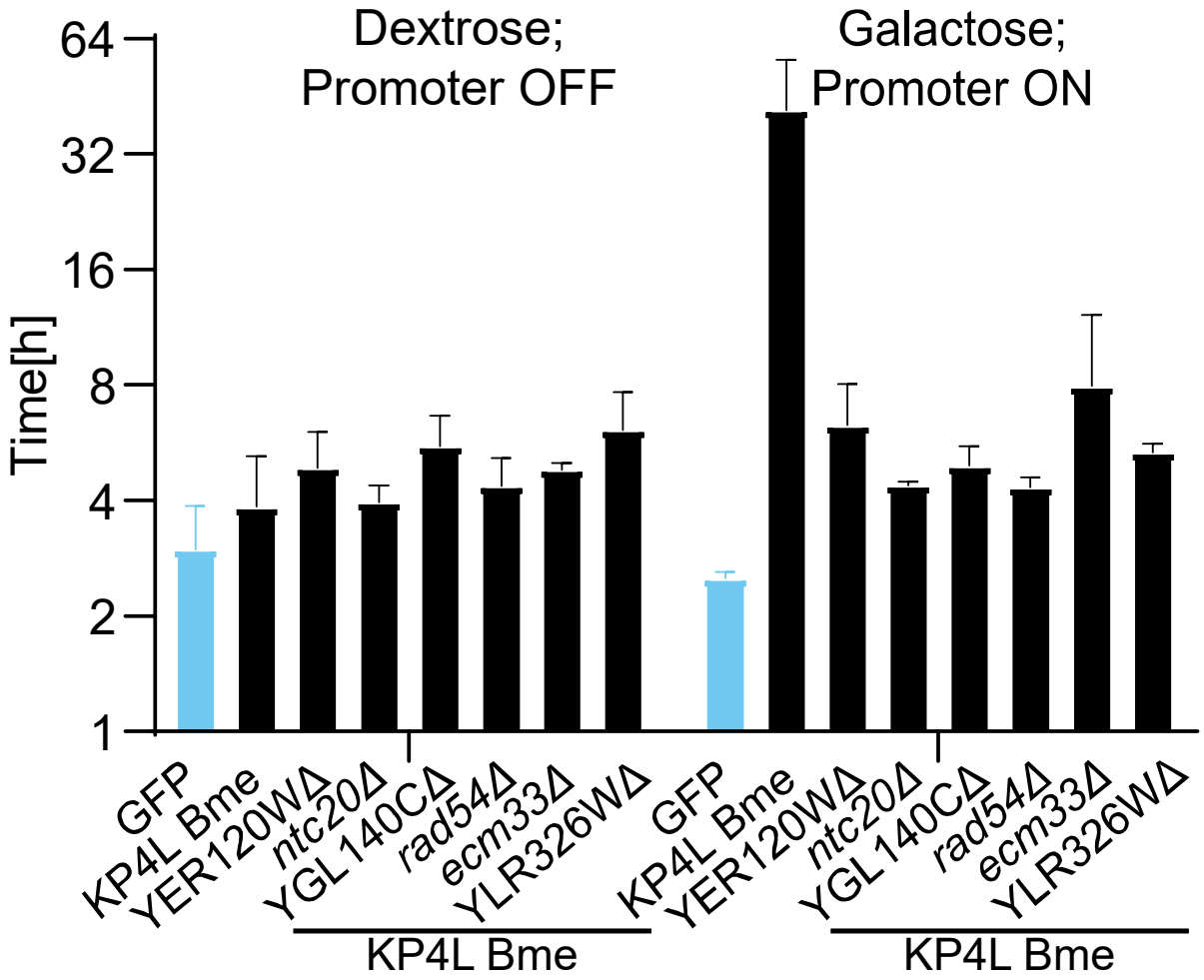

Figure 3.15. Doubling time of deletion collection strains transformed with KP4L B. meristosporus*. Bme = KP4L B. meristosporus α. Growth assays were performed, starting the eight strains in 20 mL CM -uracil raffinose media. After four time points were collected that indicated cultures were in exponential growth phase, protein production was induced with 10% galactose or 10% dextrose in the culture. After induction, an additional four time points were taken. Doubling time was calculated from the exponential growth equation and performed in excel.*

Determining the Cellular Location of the KP4L Proteins

Localization was visualized with the addition of a C-terminal C-tag of four amino acids, "EPEA", of the *B. meristosporus* KP4L protein in *S. cerevisiae* (Figure 3.16.). Other tags were considered but there was a loss of lethality when the protein was expressed. Identified deletion strains that had confirmed loss of cytotoxicity were transformed with C-tagged KP4L proteins and used in Western blotting. A GAPDH control was used to show that there was no cell lysis in the spent media sample.

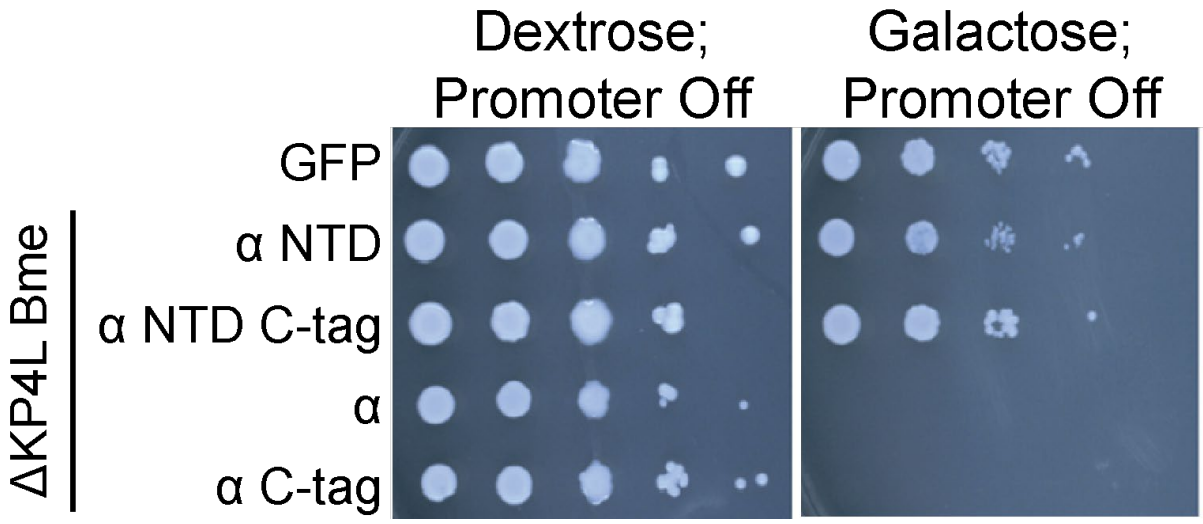

Figure 3.16. Ectopic expression of KP4L B. meristosporus and the N terminal truncation mutant with the C-tag. *KP4L Bme = KP4L B. meristosporus α, NTD = N terminal truncation. Cultures were standardized at OD600 1.5 and then had a 1:100 dilution out to 10-6. Plated on a dextrose control and galactose for protein induction. GFP and non-tagged strains were used as controls.*

Western blotting results show a band present in the cell lysis and in the spent media of the BY4741 strain of the wildtype KP4L *B. meristosporus* protein (KP4L Bme α) but not the signal sequence truncation mutant (Figure 3.19.). All strains tested showed KP4L *B. meristosporus* in the cell lysis fraction (Figure 3.17.). Except the KP4L *B. meristosporus* strain induced with dextrose was very faint probably due to leaky expression. KP4L *B. meristosporus* was also detected in the cell wall and membrane portion of all strains except *scs2*Δ and YGL140WΔ (Figure 3.18.).

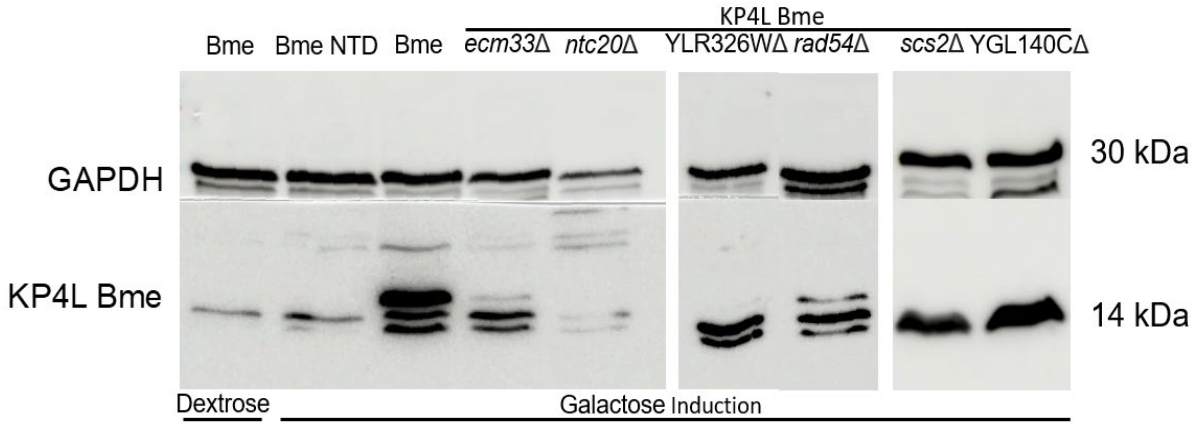

Figure 3.17. Western blots of cell fraction of strains expressing KP4L B. meristosporus*. Strains were grown overnight in raffinose and induced with galactose. Optical density was standardized at 3.0 after induction.*

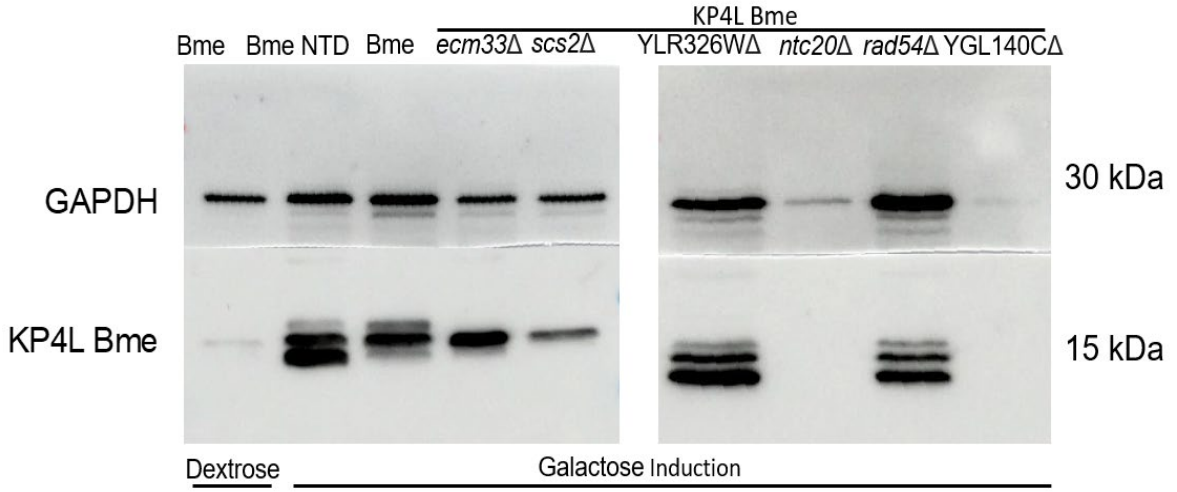

Figure 3.18. Western blots of cell membrane fraction of strains expressing KP4L B. meristosporus. *Strains were grown overnight in raffinose and induced with galactose. Optical density was standardized at 3.0 after induction.*

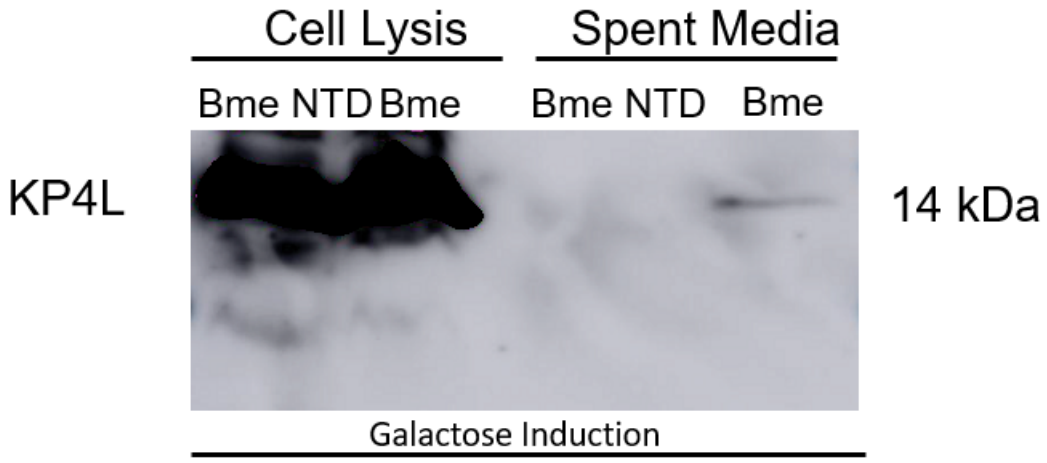

Figure 3.19. Western blots of cell lysis fraction and spent media protein precipitation of strains expressing KP4L B. meristosporus. *Strains were grown overnight in raffinose and induced with galactose. Optical density was standardized at 3.0 after induction.*

Discussion

The induction of KP4L proteins in *S. cerevisiae* resulted in a surprising phenotype. For several strains (*B. meristosporus, E. lata, T. virens*), induction caused a dramatic lethality in the expressing strain (Figure 3.3.). KP4 can be expressed as a heterologous system in *S. cerevisiae,* and it inhibits a sensitive lawn strain of *Ustilago maydis* (Park et al., 1994). The induced lethality of the *S. cerevisiae* could be a byproduct of the expression of foreign proteins. Or potentially, the lethality is from the KP4L proteins being excreted and interacting with the cell surface of the yeast cells. The sequence diversity between KP4L proteins and KP4 could allow for the differentiation of channel targets. There is a calcium channel, *cch1*, that was predicted to be similar to the one KP4 acts upon in *Ustilago maydis.* The KP4L proteins could be targeting a different type of ion channel. However, *CCH1* deletion mutant and no deletion mutants related to ion channels were identified in the deletion collection screen (Table 3.6.) KP4L *B. meristosporus* showed the strongest phenotype, with a complete lack of growth on galactose media (Figure 3.3.). The liquid growth assay supported the phenotype. Upon induction there was a plateau of growth within two hours. The optical density remained constant for upwards of eight hours. The calculated doubling time was approximately forty hours (Figure 3.4.). This essentially shows that the culture will not double in cell mass. KP4L *E. lata* had a similar phenotype, but less severe. It was difficult to see unless the plate was held to a light, but some growth develops on galactose media at the first dilution in the serial dilution assay (Figure 3.3.). The liquid growth assay, similarly, has a large doubling time of approximately eighteen hours (Figure 3.4.). These two proteins have the most amino acid similarity to the viral KP4 protein (Table 2.1.). In phylogenetic analysis, KP4L *B. meristosporus* is the sister taxa to KP4, and KP4L *Eutypa lata* is located in a nearby clade (Figure 2.3). The other six proteins did not change much compared to their dextrose controls, but the proteins are also closely placed near KP4 in the phylogeny.

The expression of these foreign proteins alone could have been toxic to *S. cerevisiae.* To help answer the question of whether the production or exocytosis of these proteins is toxic to the cell, a signal sequence truncation mutant was created of the KP4L *B. meristosporus* protein. Assays revealed that signal sequence within these proteins seems critical for the lethality function. Removal of this signal sequence revives the growth phenotype when expressed in galactose (Figures 3.6. & 3.7.). The data provides support for the exocytosis

hypothesis. Even variation in the signal sequence disrupts the lethality phenotype. The *beta* variant of *B. meristosporus* had a revival of growth with only two amino acid mutations in the signal sequence, while the KP4L domain was identical (Figure 3.5.). The revival of this variant could be related to a change in the ER translocation or efficiency of transportation out of the cell. Truncation of the signal sequence also saw growth like the positive control. The data shows that signal sequence, and perhaps therefore excretion, is a necessary component of the cytotoxicity of the KP4L proteins. This supports the hypothesis that KP4L proteins are extracellular toxins.

The cell count and budding index experiments may have revealed a portion of the mechanism of action for the KP4L proteins (Figure 3.8. & 3.9.). Before the induction of the KP4L proteins, the budding index in the KP4L *B. meristosporus* strain was similar to the GFP control strain. The cells with no bud, small buds, and large buds were roughly similar percentages of the population of cells. However, after induction, the KP4L *B. meristosporus* strain had a staggering drop of small and large budding cells (Figure 3.8.). 73% of the population had no buds present two hours after protein induction, and only 10% of the cells had large buds. Additionally, the cell size dramatically increased, compared to cells before induction and the GFP control. KP4 has been shown to be a fungistatic protein that is proposed to halt cell division between the S and G1 transition by competitively binding to the calcium channels (Gage et al., 2001). The budding analysis aligns with this hypothesis, although further studies will be needed to confirm.

Despite previous literature indicating that excess calcium can abrogate KP4L toxicity, a serial dilution assay of KP4L proteins from *B. meristosporus* and *E. lata* does not show a recovery of growth. Various concentrations (0.2 M, 0.1M, 70mM, and 40 mM) of calcium, magnesium, potassium, and sodium were used, but no growth revival was seen on any of the galactose plates (Figure 3.10.). However, when protein production was induced, the growth assay reflected a growth recovery in all treatments (Figure 3.11.). This result could indicate that an ion channel is inhibited by KP4L proteins, but the data is not conclusive. An average doubling time of ten hours is not a strong indication of nullification of the cytotoxicity effect from the three excess ion treatments. Although, two of the calcium repeats were found to have a doubling time of five hours and had strong growth after induction. Further data will need to be collected to understand this effect.

Forty-four strains were identified from the yeast genome collection that caused growth revival (Table 3.3.). GO analysis identified that the primary gene categories responsible for this effect were metabolism, stress, unclear or unknown function, and cell wall and cell membrane (Figure 3.12.). Metabolism genes are most likely an artifact of the galactose promoter system used for expression. The categories were transport, transcription and translation, and signaling could be related to modification of the protein production chain to confer resistance to the cell. The main category of interest for the purpose of this study is the cell wall and membrane category. These strains can potentially secrete the KP4L proteins because of the change in the cell wall or cell membrane. Fourteen strains of the forty-four were picked for reconfirmation of the revival of growth phenotype. One strain was chosen for each category of the go analysis, and all strains relating to the cell membrane or cell walls were chosen. This was done to find a strain that could withstand exocytosis of the KP4L proteins if they were being secreted. Other strains, while conferring resistance, may have been altering the cells' ability to secrete the KP4L protein.

The fourteen strains that were picked for reconfirmation had a variety of strengths in growth revival phenotypes. All strains eventually showed growth, but visible colony growth took between four days to several weeks after plating. Comparatively the BY4741 strain with KP4L from *B. meristosporus* protein never showed any growth during the extended incubation. Growth revival plates from the transformation of the deletion collection were incubated for several weeks to identify slow-growing colonies with resistance. It is within the limits of the transformation parameters that these strains took so long to grow.

While all deletion collection growth revival strains eventually grew, only six strains had reasonable growth times to be used for the Western blots. The subset of the deletion collection strains and BY4741 were transformed with a C-tagged KP4L *B. meristosporus* protein to be identified by Western blotting. BY4741 transformed with the truncated signal sequence mutant of KP4L *B. meristosporus* as a control. Many tags were tried for the KP4L proteins, including a HA tag and Myc tag, but they broke the lethality phenotype. The C-tag, a four amino acid "EPEA" tag on the C terminal end, was the only tag that maintained the lethality phenotype (Figure 3.16.).

The Western blot posed a unique challenge to potentially detect the tagged KP4L protein. Induction of the protein causes inhibition of the growth of BY4741 and then prevents

further protein production. Data from the growth assays and from a time series of protein precipitation was done to identify a time point that would have the best chance of detecting KP4L proteins present in the spent media. Between two and three hours were identified to have reasonable protein production while limiting the exposure of the cell to the protein. The deletion strains were used as a potential way to precipitate a larger amount of protein from the spent media, since the induction will not prevent growth. In the spent media, a light but detectable band was identified in the wildtype KP4L *B. meristosporus* protein (KP4L Bme α) in the BY4741 strain (Figure 3.19.). Strong bands are easily detectable in cell fraction for all strains tested, except for the strain that did not get induced (Figure 3.17.). The difficulty of detecting the proteins could be due to the small amount of protein secretion, cell growth inhibition, and the protein binding to the cell membrane. Strong bands were detected in most of the strains tested the membrane fraction of the cell lysis (Figure 3.18.).

The data largely supports the hypothesis that the KP4L proteins are extracellular toxins and that they target the cell surface for toxicity. The signal sequence truncation mutants showed the importance of signal sequence for the lethality phenotype. The Yeast Genome Deletion Collection screen revealed many strains with cell wall or cell membrane knock out had strong growth revival. Most importantly, the KP4L *B. meristosporus* protein was found in the spent media fraction of the Western blot data.

CHAPTER 4: IDENTIFICATION OF CRITICAL RESIDUES REQUIRED FOR KP4L FUNCTION.

Introduction

The previous two chapters have established the structural relation between KP4L proteins and KP4, as well as shown that the KP4L proteins are extracellular toxins. To further explore the structure and function relationship of the KP4L proteins a large-scale mutational library will be utilized to identify critical residues for functionality.

KP4's structure has been crystallized, it is known that lysine residue 42 is critical for toxicity as well as the location of disulfide bonds and secondary structure elements (Gu et al., 1995, Gage et al., 2001). Alignments from previous literature have shown Valine or Isoleucine present at this spot in the KP4-Like proteins (Brown, 2011; Lu & Faris, 2019). In Chapter 1 of this document, cysteine was shown to be conserved in 95% of the KP4L proteins next to the lysine 42 residue and to have no residues align to the exact lysine 42 position. Exploring residues for protein function could elucidate specific sites important for cytotoxicity or the location of the active site. A mutational library for two KP4L proteins, *B. meristosporus* and *E. lata,* is used to identify critical residues within those proteins in this study.

Materials and Methods

Mutation Screen of KP4L Proteins

Pooling of Oligonucleotides

A site-saturated mutational library was ordered from Twist Bioscience for KP4L proteins from *B. meristosporus* and *E. lata*. The site-saturated library came in ninety-six plate formats with one site being mutated in the protein per well. Within each well was nineteen mutations present at one residue with no "wildtype" amino acid present (Figure 4.1.). Signal sequence mutations through the end of the protein was included in the mutational library. The well of oligonucleotides were suspended in ten microliters of TE buffer. The wells were then combined into groups of five for the *B. meristosporus* collection and groups of twelve wells for *E. lata*. The mutational library for *B. meristosporus* had five different wells and therefore five different mutated residues in the protein present in each group. *E. lata* had twelve wells per group and therefore twelve different mutated residues in the KP4L *E. lata* protein in each group.

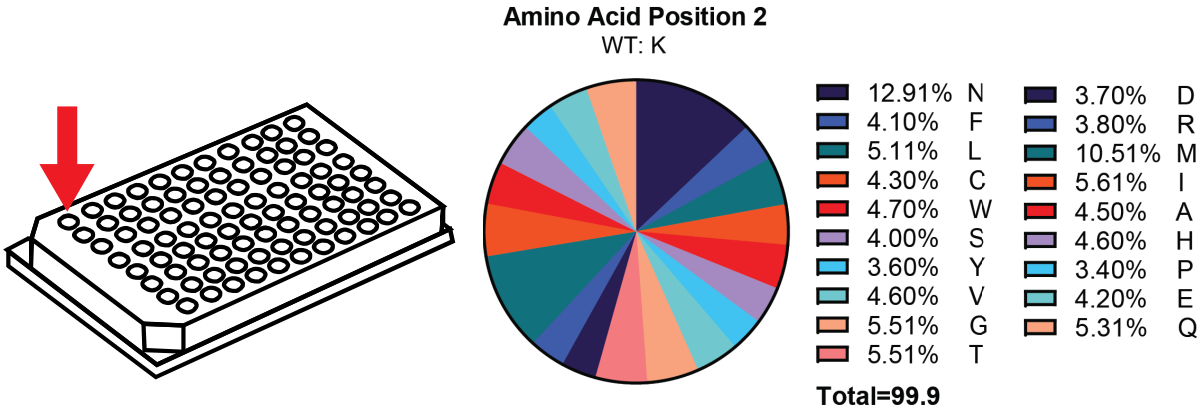

Figure 4.1. Site Saturated Library site one diagram. *Site one is position two in the protein because the start codon cannot be mutated to other amino acids. Red arrow indicates the location on the 96 well plate where site one can be found. Pie chart indicates the relative abundance of each amino acid mutation within the well.*

PCR Amplification of Oligonucleotides

Then groups were amplified using PCR using primers MH013 and MH014 and using the following reaction:

Table 4.1. Primers for amplification of the mutational libraries.

Primer	Target	Sequence
MH013	Mutational Library 5' end (Outside of gene)	CACAAGTTTGTACAAAAAAGCAGGCTTAAAAATG
MH014	Mutational Library 3' end (Outside of gene)	CACCACTTTGTACAAGAAAGCTGGGTCTA

1 µL of MH013

1 µL of MH014

7 µL nuclease-free water

100 ng of the site-saturated library group OR 5 ng of one site from the library

10 µL of Master Mix

The PCR settings are as follows:

Table 4.2. PCR settings for amplification of the mutational libraries.

Amplification of Mutational Library PCR Settings	
Denature	30 seconds at 94°C
Anneal	30 seconds at 65°C
Extend	5 minutes at 72°C
Repeat Cycle	30 cycles
	72°C ten minutes
	4°C infinite hold

The amplified oligonucleotides were then PCR purified using the Monarch PCR & DNA purification kit.

Molecular Ratio Optimization of Gateway Reactions

Optimization of the molecular ratio of oligonucleotides to the entry vector of 1:1, 1:2, 1:5, and 1:10 was performed. The different ratios underwent gateway cloning and then were transformed into *E. coli.* Then the efficiency for the transformation plates for each ratio was calculated. The ratio with the highest efficiency was used for all subsequent Gateway reactions.

BP Gateway of Oligonucleotide pools to Entry Vector (Phase One)

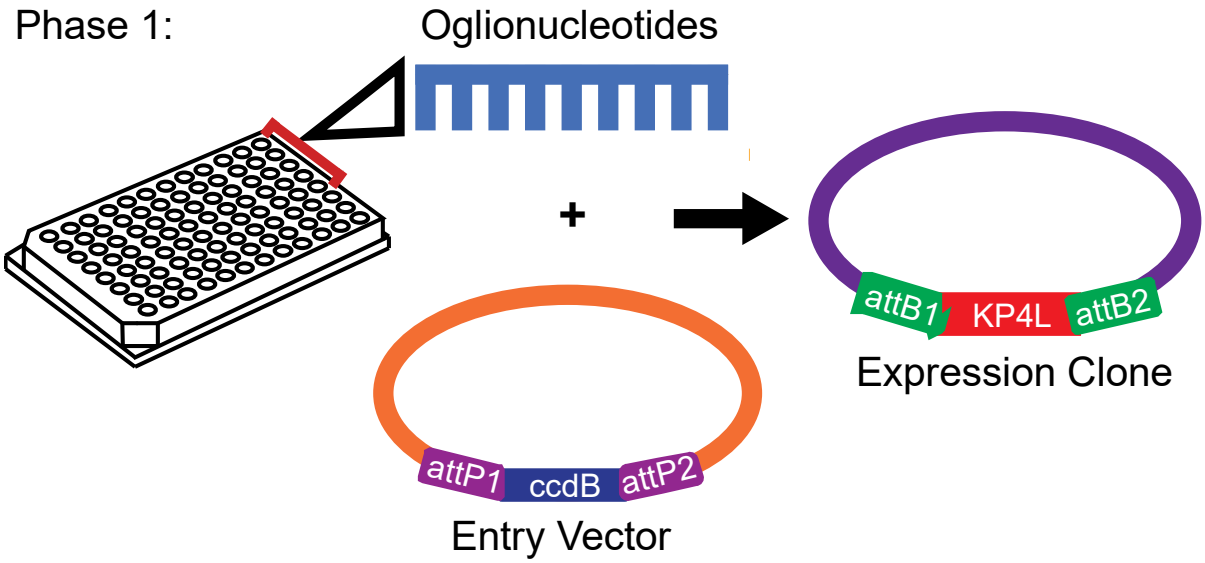

Figure 4.2. Diagram of the Gateway BP Clonase reaction from the oligonucleotides from the mutational library well plate. *pDONR221 was used for the entry vector. Expression clone will be used for the LR Gateway reaction to the yeast vector pAG426GAL.*

A BP Gateway reaction was then done to insert the mutated KP4L genes into the pDONR221 entry vector (Figure 4.2.). The reaction used follows:

10 ng oligonucleotide PCR product

119 ng of pDONR221 entry vector

4.5 µL of nuclease-free water

1 µL BP Clonase II enzyme

The reaction mix was incubated at room temperature overnight. 0.5 µL of Proteinase K was added and then tubes were incubated at 37°C for ten minutes. The mix was transformed using electroporation into *E. coli*.

Creating Electro-competent E. coli cells

DH10-Beta cell line was streaked out to single colonies on LB plates. A single colony was used to inoculate a 2 mL overnight culture of LB liquid media. The overnight culture was used to inoculate a 100 mL LB liquid culture to an OD of 0.05. The cells were then grown for approximately 2 to 3 hours to reach the mid-exponential log phase (OD_{600} of 0.4-0.6). The cells were transferred to two 50 mL conical tubes and spun for 10 minutes at 3,000 *x g* at 4°C. The supernatant was then removed, and the cells were washed with 40 mLs of chilled 10% glycerol and vortexed until homogenous. Then the suspension was spun for 7 minutes at 3,000 *x g*. This was repeated three additional times. After the last wash, the cells were resuspended into 500 µL of chilled 10% glycerol and divided into 50 µL aliquots into prechilled 1.5 mL microcentrifuge tube tubes. Aliquots were immediately frozen at -80.

Electroporation of E. coli using BP Reaction

E. coli aliquots were chilled on ice for ten minutes prior to transformation. 50 µL of cells were added to chilled electroporation cuvettes (1 mm) with 5 µL of the BP Clonase reaction. The cells were then shocked at 1.8 mV, 100 ohms resistance, and 25 cap. The time constant needed to be between 4 seconds and 5 seconds with a preference for a time constant between 4.3 seconds and 4.8 seconds. After shocking, 250 µL of warmed SOC media was added, and then cells and media were carefully pipetted into a sterile 1.5 mL microcentrifuge tube tube. The tube was incubated at 37°C and 250 rpms for one hour. 100 µL of the reaction was used to inoculate a 3mL overnight culture with selective media. 100 µL of the reaction was plated on selective plate media for colony count and was a back-up for making a -80 stock of the group and DNA extraction of the plasmid.

Efficiency Calculation of E. coli transformation

A minimum of one thousand colonies per group were needed per group to ensure all mutations were retained. 100 µL of the *E. coli* reaction was used to make a serial dilution out to 10^{-2}. 100 µL of the 10^{-2} dilution were plated for countable colonies to determine reaction efficiency. At least ten colonies needed to be present to move forward with the group. If a successful colony count was achieved, then 1 mL of the overnight culture was used to make a glycerol stock for -80 C storage. The remaining 2 mL were used for DNA extraction of the plasmids.

LR Gateway of Entry Vector to Destination Vector (Phase Two)

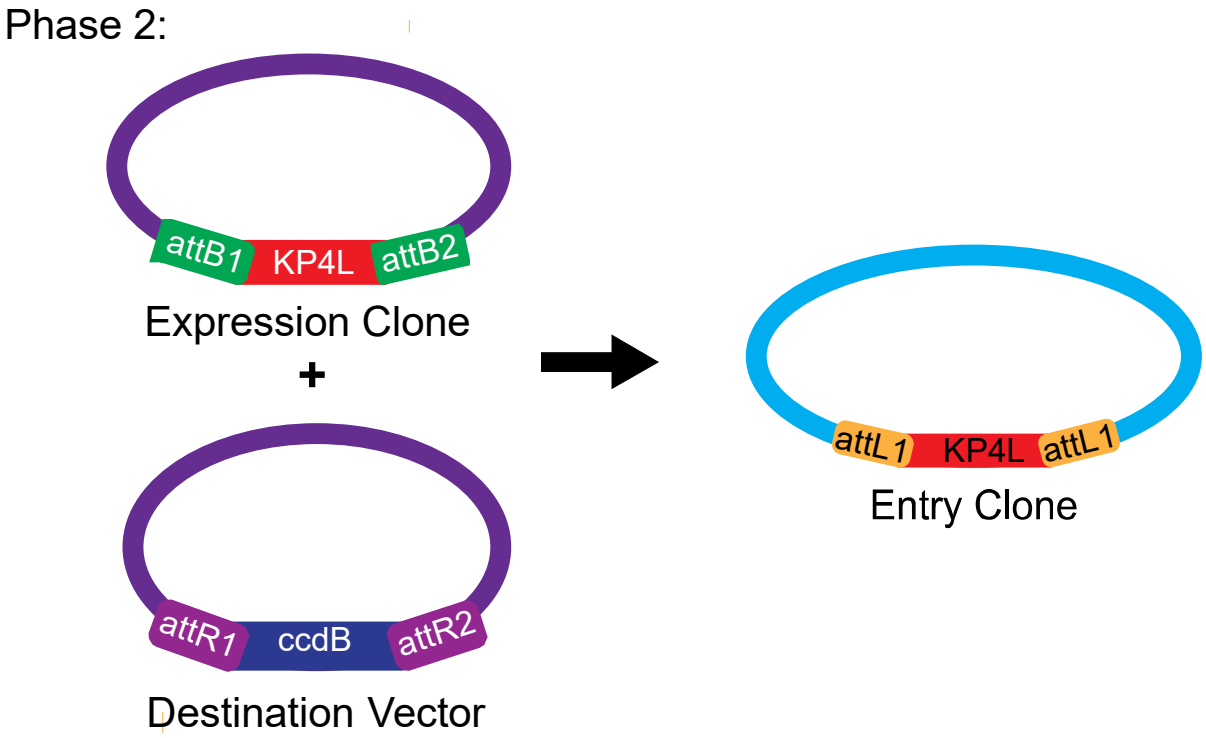

Figure 4.3. Diagram of the Gateway LR Clonase reaction converting the expression clone in the pDONR221 backbone into a yeast expression vector of pAG426GAL.

The extracted plasmids were then combined to create a library for LR gateway reaction to the destination vector of a yeast expression plasmid pAG426 (Figure 4.3.). The LR gateway reaction was repeated ten times to ensure the mutational library diversity was retained. The LR gateway reaction was as follows:

100 ng of pDONR221 plasmid containing the groups of the mutational library of KP4L Bme (entry clone)

150 ng of Destination Vector pAG426

Fill to 8 µL of nuclease-free water

1 µL of LR Clonase

The reaction was incubated overnight at room temperature. Then Proteinase K was added, and the reactions were incubated at 37°C for ten minutes. The samples were then immediately transformed into *E. coli* following the previously detailed protocol. Like the BP reaction, the *E. coli* reactions were plated for efficiency, and a 3 mL overnight culture was

created for DNA extraction and -80 storage if there was the correct level of efficiency. Ten *E. coli* reactions of successful efficiency were used to create the destination clones of site saturated library.

Destination Vector Transformation into Saccharomyces cerevisiae

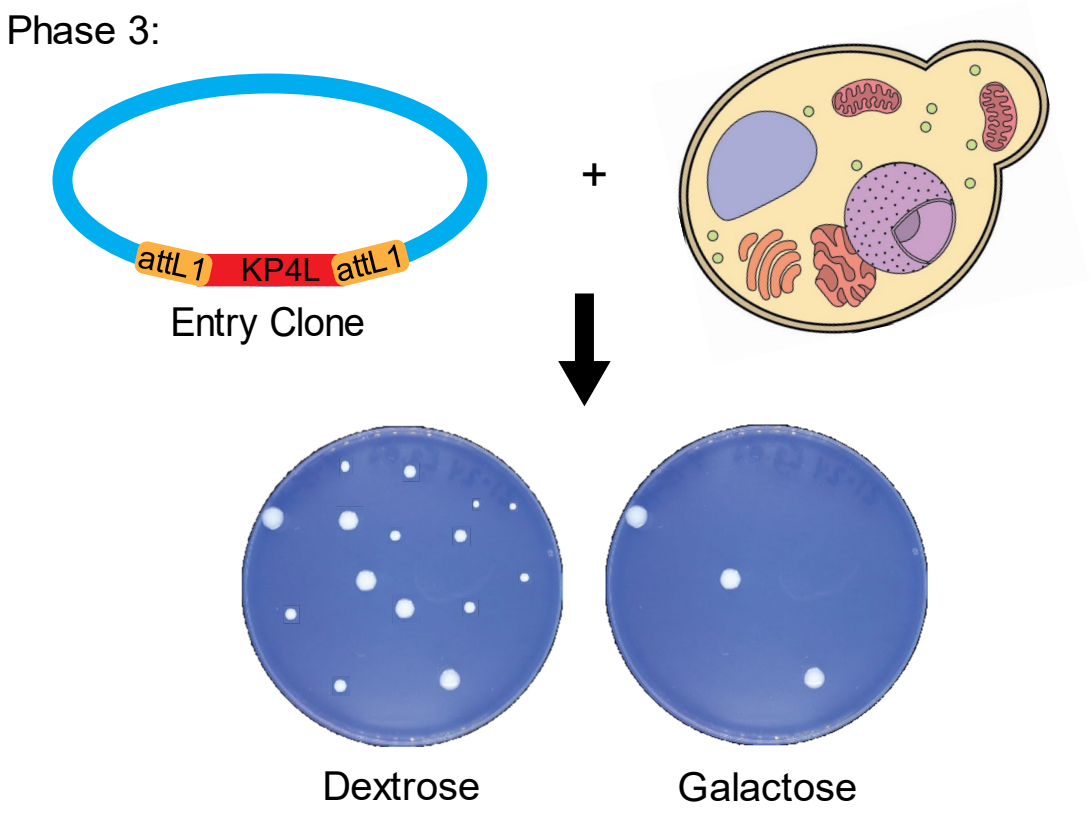

Figure 4.4. Yeast transformation of the mutational library in the yeast expression vector. *The yeast transformation is plated on dextrose and galactose to identify growth revival mutants.*

The expression clones were transformed into *S. cerevisiae* and plated on dextrose and galactose to identify growth revival mutants (Figure 4.4.). The 2mL YPD overnight cultures of BY4741 were created the day before the transformation. The OD_{600} was recorded and then a 1:50 dilution in YPD of the overnight culture was created. The 50 mL culture was grown at 30°C for six hours until it had an OD_{600} between 1.0 and 0.5. The cells were then spun for 30 seconds at 1,900 *x g*, and the supernatant was discarded. The pellet was suspended in a one-to-one ratio of sterile water and incubated at room temperature for ten minutes. The culture was then spun again for the same duration and the supernatant was removed. The pellet was then suspended in 5 mLs of 100mM lithium acetate solution per reaction. The suspension was then

incubated for ten minutes at 30°C. After incubation, the suspension was spun for the same duration and the supernatant was removed. The cells then were resuspended in the residual lithium acetate and equal amounts were transferred to sterile 1.5 mL microcentrifuge tube tubes. Then the new tubes were spun for thirty seconds for 4,000 *x g*. Then the pellets were overlaid with the following:

240 µL PEG_{4000} (50% w/v)

36 µL Lithium acetate [1M]

50 µL Carrier DNA (ssDNA, 2mg, mL)

25 µL of plasmid

25 µL of sterile ddH_2O

The overlay had to be done in order and gently. Then the cells were suspended in the transformation overlay by stirring the pipette tip gently. Controls for the experiment were water (negative control) and GFP plasmid pPAR100 (positive control). The suspension then incubated for thirty minutes at 30°C and then twenty minutes at 42°C. Samples were then spun for 30 seconds at 4,000 *x g*, and then the supernatant was removed via pipetting. Cells were then gently resuspended in 100 µL of sterile ddH_20.

One tube of cells with KP4L plasmid was used to plate on CM-ura dextrose plates, and the remaining tubes were used to plate on CM-ura galactose plates. The plates were grown at 30°C and checked first at 48 hours, and then were allowed to grow for one week.

Galactose Survivors Identification

Galactose survivors were picked from the galactose plate and used to inoculate an overnight culture (12 mL). The larger portion of the overnight culture, 10 mL, was used for total DNA extraction, and 1 mL was used for stocking at -80C.

Galactose Survivors DNA Extraction

The 10 mL culture was then spun for 5 minutes at 1200 x g . The supernatant was removed, and the cells were resuspended in 500 µL water. The suspension was then transferred to a new microcentrifuge tube. The supernatant was removed, and the cell pellet was disrupted by vortexing briefly. Then the cells were suspended in 200 µL breaking buffer. 0.3g of glass beads and 200 µL phenol chloroform isoamyl alcohol was added to the mixture. Then the mixture was vortexed at the highest speed for 3 minutes. After vortexing, 200 µL TE buffer was added and vortexed briefly again. The tube was then spun for 5 minutes at 20,000 *x g* at

room temperature. The aqueous layer within the tube was then transferred to a clean microcentrifuge tube. To this new tube with the aqueous layer, 1 mL of ethanol was added and mixed via inversion. The tube was then spun at 20,000 *x g* for 3 minutes. The supernatant was then removed, and the pellet was resuspended in 400 µL of TE buffer. Then 30 µL of 1 mg/mL DNase-free RNase A was added, mixed, and incubated for 5 minutes at 37°C. After 5 minutes, 10 µL of 4M ammonium acetate and 1 mL of 100% ethanol was added and mixed by inversion. The tube was then spun for 3 minutes at 20,000 *x g*. The supernatant was then discarded, and the pellet was dried. The dried pellet was then resuspended in TE buffer.

Breaking Buffer

2% (v/v) Triton X-100

1% (w/v) SDS

100 mM NaCl

10 mM Tris-HCl, pH 8.0

1 mM EDTA, pH 8.0

TE Buffer

100 mLs

1 mL Tris-HCl, pH 7.5 or 8.0 of 10 mM stock

0.2 mL EDTA of 0.5M stock

Fill to 100 mL with sterile ddH_20

Results

All pools for the mutational libraries *B. meristosporus* and *E. lata* were successfully amplified (Figure 4.5.; Figure 4.6.). Groups for *B. meristosporus* with extremely low efficiency were broken out and each site was amplified individually (Figure 4.7.). The first phase of the *B. meristosporus* mutational library was 75% completed. The groups of sites needed a minimum of 1000 colonies to move to phase two of the library creation. The remaining thirty-five sites had very low efficiency (0-10 total colonies), even when broken out into individual sites. The *Eutypa lata* mutational library was attempted, but low transformation efficiency prevented it from moving to phase two.

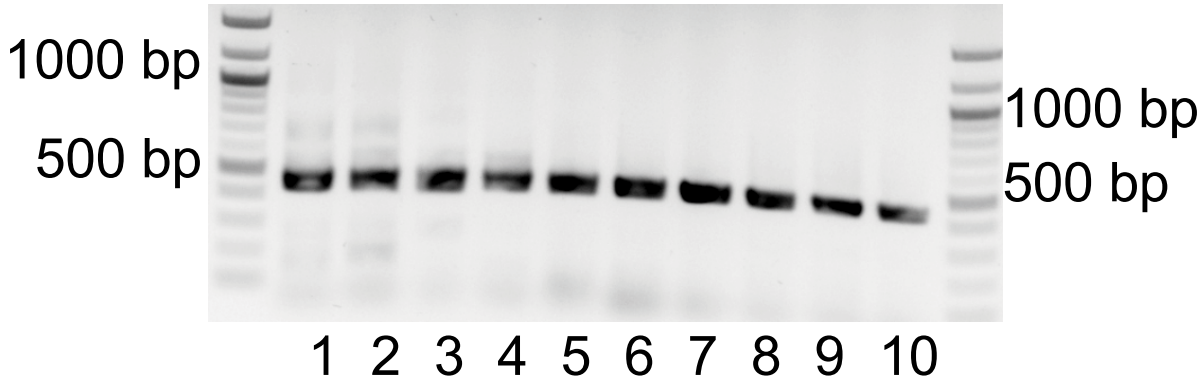

Figure 4.5. Amplification of pools in the mutational library B. meristosporus. *Lanes 1-10 represent groups 1-10 from the mutational library. The product size is approximately 450 base pairs.*

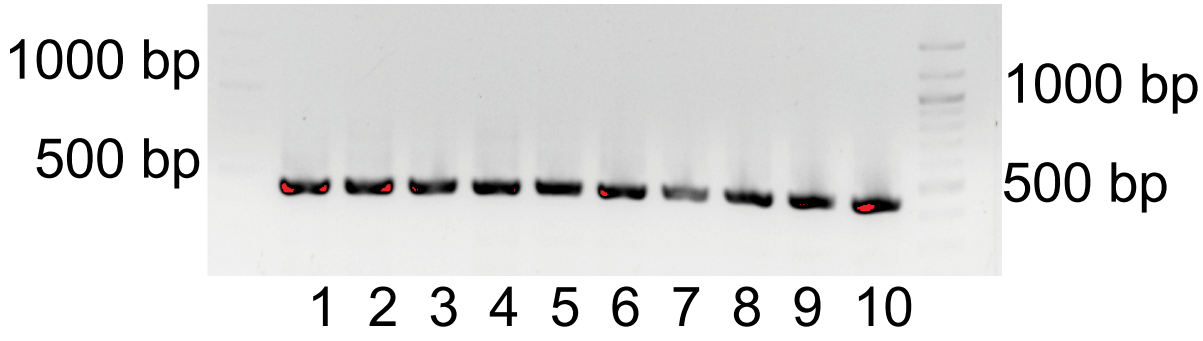

Figure 4.6. Amplification of pools in the mutational library E. lata. *Lanes 1-10 represent groups 1-10 from the mutational library. The product size is approximately 450 base pairs.*

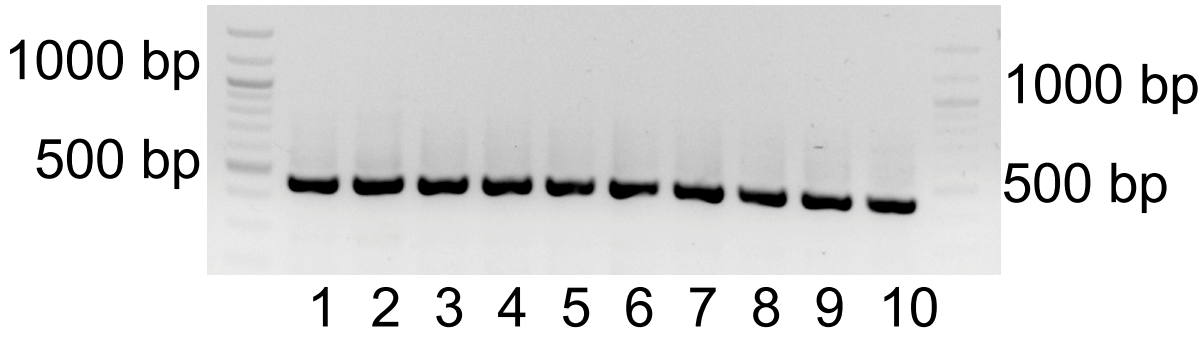

Figure 4.7. Amplification of individual sites in the mutational library B. meristosporus. *Lanes 1 = location F6, lane 2 = F7, lane 3 = F8, lane 4 = F9, lane 5 = F10, lane 6 = G6, lane 7 = G7, lane 8 = G8, lane 9 = G9, and lane 10 = G10. Locations correspond to a location on the mutational library well plate. The product size is approximately 450 base pairs.*

Upon library creation and transformation into *S. cerevisiae*, galactose surviving colonies will be sequenced to identify what residue mutation cause the break in the protein. The list of residues resulting in a broken protein will be compared to modeling data that has predicted mutations that will disrupt structure.

Discussion

The mutational library efficiency was a consistent problem in converting from the oligonucleotides to a yeast expression vector. Even some individual sites were unable to reach the transformation efficiency required to keep the diversity of mutations. PCR amplification of the mutational library dramatically increased the number of reactions able to be performed. Previously, only a maximum of five reactions were possible for each site. PCR amplification enabled the maximization of efficiency tests for sites.

The amplified oligonucleotides also had efficiency issues (10 colonies or less). A PCR gateway control was created from a plasmid containing the KP4L *B. meristosporus* gene that matched the primers. Another gateway control was from a plasmid containing the KP4L *B. meristosporus* gene that was gateway ready and had the correct ATT sites to be cloned into the pDONR221 entry vector. The efficiency of the gateway controls and the pUC19-positive *E. coli* transformation control was high (1000s of colonies).

Other labs in the Biological Sciences department also had difficulty with the efficiency of converting mutational libraries. The difficulty in the transformation of the mutational libraries, despite the success of the controls, leads to the possibility of the mutational library itself having problems.

To minimize monetary costs and continue moving forward individual sites were amplified and then combined into smaller groups (groups of three). However, the smaller groups also had very low transformation efficiency. Yeast transformation and DNA extraction were not able to be performed on the mutational library due to the transformation efficiency problems. However, the protocol was optimized and confirmed to work for the eventual transformation of the libraries. Due to the transformation efficiency problems no sequencing data is yet available.

APPENDIX A

Recipes

Uracil Dropout Mix

Adenine	5 g
Alanine	20 g
Arginine	20 g
Asparagine	20 g
Aspartic Acid	20 g
Cysteine	20 g
Glutamine	20 g
Glutamic Acid	20 g
Glycine	20 g
Isoleucine	20 g
Methionine	20 g
Phenylalanine	20 g
Proline	20 g
Serine	20 g
Threonine	20 g
Tyrosine	20 g
Lysine	20 g
Histidine	20 g
Leucine	100 g
Tryptophan	20 g

Add together into a labeled bottle. Mix thoroughly before each use.

YPD Liquid Media

Yeast Extract	10 g
Peptone	20 g
Dextrose	20 g
ddiH_20	1 L

Cover the beaker with foil, add autoclave tape, and autoclave on liquid setting for at least 45 minutes, leaving stir bar in the medium.

YPD Plate Media

Follow liquid media recipe and add:

Agar	20 g

Cover the beaker with foil, add autoclave tape, and autoclave on liquid setting for at least 45 minutes, leaving stir bar in the medium. Pour plates and let dry for a few days. Label, bag, and store in the cold room.

YPD-G418 Plate Media

Follow YPD Plate Media Instructions.

After autoclaving allow medium to cool and add 1 mL (200 µg/mL) or 2 mL (400 µg/mL) 1000X G418 (frozen aliquot).

Pour plates and let dry. Label, bag, and store in the cold room.

Complete Medium (CM) Yeast Uracil Drop-Out Liquid Media

Uracil Drop-Out Mix	2.5 g
Yeast Nitrogen Base	1.7 g
Dextrose/Galactose/Raffinose	20 g
ddiH_20	1 L

Mix the powders for at least 30 mins in a beaker to ensure all amino acids have dissolved. Cover the beaker with foil, add autoclave tape, and autoclave on liquid setting for at least 45 minutes, leaving stir bar in the medium.

Complete Media (CM) Yeast Uracil Drop-Out Plate Media

Follow the CM Yeast Uracil Drop-Out Liquid Media and add to a beaker:

Agar	20 g

Mix the powders for at least 30 mins to ensure all amino acids have dissolved. Cover the beaker with foil, add autoclave tape, and autoclave on liquid setting for at least 45 minutes, leaving stir bar in the medium. Pour plates and let dry for a few days. Label, bag, and store in the cold room.

Glycerol Stock Tubes

30% Glycerol Stock (volume/volume)

ddiH_20	70 mL
100% Glycerol	30 mL

Mix in an appropriate size beaker.

Pour into individual bottle (250 mL). Autoclave the bottle at liquid settings for 30 minutes.

Use sterile cryotubes to make stock tubes. Pipette 900 µL to each cryotube. Place into stock boxes and place autoclave table on top of the box. Autoclave on liquid settings for 30 minutes. As soon as autoclaving is done tighten the caps, so the solution does not evaporate out. Leave at room temperature to cool and store on shelf. To use add 900 µL of liquid culture to each stock tube, mix, and store at -80°C.

50% w/v of Polyethylene Glycol 3350

PEG 3350	50 g
In a final volume of	100 ml

This means weigh 50 g of PEG into a graduated cylinder or volumetric flask and bring the final volume to 100 mL with water.

100mg/ml (1000X) Ampicillin (AMP)

Mix 5 g ampicillin powder in 50 mL ddiH2O in a 50 mL conical falcon tube. Allow to dissolve with shaking. While powder is dissolving, label and date 50 1.5 mL Eppendorf tubes. Filter sterilize the solution and aliquot 1 mL liquid stock into each tube using a repeat pipettor. Store aliquots in the –20°C freezer box.

200mg/ml (1000X) G418

Mix 10 g G418 powder in 50 mL ddiH2O in a 50 mL conical falcon tube. Allow to dissolve with shaking. While powder is dissolving, label and date 50 1.5 mL Eppendorf tubes. Filter sterilize the solution and aliquot 1 mL liquid stock into each tube using a repeat pipettor. Store aliquots in the –20°C freezer box.

60mg/ml (1000X) Kanamycin (KAN)

Mix 3 g kanamycin powder in 50 mL ddiH2O in a 50 mL conical falcon tube. Allow to dissolve with shaking. While powder is dissolving, label and date 50 1.5 mL Eppendorf tubes. Filter sterilize the solution and aliquot 1 mL liquid stock into each tube using a repeat pipettor. Store aliquots in the –20°C freezer box.

15mg/ml (1000X) chloramphenicol (Cm)

Mix 0.75 g (750 mg) chloramphenicol powder in 50 mL EtOH in a 200 mL glass bottle. Allow to dissolve with shaking. While powder is dissolving, label and date 50 1.5 mL Eppendorf tubes. Screw 0.2 µm membrane filter onto a 50 mL syringe. Push the liquid through the syringe into a sterile tube or bottle. Aliquot 1 mL liquid stock into each tube using a repeat pipettor. Store aliquots in the –20°C freezer box.

20% glucose

Combine 400 g glucose (dextrose) and 1200 mL ddH_2O in a 2 L beaker. Microwave 8 min. on high or until dissolved. Stir until sugar is completely dissolved (i.e., solution is clear). Pour into a 2 L graduated cylinder and adjust volume to 2000 mL with ddH_2O. Return solution to beaker and stir until well mixed. Aliquot 500 mL into each of four labeled 1 L glass bottles, or 100 mL into each of 20 milk bottles (or some combination of the two). Autoclave 20 minutes liquid cycle. Label and store on bench.

20% galactose

Combine 100 g galactose and 400 mL ddH_2O in a 1 L beaker. Mix until fully dissolved and the solution is clear. DO NOT HEAT. This process takes a while, sometimes >1 hour. When powder is dissolved, pour into a 1 L graduated cylinder and adjust volume to 500 mL with ddH_2O. Return solution to beaker and stir until well mixed. Filter sterilize the 250 mL of solution into sterile bottles. Label and store on bench.

Ethidium Bromide (EtBr) Stock Solution

CAUTION – EtBr is a mutagen – Consult MSDS

(10mM Tris-HCl, 1 mM EDTA, 1 mg/mL ethidium bromide)

1M Tris-HCl, pH 8.0	0.5 mL
0.5 M EDTA	0.1 mL
EtBr	1 mg

Add EtBr to Tris-HCl, EDTA and 25 mL of the water, stir overnight to dissolve. Make up to 50 mL with water. Store in a light-proof bottle at room temperature.

2 mg/ml salmon sperm DNA

Mix 0.1 g (100 mg) salmon sperm DNA (looks like a cotton ball) in 50 mL TE in a 50ml conical falcon tube. Allow to dissolve with shaking overnight. Label and date 50 1.5 mL screw-cap tubes. When solution is fully uniform, aliquot 1 mL liquid stock into each tube using a repeat pipettor. DO NOT FILTER STERILIZE. Store aliquots in the –20°C freeze

LB Liquid Media

ddiH20	1 L
LB Broth	25 g
Agar	20 g

LB-Antibiotic Plate Media

In 3 L plastic beaker, add the following:

ddiH20	1 L
LB Broth	25 g
Agar	20 g

Add stir bar. Mix solution on stir plate to dissolve powders. Cover the beaker with foil and place autoclave tape on foil and autoclave for 45 minutes at 121°C (liquid cycle). Remove from the autoclave and stir the media on a stir plate (gently – avoids bubbles). The beaker should be cool enough to hold comfortably in your hands before pouring (~20 min). Take out 1 tube of Antibiotic (1 mL), wrap it in foil, and allow to thaw at room temperature. Add 1 mL of Antibiotic and briefly mix the beaker on the stir plate. Pour stacks of plates, starting from the bottom up, filling Petri dishes with ~25-30 mL of molten agar medium. Mark a line down the side of the dishes with the designated color of LB-Antibiotic. Label bag with "LB-Antibiotic", date, and initials. Allow the agar plates to harden at room temperature. Store at 4°C in lab refrigerator.

E. coli strains

DH10a electrocompetent and chemical competent cells.

One Shot™ ccdB Survival™ 2 T1R Chemically Competent Cells (From ThermoFisher).

NEB® 10-beta Competent E. coli (High Efficiency) (From NEB)

Yeast Strains

BY4741

References

Allen, A., Chatt, E. & Smith, T. J. (2013). The Atomic Structure of the Virally Encoded Antifungal Protein, KP6. *Journal of Molecular Biology*, *425*(3), 609–621. https://doi.org/10.1016/j.jmb.2012.11.033

Allen, A., Islamovic, E., Kaur, J., Gold, S., Shah, D. & Smith, T. J. (2011). Transgenic maize plants expressing the Totivirus antifungal protein, KP4, are highly resistant to corn smut. *Plant Biotechnology Journal*, *9*(8), 857–864. https://doi.org/10.1111/j.1467-7652.2011.00590.x

Allen, A., Islamovic, E., Kaur, J., Gold, S., Shah, D. & Smith, T. J. (2013). The virally encoded killer proteins from Ustilago maydis. *Fungal Biology Reviews*, *26*(4), 166–173. https://doi.org/10.1016/j.fbr.2012.10.001

Allen, A., Snyder, A. K., Preuss, M., Nielsen, E. E., Shah, D. M. & Smith, T. J. (2008). Plant defensins and virally encoded fungal toxin KP4 inhibit plant root growth. *Planta*, *227*(2), 331–339. https://doi.org/10.1007/s00425-007-0620-1

Anderson, P. K., Cunningham, A. A., Patel, N. G., Morales, F. J., Epstein, P. R. & Daszak, P. (2004). Emerging infectious diseases of plants: pathogen pollution, climate change and agrotechnology drivers. *Trends in Ecology & Evolution*, *19*(10), 535–544. https://doi.org/10.1016/j.tree.2004.07.021

Armenteros, J. J. A., Tsirigos, K. D., Sønderby, C. K., Petersen, T. N., Winther, O., Brunak, S., Heijne, G. von & Nielsen, H. (2019). SignalP 5.0 improves signal peptide predictions using deep neural networks. Nature Biotechnology, 37(4), 420–423. https://doi.org/10.1038/s41587-019-0036-z

BEVAN, E. A., HERRING, A. J. & MITCHELL, D. J. (1973). Preliminary Characterization of Two Species of dsRNA in Yeast and their Relationship to the “Killer” Character. Nature, 245(5420), 81–86. https://doi.org/10.1038/245081b0

Benítez-Chao, D. F., León-Buitimea, A., Lerma-Escalera, J. A. & Morones-Ramírez, J. R. (2021). Bacteriocins: An Overview of Antimicrobial, Toxicity, and Biosafety Assessment by in vivo Models. *Frontiers in Microbiology*, *12*, 630695. https://doi.org/10.3389/fmicb.2021.630695

Brown, D. W. (2011). The KP4 killer protein gene family. *Current Genetics*, *57*(1), 51–62. https://doi.org/10.1007/s00294-010-0326-y

Cheng, F. & Cheng, Z. (2015). Research Progress on the use of Plant Allelopathy in Agriculture and the Physiological and Ecological Mechanisms of Allelopathy. *Frontiers in Plant Science*, *6*, 1020. https://doi.org/10.3389/fpls.2015.01020

Chengxu, W., Mingxing, Z., Xuhui, C. & Bo, Q. (2011). Review on Allelopathy of Exotic Invasive Plants. *Procedia Engineering*, *18*, 240–246. https://doi.org/10.1016/j.proeng.2011.11.038

Clausen, M., Kräuter, R., Schachermayr, G., Potrykus, I. & Sautter, C. (2000). Antifungal activity of a virally encoded gene in transgenic wheat. *Nature Biotechnology*, *18*(4), 446–449. https://doi.org/10.1038/74521

Day, P. R. (1973). The Killer System in Ustilago maydis: Heterokaryon Transfer and Loss of Determinants. *Phytopathology*, *63*(8), 1017. https://doi.org/10.1094/phyto-63-1017

Díaz, M. A., Pereyra, M. M., Picón-Montenegro, E., Meinhardt, F. & Dib, J. R. (2020). Killer Yeasts for the Biological Control of Postharvest Fungal Crop Diseases. *Microorganisms*, *8*(11), 1680. https://doi.org/10.3390/microorganisms8111680

Drozdetskiy, A., Cole, C., Procter, J. & Barton, G. J. (2015). JPred4: a protein secondary structure prediction server. Nucleic Acids Research, 43(W1), W389–W394. https://doi.org/10.1093/nar/gkv332

Fisher, M. C., Gow, N. A. R. & Gurr, S. J. (2016). Tackling emerging fungal threats to animal health, food security and ecosystem resilience. *Philosophical Transactions of the Royal Society B: Biological Sciences*, *371*(1709), 20160332. https://doi.org/10.1098/rstb.2016.0332

Fisher, M. C., Henk, Daniel. A., Briggs, C. J., Brownstein, J. S., Madoff, L. C., McCraw, S. L. & Gurr, S. J. (2012). Emerging fungal threats to animal, plant and ecosystem health. *Nature*, *484*(7393), 186–194. https://doi.org/10.1038/nature10947

Food Security | USDA. (n.d.). Retrieved October 17, 2021, from https://www.usda.gov/topics/food-and-nutrition/food-security

Gage, M. J., Bruenn, J., Fischer, M., Sanders, D. & Smith, T. J. (2001). KP4 fungal toxin inhibits growth in Ustilago maydis by blocking calcium uptake. *Molecular Microbiology*, *41*(4), 775–785. https://doi.org/10.1046/j.1365-2958.2001.02554.x

Gage, M. J., Rane, S. G., Hockerman, G. H. & Smith, T. J. (2002). The Virally Encoded Fungal Toxin KP4 Specifically Blocks L-Type Voltage-Gated Calcium Channels. *Molecular Pharmacology*, *61*(4), 936–944. https://doi.org/10.1124/mol.61.4.936

Giaever, G., Chu, A. M., Ni, L., Connelly, C., Riles, L., Véronneau, S., Dow, S., Lucau-Danila, A., Anderson, K., André, B., Arkin, A. P., Astromoff, A., Bakkoury, M. E., Bangham, R., Benito, R., Brachat, S., Campanaro, S., Curtiss, M., Davis, K., … Johnston, M. (2002). Functional profiling of the Saccharomyces cerevisiae genome. Nature, 418(6896), 387–391. https://doi.org/10.1038/nature00935

Ghoul, M. & Mitri, S. (2016). The Ecology and Evolution of Microbial Competition. *Trends in Microbiology*, *24*(10), 833–845. https://doi.org/10.1016/j.tim.2016.06.011

Godfray, H. C. J., Mason-D'Croz, D. & Robinson, S. (2016). Food system consequences of a fungal disease epidemic in a major crop. *Philosophical Transactions of the Royal Society B: Biological Sciences*, *371*(1709), 20150467. https://doi.org/10.1098/rstb.2015.0467

Grinter, R., Milner, J. & Walker, D. (2012). Bacteriocins active against plant pathogenic bacteria. *Biochemical Society Transactions*, *40*(6), 1498–1502. https://doi.org/10.1042/bst20120206

Gu, F., Khimani, A., Rane, S. G., Flurkey, W. H., Bozarth, R. F. & Smith, T. J. (1995). Structure and function of a virally encoded fungal toxin from Ustilago maydis: a fungal and mammalian Ca2+ channel inhibitor. *Structure*, *3*(8), 805–814. https://doi.org/10.1016/s0969-2126(01)00215-5

Kahl, C. R. & Means, A. R. (2003). Regulation of Cell Cycle Progression by Calcium/Calmodulin-Dependent Pathways. *Endocrine Reviews*, *24*(6), 719–736. https://doi.org/10.1210/er.2003-0008

Kandel, J. & Koltin, Y. (1978). Killer phenomenon in Ustilago maydis: Comparison of the killer proteins. *Experimental Mycology*, *2*(3), 270–278. https://doi.org/10.1016/s0147-5975(78)80020-6

Khan, R. S., Iqbal, A., Malak, R., Shehryar, K., Attia, S., Ahmed, T., Khan, M. A., Arif, M. & Mii, M. (2019). Plant defensins: types, mechanism of action and prospects of genetic engineering for enhanced disease resistance in plants. *3 Biotech*, *9*(5), 192. https://doi.org/10.1007/s13205-019-1725-5

Koltin, Y. & Day, P. R. (1976). Inheritance of killer phenotypes and double-stranded RNA in Ustilago maydis. *Proceedings of the National Academy of Sciences*, *73*(2), 594–598. https://doi.org/10.1073/pnas.73.2.594

Lacerda, A. F., Vasconcelos, É. A. R., Pelegrini, P. B. & Sa, M. F. G. de. (2014). Antifungal defensins and their role in plant defense. *Frontiers in Microbiology*, *5*, 116. https://doi.org/10.3389/fmicb.2014.00116

Li, N., Erman, M., Pangborn, W., Duax, W. L., Park, C.-M., Bruenn, J. & Ghosh, D. (1999). Structure of Ustilago maydis Killer Toxin KP6 α-Subunit A MULTIMERIC ASSEMBLY WITH A CENTRAL PORE*. *Journal of Biological Chemistry*, *274*(29), 20425–20431. https://doi.org/10.1074/jbc.274.29.20425

Lu, S. & Faris, J. D. (2019). Fusarium graminearum KP4-like proteins possess root growth-inhibiting activity against wheat and potentially contribute to fungal virulence in seedling rot. *Fungal Genetics and Biology*, *123*, 1–13. https://doi.org/10.1016/j.fgb.2018.11.002

Lukša, J., Podoliankaitė, M., Vepštaitė, I., Strazdaitė-Žielienė, Ž., Urbonavičius, J. & Servienė, E. (2015). Yeast β-1,6-Glucan Is a Primary Target for the Saccharomyces cerevisiae K2 Toxin. *Eukaryotic Cell*, *14*(4), 406–414. https://doi.org/10.1128/ec.00287-14

Madgwick, J. W., West, J. S., White, R. P., Semenov, M. A., Townsend, J. A., Turner, J. A. & Fitt, B. D. L. (2011). Impacts of climate change on wheat anthesis and fusarium ear blight in the UK. *European Journal of Plant Pathology*, *130*(1), 117–131. https://doi.org/10.1007/s10658-010-9739-1

Martínez-Espinoza, A. D., García-Pedrajas, M. D. & Gold, S. E. (2002). The Ustilaginales as Plant Pests and Model Systems. *Fungal Genetics and Biology*, *35*(1), 1–20. https://doi.org/10.1006/fgbi.2001.1301

Mirzaee, H., Peralta, N. L. N., Carvalhais, L. C., Dennis, P. G. & Schenk, P. M. (2021). Plant-produced bacteriocins inhibit plant pathogens and confer disease resistance in tomato. *New Biotechnology*, *63*, 54–61. https://doi.org/10.1016/j.nbt.2021.03.003

Park, C., Banerjee, N., Koltin, Y. & Bruenn, J. A. (1996). The Ustilago maydis virally encoded KP1 killer toxin. *Molecular Microbiology*, *20*(5), 957–963. https://doi.org/10.1111/j.1365-2958.1996.tb02537.x

Park, C., Bruenn, J. A., Ganesa, C., Flurkey, W. F., Bozarth, R. F. & Koltin, Y. (1994). Structure and heterologous expression of the Ustilago maydis viral toxin KP4. *Molecular Microbiology*, *11*(1), 155–164. https://doi.org/10.1111/j.1365-2958.1994.tb00297.x

Puhalla, J. E. (1968). COMPATIBILITY REACTIONS ON SOLID MEDIUM AND INTERSTRAIN INHIBITION IN USTILAGO MAYDIS. *Genetics*, *60*(3), 461–474. https://doi.org/10.1093/genetics/60.3.461

Reece-Hoyes, J. S. & Walhout, A. J. M. (2018). Gateway Recombinational Cloning. Cold Spring Harbor Protocols, 2018(1), pdb.top094912. https://doi.org/10.1101/pdb.top094912

Rooney, W. M., Chai, R., Milner, J. J. & Walker, D. (2020). Bacteriocins Targeting Gram-Negative Phytopathogenic Bacteria: Plantibiotics of the Future. *Frontiers in Microbiology*, *11*, 575981. https://doi.org/10.3389/fmicb.2020.575981

Rossman, A. Y. (2009). The impact of invasive fungi on agricultural ecosystems in the United States. *Biological Invasions*, *11*(1), 97–107. https://doi.org/10.1007/s10530-008-9322-2

Ruiz-Herrera, J., & Martínez-Espinoza, A. D. (1998). The fungus Ustilago maydis, from the aztec cuisine to the research laboratory. *International Microbiology*, *1*(2), 149-158.

Sayers, E. W., Bolton, E. E., Brister, J. R., Canese, K., Chan, J., Comeau, D. C., Connor, R., Funk, K., Kelly, C., Kim, S., Madej, T., Marchler-Bauer, A., Lanczycki, C., Lathrop, S., Lu, Z., Thibaud-Nissen, F., Murphy, T., Phan, L., Skripchenko, Y., Tse, T., … Sherry, S. T.

(2022). Database resources of the national center for biotechnology information. *Nucleic acids research*, *50*(D1), D20–D26. https://doi.org/10.1093/nar/gkab1112

Schlaich, T., Urbaniak, B. M., Malgras, N., Ehler, E., Birrer, C., Meier, L. & Sautter, C. (2006). Increased field resistance to Tilletia caries provided by a specific antifungal virus gene in genetically engineered wheat. *Plant Biotechnology Journal*, *4*(1), 63–75. https://doi.org/10.1111/j.1467-7652.2005.00158.x

Schmitt, M. J. & Breinig, F. (2006). Yeast viral killer toxins: lethality and self-protection. Nature Reviews Microbiology, 4(3), 212–221. https://doi.org/10.1038/nrmicro1347

SCHMITT, M., BRENDEL, M., SCHWARZ, R. & RADLER, F. (1989). Inhibition of DNA Synthesis in Saccharomyces cerevisiae by Yeast Killer Toxin KT28. *Microbiology*, *135*(6), 1529–1535. https://doi.org/10.1099/00221287-135-6-1529

Schmitt, M. J. & Tipper, D. J. (1990). K28, a unique double-stranded RNA killer virus of Saccharomyces cerevisiae. *Molecular and Cellular Biology*, *10*(9), 4807–4815. https://doi.org/10.1128/mcb.10.9.4807-4815.1990

Schmitt, M. & Radler, F. (1987). Mannoprotein of the Yeast Cell Wall as Primary Receptor for the Killer Toxin of Saccharomyces cerevisiae Strain 28. *Microbiology*, *133*(12), 3347–3354. https://doi.org/10.1099/00221287-133-12-3347

Schmitt, M. J. & Reiter, J. (2008). Viral induced yeast apoptosis. Biochimica et Biophysica Acta (BBA) - Molecular Cell Research, 1783(7), 1413–1417. https://doi.org/10.1016/j.bbamcr.2008.01.017

Schulz, M., Marocco, A., Tabaglio, V., Macias, F. A. & Molinillo, J. M. G. (2013). Benzoxazinoids in Rye Allelopathy - From Discovery to Application in Sustainable Weed Control and Organic Farming. *Journal of Chemical Ecology*, *39*(2), 154–174. https://doi.org/10.1007/s10886-013-0235-x

Schrödinger, L., & DeLano, W. (2020). *PyMOL*. Retrieved from http://www.pymol.org/pymol

Skolnick, J., Gao, M., Zhou, H. & Singh, S. (2021). AlphaFold 2: Why It Works and Its Implications for Understanding the Relationships of Protein Sequence, Structure, and Function. Journal of Chemical Information and Modeling, 61(10), 4827–4831. https://doi.org/10.1021/acs.jcim.1c01114

Simons, A., Alhanout, K. & Duval, R. E. (2020). Bacteriocins, Antimicrobial Peptides from Bacterial Origin: Overview of Their Biology and Their Impact against Multidrug-Resistant Bacteria. *Microorganisms*, *8*(5), 639. https://doi.org/10.3390/microorganisms8050639

Spelbrink, R. G., Dilmac, N., Allen, A., Smith, T. J., Shah, D. M. & Hockerman, G. H. (2004). Differential Antifungal and Calcium Channel-Blocking Activity among Structurally

Related Plant Defensins. *Plant Physiology*, *135*(4), 2055–2067. https://doi.org/10.1104/pp.104.040873

Stothard P (2000) The Sequence Manipulation Suite: JavaScript programs for analyzing and formatting protein and DNA sequences. Biotechniques 28:1102-1104.

Talbot, N. J. (2003). ON THE TRAIL OF A CEREAL KILLER: Exploring the Biology of Magnaporthe grisea. *Annual Review of Microbiology*, *57*(1), 177–202. https://doi.org/10.1146/annurev.micro.57.030502.090957

Tamura, K., Stecher, G. & Kumar, S. (2021). MEGA11: Molecular Evolutionary Genetics Analysis version 11. *Molecular Biology and Evolution*, *38*(7), msab120-. https://doi.org/10.1093/molbev/msab120

TAO, J., GINSBERG, ' IDIT, BANERJEE, 2 NANDITTA, HELD, ' W., KOLTIN, 3 YIGAL & BRUENNl, 2 AND JEREMY A. (1990). Ustilago maydis KP6 Killer Toxin: Structure, Expression. *Molecular and Cellular Biology*.

Thompson, J. D., Higgins, D. G. & Gibson, T. J. (1994). CLUSTAL W: improving the sensitivity of progressive multiple sequence alignment through sequence weighting, position-specific gap penalties and weight matrix choice. *Nucleic Acids Research*, *22*(22), 4673–4680. https://doi.org/10.1093/nar/22.22.4673

Weerden, N. L. van der, Lay, F. T. & Anderson, M. A. (2008). The Plant Defensin, NaD1, Enters the Cytoplasm of Fusarium Oxysporum Hyphae. *Journal of Biological Chemistry*, *283*(21), 14445–14452. https://doi.org/10.1074/jbc.m709867200

WHITE, P. J. (1998). Calcium Channels in the Plasma Membrane of Root Cells. *Annals of Botany*, *81*(2), 173–183. https://doi.org/10.1006/anbo.1997.0554